NTNU
Norwegian University of Science and Technology
Department of Marine Technology

M.Sc.THESIS

Title:	**Delivered:**
Design analysis and optimisation of mooring system for floating wind turbines	14.06.2011
	Availability: Open
Student: Tore Hordvik	**Number of pages:** 71

Abstract:

Lately, focus is put on renewable energy resources as the environmental concerns regarding exploitation of hydrocarbons are increasing. The enormous energy potential found in offshore wind fields is proposed utilized by installing floating wind turbines in interconnected wind farms. As for all other floating structures operating within a limited area, stationkeeping is needed in order to keep the motions of the floating structure within permissible limits. In this study, methods for selecting and optimising the mooring system for floating wind turbines in shallow water are investigated. The design of the mooring system is checked against the governing rules and standards.

Initially, the forces and moments associated with such structures are identified as the various terms in the equations of motions.

Furthermore, the different mooring system concepts investigated in the study are described. They include distributed mass-, clump weight-, and buoyancy element mooring system. They are all based on the Hywind design with three distributed main mooring lines, each split into two delta-lines. Software programs suitable for analysing the system behaviour are recognized as SIMO, Riflex and TDHMILL3D. The analysis methods include quasi-static catenary analysis, eigenvalue analysis and decay analysis, in addition to integrated time domain analysis.

The mooring system concepts are studied, and the clump weight mooring system is shown to be the preferred one with respect to limiting peak tensions in the mooring lines. The selected design concept is subjected to an optimisation procedure, where the main focus is to select mooring line segments with adequate breaking strength to sustain the maximum line tension with sufficient margins and to avoid vertical forces on the anchors. From parameter studies, the size of the clump weight is shown to be the most influential design parameter. Other parameters investigated include the position of the clump weight, pretension, overall length of the mooring system, chain and wire weight/dimension, vertical fairlead position and the delta-line length.

Finally, the intact optimised mooring system is checked against the Ultimate limit state, while Accidental limit state control is performed for the mooring system in damaged condition. Both the cases of loss of line and loss of clump weight are investigated. The Troll field is selected as design location. For the Ultimate limit state, the criteria given in the standards are fulfilled for all directions. For the Accidental limit state, the mooring system design fails to meet the criteria given in the standards. Lack of redundancy is shown as this may cause loss of additional anchorlines.

Keyword:

Floating wind turbine
Mooring system
Optimisation

Advisor:

Professor Carl Martin Larsen

Address:
NTNU
Department of Marine Technology
N-7491 Trondheim

Location
Marinteknisk Senter
O. Nielsens vei 10

Tel. +47 73 595501
Fax +47 73 595697

NTNU Trondheim
Norwegian University of Science and Technology
Faculty of Engineering Science and Technology
Department of MarineTechnology

M.Sc. thesis 2011

for

Stud.tech. Tore Hordvik

Design analysis and optimisation of mooring system for floating wind turbines

Renewable energy is considered to be the only sustainable way for future energy supply. Norway is blessed with topography and sufficient rainfall that makes it possible to produce sufficient electricity from hydropower. However, future growth in domestic energy demand and export will require unwanted encroachments on rivers and lakes. Alternative energy production is therefore encouraged. Wind energy is an obvious alternative, but wind turbines are not always wanted on land. Offshore windmills have therefore been proposed. For several reasons one would prefer to have such installations at some distance from the coast, but the water depth on the Norwegian continental shelf is too large for the use of bottom fixes turbines. It is therefore proposed to have floating wind turbines and the design of cheap but reliable mooring systems for such structures will hence crucial for the economy of this concept.

The purpose of this project is to describe a rational method for design verification analysis and mooring line optimisation for floating wind turbines on shallow water.

The work is a continuation of the pre-project that reported basic features of floating wind turbines and relevant analysis methods. Subjects that have been reported in the pre-project should not be repeated in the MSc thesis.

The work may be carried out in steps as follows:

1. Select realistic design parameters for a floating wind turbine that might be applied for large scale power production on 85-100 meters water depth in Norwegian waters.
2. Discuss alternative mooring system designs, and select the topography for a system that should be subjected to further studies.
3. Define all needed parameters for the selected system, either from optimisation or based on experience and sound engineering judgement.
4. Describe methods for a complete design verification including the use of actual computer programs and analysis procedures.
5. Carry out and report selected parts of a design verification. The selection of actual analyses should be discussed with the supervisor.

The will be carried out in cooperation with Statoil Bergen, where student will stay most of the time during the MSc thesis period.

The work may show to be more extensive than anticipated. Some topics may therefore be left out after discussion with the supervisor without any negative influence on the grading.

The candidate should in her/his report give a personal contribution to the solution of the problem formulated in this text. All assumptions and conclusions must be supported by mathematical models and/or references to physical effects in a logical manner.
The candidate should apply all available sources to find relevant literature and information on the actual problem.

The report should be well organised and give a clear presentation of the work and all conclusions. It is important that the text is well written and that tables and figures are used to support the verbal presentation. The report should be complete, but still as short as possible.

The final report must contain this text, an acknowledgement, summary, main body, conclusions and suggestions for further work, symbol list, references and appendices. All figures, tables and equations must be identified by numbers. References should be given by author name and year in the text, and presented alphabetically by name in the reference list. The report must be submitted in two copies unless otherwise has been agreed with the supervisor.

The supervisor may require that the candidate should give a written plan that describes the progress of the work after having received this text. The plan may contain a table of content for the report and also assumed use of computer resources.

From the report it should be possible to identify the work carried out by the candidate and what has been found in the available literature. It is important to give references to the original source for theories and experimental results.

The report must be signed by the candidate, include this text, appear as a paperback, and - if needed - have a separate enclosure (binder, DVD/ CD) with additional material.

Supervisor at NTNU: Carl M. Larsen
Contact person at Statoil: Tor Hanson

Trondheim, January 2011

Carl M. Larsen

Submitted: January 2011
Deadline: June 2011

Preface

This report is the result of the course TMR4900 Marine Structures - Master thesis at the Department of Marine Technology at the Norwegian University of Science and Technology (NTNU) in Trondheim. The work is carried out at the Statoil research centre at Sandsli, Bergen. The study elaborates on optimising the mooring system design for offshore floating wind turbines in shallow water. A water depth of 100 m is assumed. The design is based on the Hywind design with modified draft, accounting for the reduced water depth.

In an attempt to maintain the motion characteristics of the Hywind pilot, the draft is only reduced by 20 m to 80 m. Whether the vertical distance between the tower bottom and the sea bed of only 20 m is sufficient from a design perspective is not investigated. The same is the case for whether a deep-draft SPAR concept is the most cost-effective concept for such water depths. Focus is mainly put on how the mooring system can be selected, optimised, and designed according to the governing rules and standards for the selected design concept.

Several people have contributed to the realization of this report. First and foremost I would like to thank NTNU and my supervisor Professor Carl Martin Larsen, and the Statoil research centre represented by my supervisor Tor David Hanson for the cooperation and contributions during the thesis work. I would also like to thank Finn Gunnar Nielsen and Rune Yttervik at the Statoil research centre for their contributions. Vryhof anchors in the Netherlands are also acknowledged for their helpfulness. Gratitude is finally addressed to my office mates Jon Erik Lygren and Ingebjørg Hage for making my stay at the Statoil research centre memorable.

Tore Hordvik

Bergen, June 14th, 2011

Abstract

Lately, focus is put on renewable energy resources as the environmental concerns regarding exploitation of hydrocarbons are increasing. The enormous energy potential found in offshore wind fields is proposed utilized by installing floating wind turbines in interconnected wind farms. As for all other floating structures operating within a limited area, stationkeeping is needed in order to keep the motions of the floating structure within permissible limits. In this study, methods for selecting and optimising the mooring system for floating wind turbines in shallow water are investigated. The design of the mooring system is checked against the governing rules and standards.

Initially, the forces and moments associated with such structures are identified as the various terms in the equations of motions.

Furthermore, the different mooring system concepts investigated in the study are described. They include distributed mass-, clump weight-, and buoyancy element mooring system. They are all based on the Hywind design with three distributed main mooring lines, each split into two delta-lines. Software programs suitable for analysing the system behaviour are recognized as SIMO, Riflex and TDHMILL3D. The analysis methods include quasi-static catenary analysis, eigenvalue analysis and decay analysis, in addition to integrated time domain analysis.

The mooring system concepts are studied, and the clump weight mooring system is shown to be the preferred one with respect to limiting peak tensions in the mooring lines. The selected design concept is subjected to an optimisation procedure, where the main focus is to select mooring line segments with adequate breaking strength to sustain the maximum line tension with sufficient margins and to avoid vertical forces on the anchors. From parameter studies, the size of the clump weight is shown to be the most influential design parameter. Other parameters investigated include the position of the clump weight, pretension, overall length of the mooring system, chain and wire weight/dimension, vertical fairlead position and the delta-line length.

Finally, the intact optimised mooring system is checked against the Ultimate limit state, while Accidental limit state control is performed for the mooring system in damaged condition. Both the cases of loss of line and loss of clump weight are investigated. The Troll field is selected as design location. For the Ultimate limit state, the criteria given in the standards are fulfilled for all directions. For the Accidental limit state, the mooring system design fails to meet the criteria given in the standards. Lack of redundancy is shown as this may cause loss of additional anchorlines.

List of abbreviations

ALS	Accidental Limit State
COB	Centre of Buoyancy
COG	Centre of Gravity
DLL	Dynamic Linked Library
DNV	Det Norske Veritas
DOF	Degree of Freedom
FFT	Fast Fourier Transform
FLS	Fatigue Limit State
JONSWAP	Joint North Sea Wave Project
LF	Low-Frequency
MPM	Most Probable Maximum
OS-E301	DNV-OS-E301 “Position Mooring”
SLS	Serviceability Limit State
ULS	Ultimate Limit State
VIV	Vortex-induced vibrations
WF	Wave-Frequency

Table of Contents

List of Figures

List of Tables

1. Introduction

1.1 General

As the demand for energy is increasing and the oil and gas deposits are limited, focus is put on renewable energy sources. Wind energy, being one of this renewable energy sources, has been utilized for agricultural purposes for centuries, and became important also for power production in the second half of the 20th century. As one wants to take advantage of the enormous wind power potential offshore, several participants in the international energy business have installed and commercialized interconnected bottom-fixed wind turbine structures in areas of shallow water. The water depth is however strongly limiting the extent of such applications, as the support structures of offshore wind turbines become highly dynamic, having to cope with combined wind and hydrodynamic loading in addition to the complex dynamic behaviour of the wind turbine itself (Hordvik, 2010). Wind turbines installed on floating substructures are therefore proposed in order to utilize the potential for harvesting wind energy in areas that are not feasible for bottom-fixed structures. Developing and the possibility of commercializing floating offshore wind turbines are presently being investigated by several developers, technology providers and research institutes worldwide. The Spar concept is one of the designs that have been proposed as substructure for floating offshore wind turbines.

1.2 Spar concept

The Spar concept is not by any means a new concept. It has been used in marine applications for decades as marker buoys and for gathering oceanographic data. Later it was scaled up and introduced as production platform in the offshore energy market. The world's first production spar was the Neptune Spar installed in 1996 by Oryx Energy Company and CNG (Chakrabarti 2005). In 2009, Statoil introduced a floating wind turbine based on the Spar concept, which is reviewed in the following section.

Simplified we can say that the Spar consists of a large cylinder floating vertically in the water. A Spar platform is weight stabilized, which implies a design where the centre of gravity (COG) is located below the centre of buoyancy (COB). The low COG is obtained by heavy ballasting in the bottom part of the cylinder. The concept is characterized by its deep draft which gives the Spar concept favourable motion characteristics compared to other floating concepts; because the wave action at the surface is damped by the counter balance effect of the structural weight (Hordvik, 2010).

Some of the key features of the Spar concept include:

- Feasible for water depths up to 3000 m.
- Possibility for a large range of payloads
- Is always stable because the COB is located above the COG

As for any other floating structure operating within a limited area, stationkeeping becomes important. Spars are traditionally moored by the means of spread catenary moorings. The restoring forces are then provided by the weight of the mooring lines. When the water depth is reduced to only 100 m, as investigated in this study, catenary mooring becomes challenging because the suspended length of the mooring lines, and hence the submerged weight, is limited. Focus is put on these issues later in the report.

1.3 Hywind pilot

As this study is investigating the mooring system of a floating wind turbine structure similar to the Hywind pilot, a short introduction to the concept is given in the following.

According to Statoil's homepage, the world's first operational deep-water floating large-capacity wind turbine is the Hywind pilot, which is a prototype of the Hywind concept. The pilot is located about ten kilometers off the coast of Karmøy on the west coast of Norway; it is still in operation, generating electricity to the Norwegian grid. The main purpose of the pilot project is to investigate how wind and waves are affecting the structure.

The design is owned by Statoil while Technip built the floater and Siemens manufactured the turbine. The concept is based on a Spar buoy type design. A 2.3 MW turbine is mounted on the tower 65 m above the water line. The draft is 100 m and the buoy is moored at a water depth of approximately 210 m. The tower and substructure is made in steel with water and rock ballasting. The installation is expected to generate about 9 GWh of electricity annually.

The Hywind mooring system consists of a three-point catenary spread with an angular spacing of 120°. The mooring lines are composed of a combination of chain and steel wire segments. A clump weight of 60 tons is attached to each mooring line. Each of the main mooring lines is split into two separate lines (forming a bridle) that are attached to the fairlead. This arrangement provides increased yaw stiffness.

The main characteristics of the Hywind pilot are collected in table 1-1.

Hywind Prototype Main Data	
WTG (Wind Turbine Generator)	2.3 MW
Turbine weight	138 tons
Nacelle height	65 m
Rotor diameter	82.4 m
Draft hull	100 m
Water depth	210 m
Displacement	5300 m^3
Diameter (Water Line)	6 m
Diameter (Submerged Body)	8.3 m
Rated wind speed	12 m/s
Mooring	3 lines
Pitch control	Dynamic

Table 1-1: Hywind prototype main data

Figure 1-1: Hywind prototype (Source: http://www.statoil.com)

2. System motions and forces

2.1 General

In this chapter, motions and forces associated with floating structures are briefly discussed. When appropriate, reference is made to the literature for further details.

It is assumed that we are dealing with a catenary moored vertical cylinder, similar to the Hywind pilot. The coordinate system for a segmented vertical column is defined in figure 2-1.

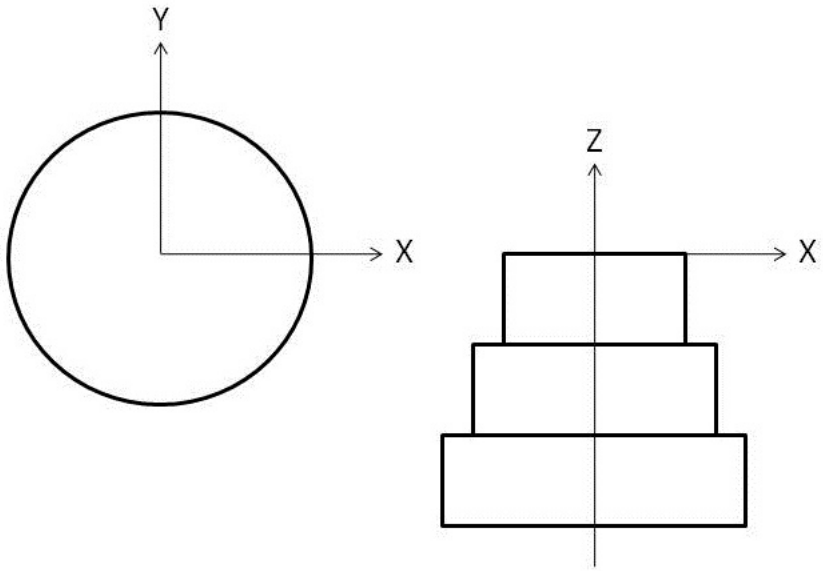

Figure 2-1: Definition of coordinate system

2.2 The equations of motions

For steady-state sinusoidal motions, Faltinsen (1990) showed that the equations of motions can be expressed as:

$$\sum_{k=1}^{6}[(M_{jk}+A_{jk})\ddot{\eta}+B_{jk}\dot{\eta}_k+C_{jk}\eta_k]=F_j e^{-i\omega_e t} \quad (j=1,...,6) \tag{2.1}$$

On the left side of the equation, the three terms represent the inertia, damping and restoring forces and moments respectively. On the right side, F_j are the complex amplitudes of the exciting forces and moment-components with the force and moment-components given by the real part of $F_j e^{-i\omega_e t}$.

For a structure with lateral symmetry (symmetry about the x-z-plane) the six coupled equations reduces to a set of two equations. We see that for the floating structure considered in figure 2-1, the motions in six degrees of freedom are described by two sets of three coupled equations; one set for surge, heave and pitch and one set for sway, roll and yaw. Hence, the lateral motions are uncoupled from the vertical and longitudinal motions.

In the following, the various terms of the equations of motions (2.1) are briefly discussed.

2.3 Mass matrix

The forces on a structure proportional to the acceleration are denoted inertia forces. These are composed of mass- and hydrodynamic forces and moments.

Keeping in mind that we are considering a structure with lateral symmetry, Nielsen (2007) showed that the mass matrix for vertical and longitudinal motions can be written as:

$$\mathbf{M} = \begin{pmatrix} M + A_{11} & 0 & Mz_G + A_{15} \\ 0 & M + A_{33} & 0 \\ Mz_G + A_{51} & 0 & I_{55} + Mz_G^2 + A_{55} \end{pmatrix} \tag{2.2}$$

Here M denotes the total mass of the system, A_{ij} are the hydrodynamic masses, z_G is the vertical position of the centre of gravity and I_{55} is the vertical moment of inertia about the centre of gravity. For a structure with no forward speed and no current present it can be shown that $A_{kj} = A_{jk}$, hence $A_{51} = A_{15}$.

2.4 Damping

Damping is the structures ability to dissipate energy and becomes very important in order to limit resonant motions of the structure.

For a floating wind turbine structure, Nielsen (2007) recognized the main contributions to the total damping as:

- Wave radiation damping
- Viscous damping on the submerged hull
- Viscous damping on the tower due to the relative wind velocity
- Damping due to the velocity dependent forces on the wind turbine

For a detailed description on how the various damping effects are found, reference is made to Nielsen (2007). Later in the report, it is outlined how the linear and quadratic damping levels can be estimated from motion decay tests.

2.5 Restoring matrix

The restoring forces will work to pull the structure back to its equilibrium position and consist of the stiffness forces proportional to the motion of the structure. For a freely floating structure the restoring forces will appear from hydrostatic and mass considerations, while for a moored structure, restoring forces from the mooring system have to be added. The total restoring matrix will therefore be:

$$\mathbf{C} = \mathbf{C}_H + \mathbf{C}_M \tag{2.3}$$

2.5.1 Hydrostatic

By considering the vertical and longitudinal motions, the hydrostatic contribution to the restoring matrix for a vertical column will be:

$$\mathbf{C}_H = \begin{pmatrix} 0 & 0 & 0 \\ 0 & \rho g \pi R_{WL}^2 & 0 \\ 0 & 0 & \rho g (I_{WL} + V z_B) - mgz_G \end{pmatrix} \tag{2.4}$$

where R_{WL} is the radius in the water line, V is the displaced volume of the column and $I_{WL} = \frac{\pi R_{WL}^4}{4}$ is the surface moment of inertia of the water line area.

2.5.2 Catenary

In general, the restoring matrix for a catenary mooring system will depend on the offset. Nielsen (2007) demonstrated how the restoring matrix for a mooring system could be calculated from the restoring matrices for the individual lines at a given offset level.

It is assumed that the line initially only will have restoring effects from motion in the catenary plane, i.e. an x-z-plane with the local x-axis parallel to the extension of the catenary. The only non-zero contributions to the line restoring matrix will therefore be $C_{11}^{(l)}, C_{13}^{(l)}, C_{31}^{(l)}, C_{33}^{(l)}$.

The catenary plane is rotated an angle θ relative to the floater coordinate system, where θ denotes the azimuth angle of the fairlead coordinates relative to the floater coordinate system.

By introducing the transformation matrix:

$$\boldsymbol{\gamma} = \begin{pmatrix} \cos(\theta) & \sin(\theta) & 0 \\ -\sin(\theta) & \cos(\theta) & 0 \\ 0 & 0 & 1 \end{pmatrix} \tag{2.5}$$

the restoring effect in a coordinate system parallel to the platform coordinates can be found as:

$$\mathbf{C}^{(0)} = \boldsymbol{\gamma}^T \mathbf{C}^{(l)} \boldsymbol{\gamma} \tag{2.6}$$

By using the line upper connection point (fairlead) coordinates $[X_T, Y_T, Z_T]$, the line's contribution to the restoring matrix for the mooring system will become:

$$\mathbf{C}_M = \begin{pmatrix} \mathbf{C}^{(0)}\boldsymbol{\alpha} & \mathbf{C}^{(0)} \\ \boldsymbol{\alpha}^T \mathbf{C}^{(0)} & \boldsymbol{\alpha}^T \mathbf{C}^{(0)} \boldsymbol{\alpha} \end{pmatrix} \tag{2.7}$$

where $\boldsymbol{\alpha}$ is given as:

$$\boldsymbol{\alpha} = \begin{pmatrix} 0 & Z_T & -Y_T \\ -Z_T & 0 & X_T \\ Y_T & -X_T & 0 \end{pmatrix} \tag{2.8}$$

Hence for a spread mooring system consisting of N_l lines, the main contributions to the 3dof (surge, heave and pitch) restoring matrix will be:

$$\begin{aligned} C_{M,11} &= \sum_{n=1}^{N_l} C_{11}^{(l)} \cos^2 \theta_n \\ C_{M,33} &= \sum_{n=1}^{N_l} C_{33}^{(l)} \\ C_{M,15} &= \sum_{n=1}^{N_l} C_{11}^{(l)} Z_T \cos^2 \theta_n \\ C_{M,55} &= \sum_{n=1}^{N_l} [C_{11}^{(l)} Z_T^2 + C_{33}^{(l)} r_M^2] \cos^2 \theta_n \end{aligned} \tag{2.9}$$

The superscript (l) refers to the line restoring coefficient C_{jk}; θ_n is the azimuth angle of line number n; Z_T is the vertical coordinate of the fairlead; and r_M is radius of mooring line attachments. For the three point equally spread mooring system utilized on the Hywind (see figure 1-1), equation (2.9) simplifies to:

$$\begin{aligned} C_{M,11} &= \frac{3}{2} C_{11}^{(l)} \\ C_{M,33} &= 3C_{33}^{(l)} \\ C_{M,15} &= \frac{3}{2} C_{11}^{(l)} Z_T \\ C_{M,55} &= \frac{3}{2} [C_{11}^{(l)} Z_T^2 + C_{33}^{(l)} r_M^2] \end{aligned} \tag{2.10}$$

One should note that only contributions to the restoring matrix from the catenary plane are included in the above derivation. These will form the main contributions, but restoring effects from out of plane motions will also be present. These effects will form the yaw stiffness of the mooring system, which is briefly discussed in Chapter 8. For further details on how the yaw restoring coefficients are derived, reference is made to Nielsen (2007).

2.6 Excitation forces and moments

The excitation forces and moments are added to the right side of the equations of motions (2.1). The external forces on the structure are typically environmental loads and may be composed of wave forces, current forces and wind forces.

2.6.1 Wave forces

By using linear theory, the wave elevation can be described as a sum of individual sinusoidal wave components. From Faltinsen (1990) we have that for N waves, the total wave elevation for a long-crested wave propagating along the positive x-axis can be expressed as:

$$\zeta = \sum_{j=1}^{N} A_j \sin(\omega_j t - k_j x + \varepsilon_j) \tag{2.11}$$

where subscript j denotes wave number j, A is the wave amplitude, ω, k and ε are the circular frequency, wave number and random phase angle respectively.

Furthermore, the relationship between the wave amplitude and wave spectrum is given as:

$$\frac{1}{2} A_j^2 = S(\omega_j)\Delta\omega \tag{2.12}$$

where $S(\omega_j)$ is the spectral density for wave component j, and $\Delta\omega$ is a constant difference between successive frequencies. By considering a wide range of frequencies, the wave spectrum will indicate which frequencies that are contributing to the total energy in the sea state.

A JONSWAP wave spectrum is typically used for describing North Sea sea states.

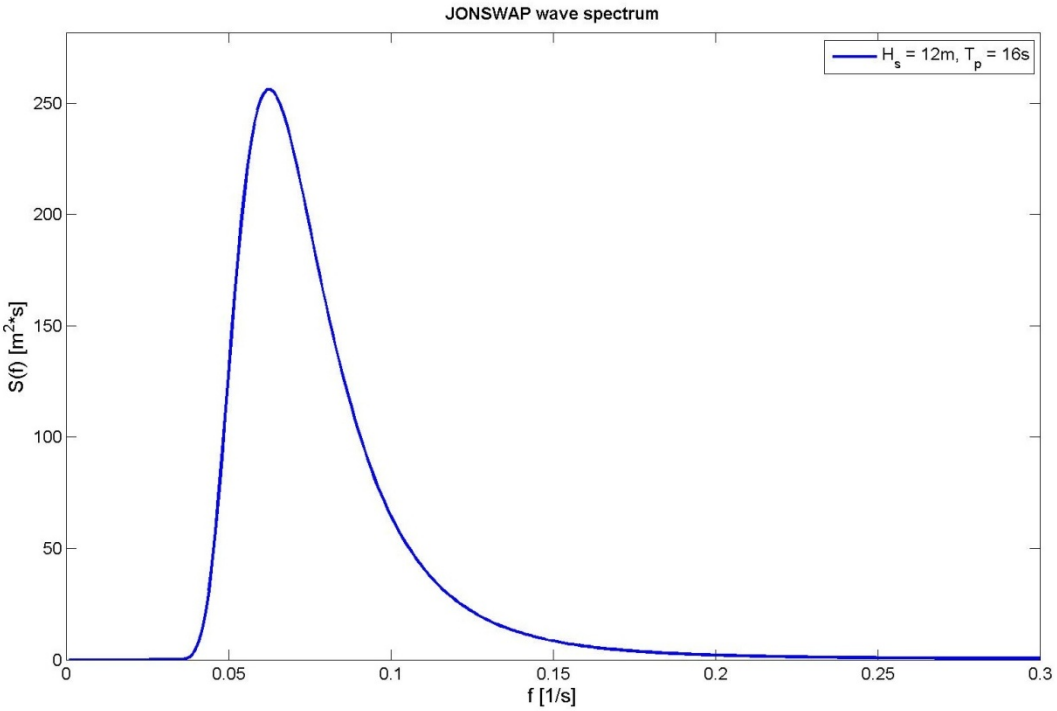

Figure 2-2: JONSWAP wave spectrum
H_S = 12m, T_P = 16s

Furthermore, a description on how linear and second-order wave forces are obtained is included in the following. A short summary is reproduced here, while reference is made to Faltinsen (1990) for further details.

By solving the linear problem, i.e. satisfying the free-surface and body boundary condition on the mean position of the free-surface and submerged hull, first-order wave forces on the structure are obtained. These forces will induce first-order motions known as wave-frequency (WF) motions. However, in order to capture motions in severe sea states and for moored structures, the problem has to be solved to the second order. This implies accounting for the zero-normal flow condition through the body at the instantaneous position of the body. The solution of the second-order problem will result in mean forces and forces oscillating with the sum and difference frequency in addition to the linear solution. The steady component is known as mean wave-drift forces, while the oscillating component may act together with environmental forces to induce low-frequency (LF) motions.

For a catenary moored structure, mean and slowly-varying wave forces (difference frequency forces) are of importance. For a lightly damped moored structure, slow-drift resonant motions occur in surge, sway and yaw.

2.6.2 Current forces

The current velocity is assumed to be constant with time, and is described by the speed and direction. For a cylinder with current perpendicular to the cylinder axis, vortices will be shed on alternating sides, giving rise to drag and lift force on the cylinder. When the vortex-shedding frequency is close to the natural frequency of the cylinder, large vibrations may occur in both cross-flow and in-line direction. These vibrations are recognized as vortex-induced vibrations (VIV). When the two frequencies coincide, the vortex-shedding frequency locks on to the natural frequency of the cylinder and large resonant motions may occur. The phenomenon is known as lock-in, which in addition to increased motion amplitudes will cause increased in-line drag forces due to a larger effective drag area.

2.6.3 Wind forces

The wind speed is typically composed of a rapidly fluctuating gust wind superimposed onto the slowly-varying mean wind speed. Haver (2010) expressed the total wind speed at time instant t as:

$$V(t) = V_m(t) + V_t(t) \tag{2.13}$$

where $V_m(t)$ is the mean wind speed and $V_t(t)$ is the turbulent (gust) wind speed at time instant t. The mean wind force will give rise to a steady-state wind force; while for a moored structure, the gust wind may excite resonant slow-drift motions of the structure.

A Kaimal wind spectrum is recommended used for representing the spectral density of the wind process (DNV-OS-J101), and is shown in figure 2-3.

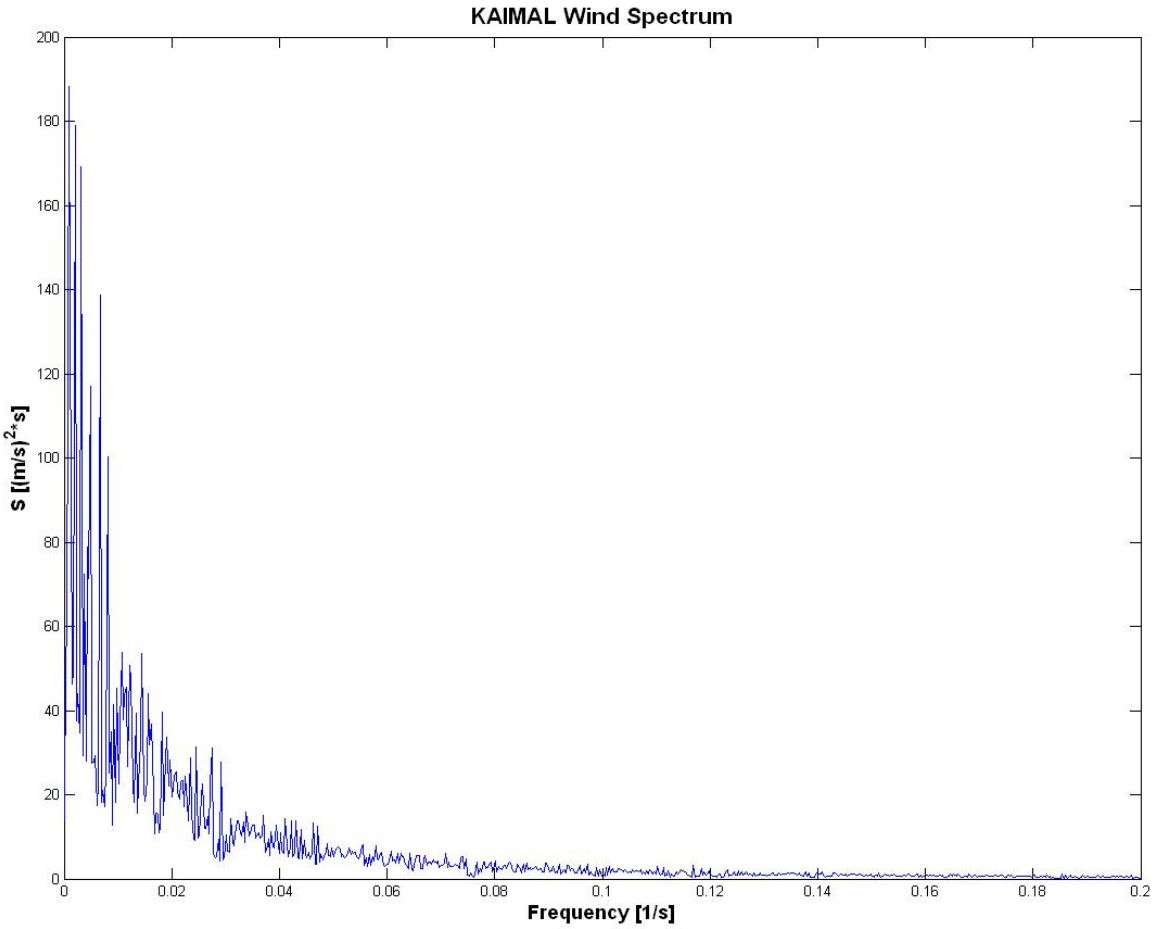

Figure 2-3: Kaimal wind spectrum
U_m = 12m/s, T_I = 0.1, λ=42

2.7 A discussion on natural periods

2.7.1 General

As the mass and stiffness matrices are found for vertical and longitudinal motions, the natural periods can be obtained for the same motion modes.

Faltinsen (1990) expresses the natural period for degree of freedom i as:

$$T_{ni} = 2\pi \left(\frac{M_{ii} + A_{ii}}{C_{ii}} \right)^{\frac{1}{2}} \tag{2.14}$$

Remembering that we defined $\mathbf{M}$ as the total mass, including the hydrodynamic mass; by using a strip theory approach to obtain the added mass, the natural period in surge is written as:

$$T_{n1} = 2\pi \left(\frac{M_{11}}{C_{11}} \right)^{\frac{1}{2}} = 2\pi \left(\frac{M + A_{11}}{C_{M,11}} \right)^{\frac{1}{2}} = 2\pi \left(\frac{2\rho_w V}{C_{M,11}} \right)^{\frac{1}{2}} \tag{2.15}$$

where ρ_w is the water density and V is the displaced volume. Since there is no hydrostatic stiffness contribution in surge, only the mooring line stiffness will contribute to the stiffness matrix.

In heave, we get:

$$T_{n3} = 2\pi\left(\frac{M_{33}}{C_{33}}\right)^{\frac{1}{2}} = 2\pi\left(\frac{M + A_{33}}{C_{H,33} + C_{M,33}}\right)^{\frac{1}{2}} \approx 2\pi\left(\frac{M + A_{33}}{\rho g \pi R_{wl}^2}\right)^{\frac{1}{2}} \tag{2.16}$$

Since the mooring line contribution to the heave stiffness is minimal compared to the hydrostatic contribution, it can be neglected. The vertical added mass will be very small compared to the mass and may also be neglected. We see that the natural period in heave is strongly dependent on the waterplane area.

By considering a reference point close to the vertical COG and assuming $\rho_w V = mg$, the natural period in pitch becomes:

$$T_{n5} = 2\pi\left(\frac{M_{55}}{C_{55}}\right)^{\frac{1}{2}} = 2\pi\left(\frac{I_{55} + A_{55}}{C_{H,55} + C_{M,55}}\right)^{\frac{1}{2}} \approx 2\pi\left(\frac{I_{55} + A_{55}}{C_{H,55}}\right)^{\frac{1}{2}} \approx 2\pi\left(\frac{I_{55} + A_{55}}{\rho V g (z_B - z_G)}\right)^{\frac{1}{2}} \tag{2.17}$$

where z_B and z_G is the vertical position of the centre of buoyancy and gravity respectively. The mooring system effect on the pitch restoring coefficient is neglected.

Typically, for moored structures, the natural period in surge is in order of minutes. For heave and pitch it is usually required that the natural periods are larger than $T = 20s$, above most wave periods in open sea (4-20s).

2.7.2 Mathieu instability

According to Nielsen (2007), the Mathieu instability is related to a time dependent restoring term in the equation of motion and is a well-known dynamic phenomenon for spar platforms.

For the coupled heave-, pitch motions, instabilities can occur when the pitch natural period is close to the heave natural period or twice the heave natural period.

Haslum (2000) showed another effect that may cause Mathieu effects. For a certain wave period, denoted $T_{wave,cr}$, the combined action of wave induced heave and resonant heave may excite pitch resonance. The critical wave period is given as:

$$T_{wave,cr} = \frac{1}{\frac{1}{T_{n5}} + \frac{1}{T_{n3}}} \tag{2.18}$$

3. Catenary mooring systems

3.1 General

As seen in the previous chapter, the mooring system contributes to providing restoring forces and moments on a floating structure, pulling the structure back against its equilibrium position. A wide selection of mooring systems are applied in the offshore industry; ranging from tension leg moorings, with small horizontal offsets and large vertical forces on the anchors, to catenary moorings, with larger horizontal offsets and no vertical forces on the anchors. In the present study, only catenary mooring systems are considered.

A catenary mooring system may be composed of one or several individual lines connected to the floating structure at the fairlead and the sea bottom at the anchors. The suspended part of each line will form a catenary, where the shape is dependent on the weight of the line in addition to the horizontal and vertical distance between the fairlead and anchor. The line arrives at the sea bottom horizontally, so that the anchor is only subjected to horizontal forces. The initial horizontal holding capacity, often referred to as the pretension, is dependent on the horizontal distance between the fairlead and the anchor. The restoring forces are provided by the weight of the line. Hence the major contribution to the stiffness matrix from the mooring system comes from the geometric stiffness of the line, i.e. stiffness due to the change of geometry of the catenary.

As the top end point of the mooring line is moved, the initial configuration of the mooring line is modified; and assuming that part of the line is resting on the sea bottom, the new position is determined by the geometric stiffness of the line. The restoring force from the mooring system will be non-linear as the catenary configuration of the mooring lines and the existence of the sag introduce geometric non-linearity (Loukogeorgaki et al. 2005). In chapter 6, it is shown how the restoring forces from each mooring line can be calculated.

Typically, the mooring lines are segmented in order to optimise the force/displacement characteristics known as the mooring line characteristics. In addition to anchors and connectors, the lines may be composed of chains, wire ropes and synthetic fiber ropes. For details regarding the different mooring components, reference is made to Hordvik (2010).

In this report, three different concepts based on catenary moorings are considered. They are presented in the following.

3.2 Distributed mass mooring system

For the distributed mass mooring system, the restoring stiffness is obtained by applying mooring line segments with large submerged weight. Typically, large diameter chains are used as they have significantly larger self-weight than wire and synthetic fiber ropes. The bottom chain can either have the same weight as the rest of the line, or larger weight for increased geometric stiffness. This mooring system concept is widely used for stationkeeping of offshore applications.

3.3 Clump weight mooring system

For the clump weight mooring system, the restoring force is mainly provided by attaching a large mass clump weight to the mooring lines. The clump weight will increase the vertical component and the total tension in the line. The stiffness of the system increases accordingly providing more restoring forces.

Luo (1992) argues that the clump weights should be installed near the line's touchdown point, causing increased stiffness and a steeper tension excursion curve as the weight is lifted off from the sea bottom. The stage when the clump weight is lifted off the bottom is referred to as the effective stage, and may be tuned to optimise the mooring characteristics. Nielsen (2011) however claims that in conventional mooring designs involving clump weights, the weights are installed so that they will not touch the sea bottom during normal operation. This reduces the risk of the clump weights digging into the soil, causing large, uncontrollable forces and overshoot in the anchor lines as they are lifted off. The restoring force is then merely provided by the line configuration.

3.4 Buoyancy element mooring system

The buoyancy element mooring system has a buoyancy element attached to the mooring lines, creating an upward force. This results in a virtual displacement of the top end point, so that the main contribution to the restoring forces is provided by the suspended part of the mooring lines below the buoyancy element. Such a layout is especially attractive for deep water applications, to limit the mooring line dynamics. As for the other concepts, combination of chain and wire segments may be used.

All three concepts are illustrated in figure 3-1.

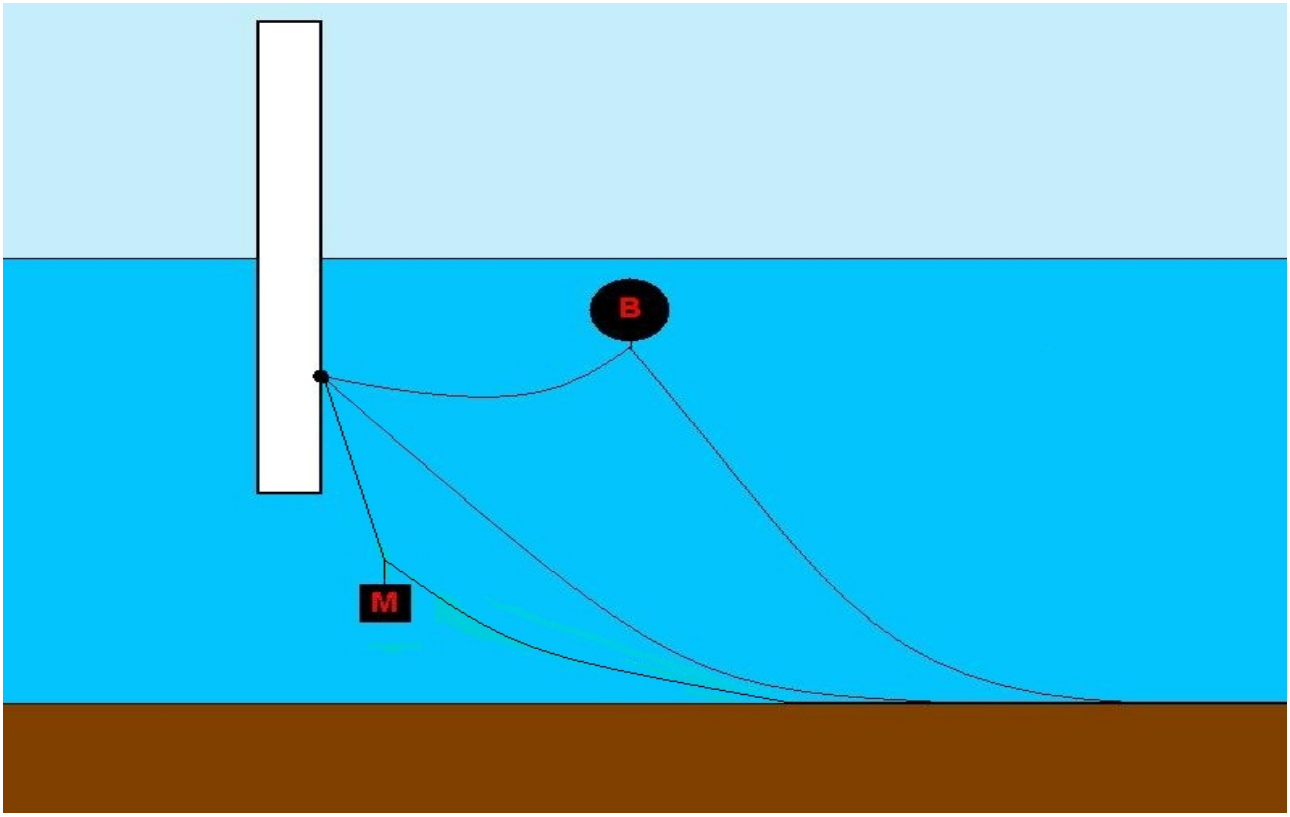

Figure 3-1: Mooring system concepts
From left to right: Clump weight-, distributed mass- and buoyancy element mooring system

4. Analysis software

In order to investigate the performance of the different mooring system concepts, various computer programs dedicated to analysis of marine structures are applied. In the following, these computer programs are presented.

4.1 SIMO

According to the user manual, SIMO (Simulation of Marine Operations) is a time domain simulation program for study of motions and stationkeeping of multibody systems. The program is typically applied for time domain simulation of surface vessels and for simulation of complex marine operations. The results are presented as time series, statistics and spectral analysis of all forces and motions of the bodies in the analysed system. SIMO is interactive and modular, i.e. the results from one module becomes the input for the next module.

In the present study, SIMO is used for environmental modelling (waves and current) and for its ability to include wind forces from an external force subroutine (TDHMILL3D) linked into the program.

Waves can be modelled by regular waves and by various model spectra for irregular waves. The current speed and direction is assumed to be constant with time. However it can vary with depth by specifying a current profile.

4.2 TDHMILL3D

TDHMILL3D is, according to the User Documentation, a simplified computer tool developed by MARINTEK for analysis of floating wind power facilities. The code is a numerical model of thrust from a wind turbine rotor onto the nacelle, and consists of coefficients for thrust (force in axial direction of the rotor axis) tabulated as a function of relative velocity between the rotor and the wind. Gyro-moments from the rotor when it is rotating about an axis in the rotor plane are also included.

The wind speed at hub height can be specified by the user directly as a time series, or by specifying a dynamic wind spectrum and let the program generate an irregular wind speed time series. The Kaimal wind spectrum (see figure 2-3) is used for generating irregular wind speed time series.

The thrust force from the rotor onto the rotor axis at time t is calculated from the wind speed time series and loaded by SIMO at runtime through a DLL (Dynamic Linked Library).

By using a built-in notch filter tuned to the pitch natural period of the system, the user can choose to include the control system in a very simplistic way. A notch filter is designed such as to remove the contribution from a certain frequency band of a given signal.

4.3 Riflex

Originally, according to the user manual, Riflex is a finite element program developed as a tool for analysing flexible marine riser systems. However the program can also be used for analysing other types of slender marine structures (e.g. mooring lines and umbilicals). The program features an extremely efficient and robust non-linear time domain formulation applicable for irregular wave analysis; and high flexibility in modelling, enabling analysis for a wide range of structures. The hydrodynamic loading is described by the generalized Morison’s equation.

4.4 Integrated analysis

By coupling the computer programs described above together, one can take advantage of the features characterizing each program and combine them. SIMO, for instance, models all structures as rigid bodies, i.e. internal forces are not captured. The complete structure (including the mooring system) is therefore modelled in Riflex, allowing for flexible modelling. SIMO does however as mentioned, offer the option of including an external force through a DLL, in addition to excellent modelling of waves and current. SIMO in combination with TDHMILL3D is therefore used for environmental modelling (wind, waves and current).

The combined SIMO-Riflex simulation is widely used to simulate floating offshore structures. In order to couple the programs together, the different modules of the programs must be run in a specific order:

1. Riflex inpmod
2. SIMO stamod
3. Riflex stamod
4. SIMO dynmod
5. Riflex dynmod

Of course additional modules for postprocessing (e.g. s2xmod and outmod) may be added subsequently. For details regarding the different modules of the program, reference is made to the respective user manuals.

5. Analysis models

5.1 General

The models used in this study are based on an early phase Hywind design with a steel tower and a concrete substructure.

The original model was used by Furunes (2010). As the study is focusing on the mooring system design and not the structural design of the support structure, this tower model is conveniently used as a starting point. All structural properties remain unchanged, while major adjustments have been made with respect to the heading of the mooring lines. Furthermore, the water depth is modified, and the mooring system is adjusted to reproduce the three concepts described in Chapter 3. The model applied for shallow water ($100m$) analysis is henceforth referred to as the test model. In the following the test model will be reviewed.

5.2 Finite element model

Figure 5-1 shows the finite element model and coordinate system for the test model. SN i refers to supernode i, while the bracket numbers refers to the Riflex line numbers. The main mooring lines and delta-lines are named Anch.line 1-3 and DL 1-6 respectively.

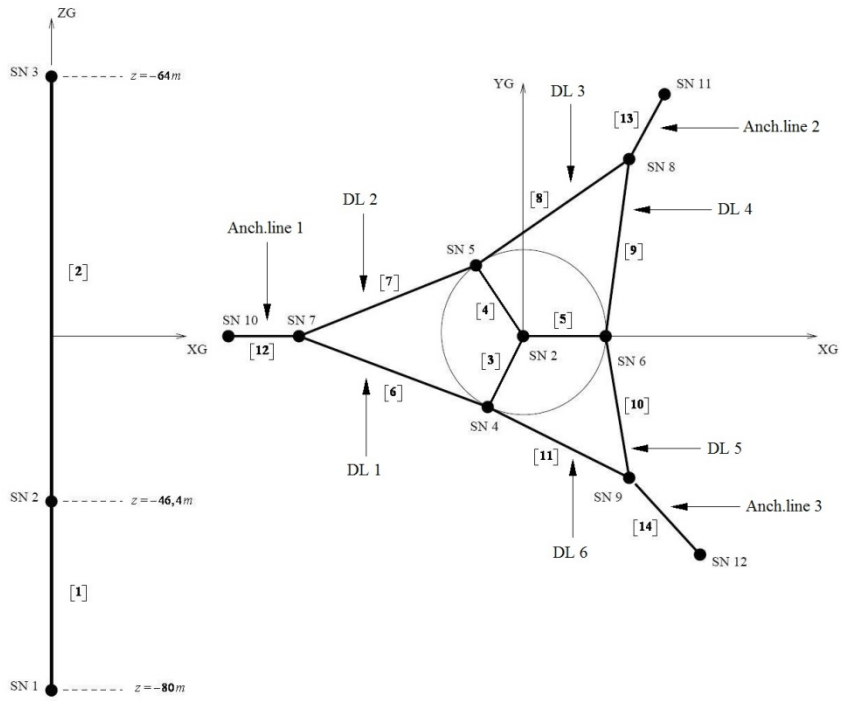

Figure 5-1: Test model, finite element model

We see that the system topology is defined in terms of branching points and terminal points called supernodes. Lines are defined between the supernodes, and subsequently split into segments consisting of equally sized elements. The element mesh is automatically computed based on the topology, line and component description. SN 1, which is the tower bottom, is fixed; while the anchornodes (SN 10 – 12) are given prescribed displacements. All other supernodes are free, i.e. nodal position and rotations are unknown prior to the analysis. SN 3, which is located at the top of the tower, is connected to a

mass free SIMO body through a floater force model, accounting for the thrust force from the wind. The substructure has a draft of 80m, and the water depth is set to 100m.

5.3 Tower structure

All the elements in the tower structure are modelled as 3D beam elements with an axi-symmetric cross section and constant axial-, bending-, and torsional stiffness. The beam element formulation uses a co-rotated ghost reference description, with three translational and three rotational degrees of freedom at each node. For further details regarding the beam theory, reference is made to the Riflex theory manual.

The tower structure layout, including section levels, diameter and weight is shown in figure 5-2.

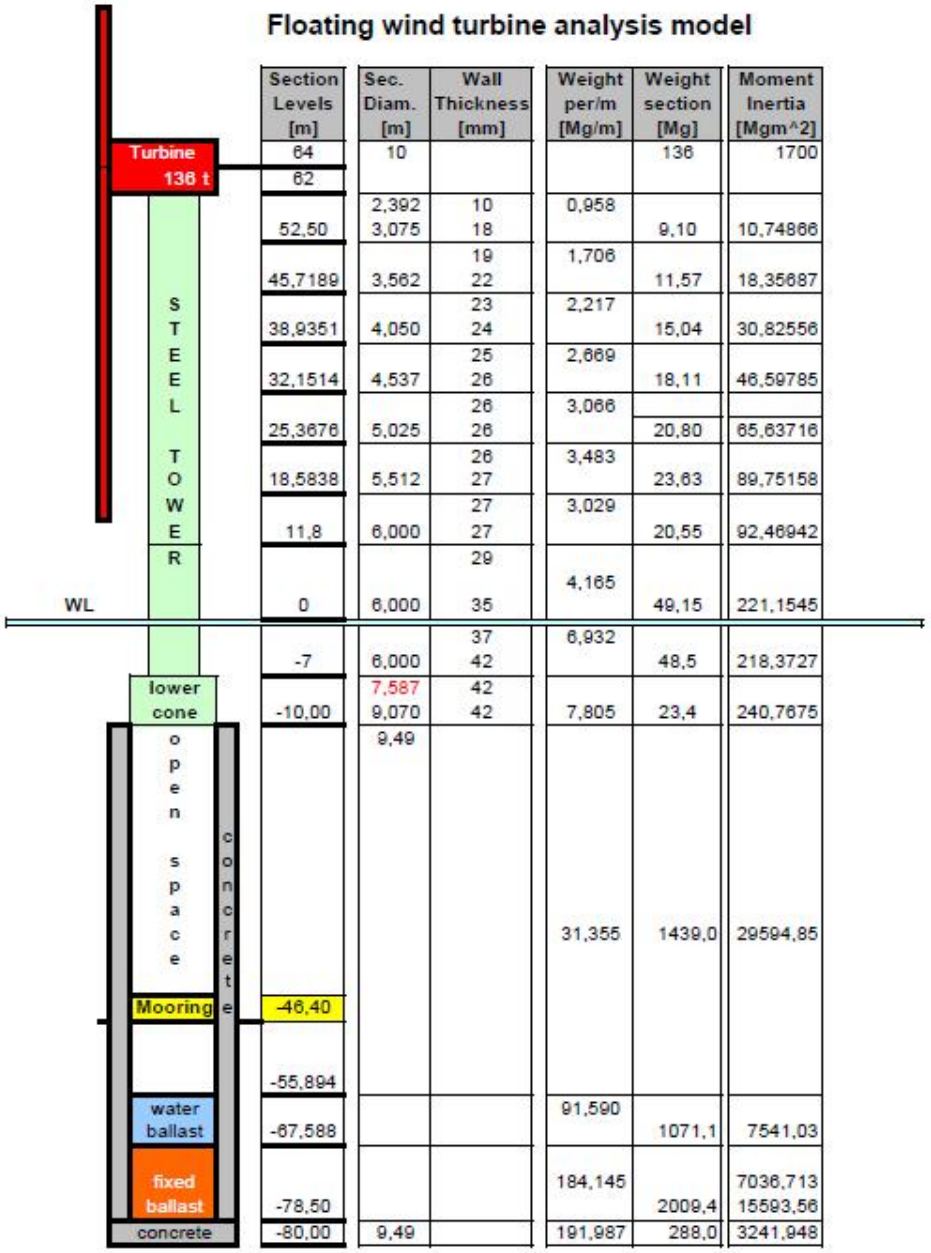

Section Levels [m]	Sec. Diam. [m]	Wall Thickness [mm]	Weight per/m [Mg/m]	Weight section [Mg]	Moment Inertia [Mgm^2]
64	10			136	1700
62					
	2,392	10	0,958		
52,50	3,075	18		9,10	10,74866
		19	1,706		
45,7189	3,562	22		11,57	18,35687
		23	2,217		
38,9351	4,050	24		15,04	30,82556
		25	2,669		
32,1514	4,537	26		18,11	46,59785
		26	3,066		
25,3676	5,025	26		20,80	65,63716
		26	3,483		
18,5838	5,512	27		23,63	89,75158
		27	3,029		
11,8	6,000	27		20,55	92,46942
		29	4,165		
0	6,000	35		49,15	221,1545
		37	6,932		
-7	6,000	42		48,5	218,3727
	7,587	42			
-10,00	9,070	42	7,805	23,4	240,7675
	9,49				
			31,355	1439,0	29594,85
-46,40					
-55,894					
			91,590		
-67,588				1071,1	7541,03
			184,145		7036,713
-78,50				2009,4	15593,56
-80,00	9,49		191,987	288,0	3241,948

Figure 5-2: Test model, tower structure
Source: Furunes (2010)

5.4 Mooring system

The mooring system is represented by 3D bar elements, specified with axial stiffness only. The bar element is described in a total Lagrangian formulation, and adjusted to a formulation based on integrated cross-section forces and small strain theory.

The three-point lateral symmetric mooring system is laid out with an angular spacing of 120^{o}. Each mooring line is attached to the tower structure at the fairlead. Two lines are connected to each fairlead point so that the upper part of each mooring line forms a bridle. These upper line segments are denoted delta-lines. In the original model, the water depth is 220m and the length of each delta-line is 50m. For the test model, the water depth is reduced to 100m. The length of each delta-line is accordingly reduced to 40m in order to have adequately vertical distance between the sea bottom and the delta-line connection points. A single line is extending from the delta-lines to the anchor. The anchornodes are given a prescribed displacement in order to obtain the desired pretension. The length of the delta-lines is further assessed in Chapter 8.

The modelling of the different mooring system concepts is reviewed in the following. The layout described here is merely used for comparing the concepts, i.e. segment lengths and weights are not optimised. The total line length is for simplicity equal for all three mooring system concepts and is set to 513 m.

The delta-lines consist of only one segment, while the main mooring lines are composed of 7 segments each. Table 5-1 shows segment lengths and total weight for the three different mooring system concepts considered.

Distributed mass mooring system		**Clump weight mooring system**		**Buoyancy element mooring system**	
Segement type	Segment length [m]	Segement type	Segment length [m]	Segement type	Segment length [m]
Chain (delta-line)	40,00	Chain (delta-line)	40,00	Chain (delta-line)	40,00
Chain	70,00	Chain	5,00	Chain	5,00
Chain	70,00	Wire	25,02	Wire	76,02
Chain	70,00	Chain	5,00	Chain	5,00
Chain	70,00	Clump weight	1,00	Buoyancy element	1,00
Chain	40,00	Chain	5,00	Chain	5,00
Chain	53,04	Wire	332,02	Wire	281,02
Chain	100,00	Chain	100,00	Chain	100,00
Total length [m]	513,04		513,04		513,04
Total submerged weight [kN]	676,03		527,03		120,12

Table 5-1: Segment lengths

5.4.1 Distributed mass mooring system

For the distributed mass mooring system, all segments are composed of chain. The layout is shown in figure 5-3, while the main parameters describing the chain modelling is given in table 5-2.

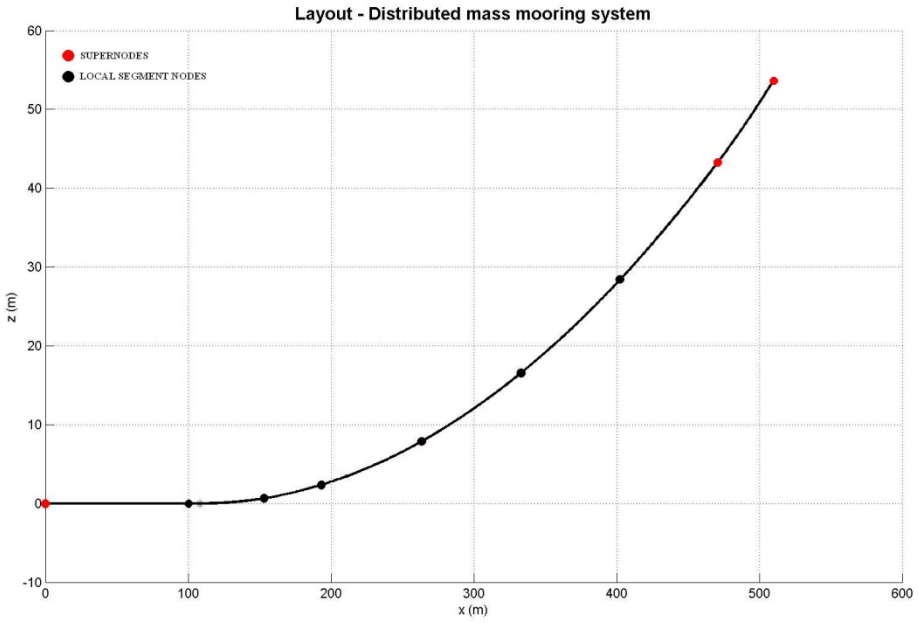

Figure 5-3: Layout, distributed mass mooring system

Segment type	Mass/unit length [t/m]	External C-S area [m^2]	Axial stiffness [kN]	Hydrodynamic diameter [m]
Chain	0,1545	0,0197	7,09 E+5	0,1583

Table 5-2: Segment properties, distributed mass mooring system

5.4.2 Clump weight mooring system

In addition to the clump weight, the clump weight mooring system is composed of a combination of chain and steel wire segments in order to introduce more elasticity and ease the handling. Chains are used for the delta-lines and for connecting different segments together. The mooring system layout and main segment properties are shown in figure 5-4 and table 5-3 respectively.

The clump weight is modelled as an axi-symmetrical line segment, i.e. a cylinder. The clump weight properties are shown in table 5-4.

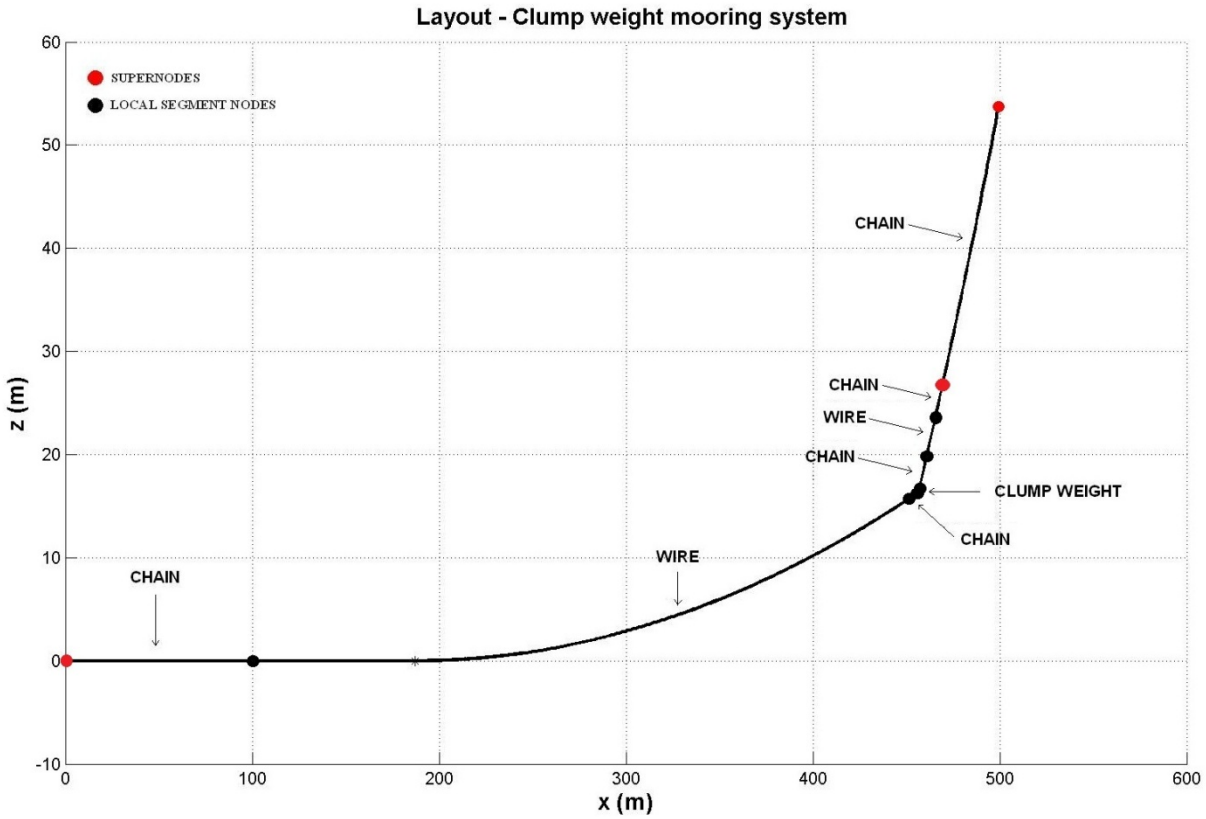

Figure 5-4: Layout, clump weight mooring system

Segment type	Mass/unit length [t/m]	External C-S area [m^2]	Axial stiffness [kN]	Hydrodynamic diameter [m]
Chain	0,1545	0,0197	7,09 E+5	0,1583
Wire	0,0379	0,0057	3,43 E+5	0,0850
Clump Weight	24,66	3,14	6,28 E+9	2,0

Table 5-3: Segment properties, clump weight mooring system

Material	STEEL
Density [kg/m^3]	7850
Young's modulus [N/m^2]	2,0 E+11
Diameter [m]	2,0
Thickness [m]	2,0
Length [m]	1,0
Volume [m^3]	3,14
Mass [kg/m]	24662
Area moment of inertia [m^4]	0,8836
Gyration radius [m]	0,53
Buoyancy force [kN]	31,59
Gravity force [kN]	241,9
Net force (positive upwards) [kN]	-210,34
Weight in water [kN/m]	210,34

Table 5-4: Clump weight properties

5.4.3 Buoyancy element mooring system

The buoyancy element mooring system is composed of a combination of chain and wire segments in addition to the buoyancy element. The mooring system layout and main segment properties are shown in figure 5-5 and table 5-5 respectively.

As for the clump weight, the buoyancy element is modelled as a line segment with axi-symmetrical cross-section. The buoyancy element modelling is based on the properties given in table 5-6.

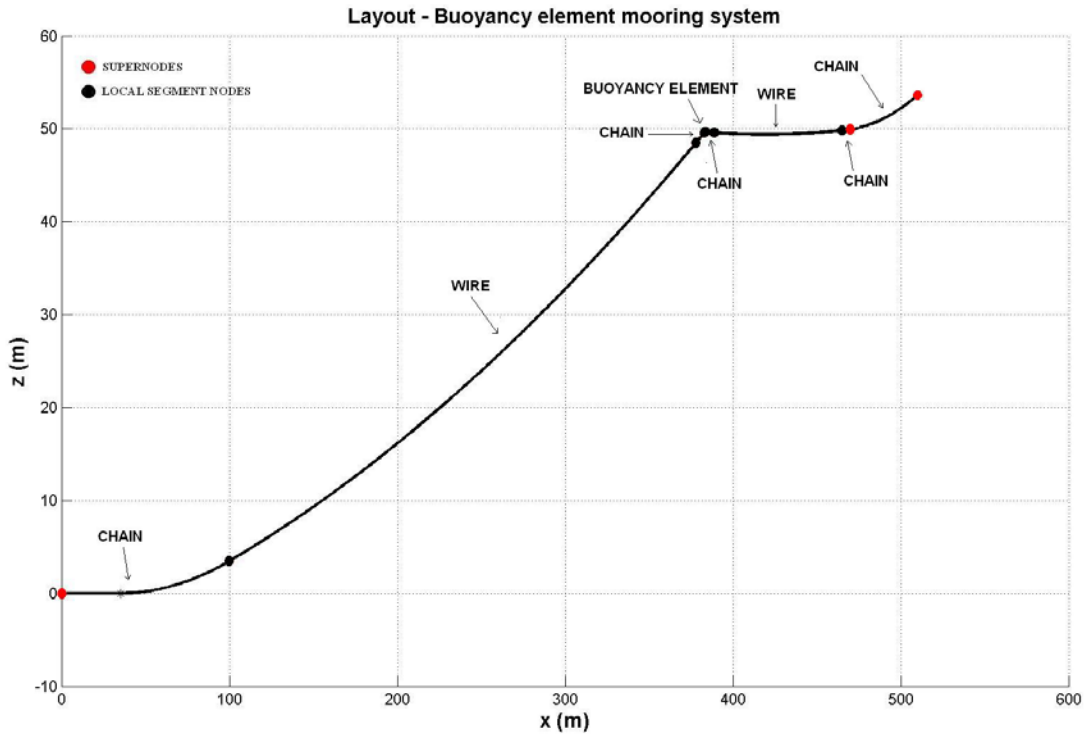

Figure 5-5: Layout, buoyancy element mooring system

Segment type	Mass/unit length [t/m]	External C-S area [m^2]	Axial stiffness [kN]	Hydrodynamic diameter [m]
Chain	0,1545	0,0197	7,09 E+5	0,1583
Wire	0,0379	0,0057	3,43 E+5	0,0850
Buoyancy element	19,41	38,48	1,10 E+9	7,0

Table 5-5: Segment properties, buoyancy element mooring system

Material	STEEL
Density [kg/m^3]	7850
Young's modulus [N/m^2]	2,0 E+11
Diameter [m]	7,0
Thickness [m]	0,025
Length [m]	1,0
Volume buoy [m^3]	38,48
Volume steel [m^3]	2,47
Mass [kg/m]	19406
Equivalent density buoy [kg/m^3]	504
Area moment of inertia [m^4]	117,5
Gyration radius [m]	1,75
Buoyancy force [kN]	387
Gravity force [kN]	190
Net force (positive upwards) [kN]	196,6
Weight in water [kN/m]	-196,6

Table 5-6: Buoyancy element properties

6. Analysis methods

In the following, the theoretical basis underlying the analysis methods used in the study are described.

6.1 Catenary analysis

In Chapter 2, it was shown how the catenary contribution to the total stiffness matrix was obtained from the single line stiffness matrix. In this section it is shown how the single line stiffness matrix is obtained.

Nielsen (2007) demonstrated a stepwise procedure for how the restoring coefficients in surge and heave may be calculated:

- Assuming that the horizontal position of the upper mooring line end is known, a small perturbation of the horizontal force is made.
- The corresponding variation in end point coordinates and vertical force are found and denoted Δx_1, Δz_1 and ΔH_1, ΔV_1 respectively.
- A similar perturbation is made for the depth, and the end point coordinates and vertical force are respectively denoted Δx_2, Δz_2 and ΔH_2, ΔV_2.
- The stiffness components are then found as:

$$\begin{aligned} C_{11}^{(l)} &= \frac{\partial H}{\partial x} \\ C_{13}^{(l)} &= \frac{\partial H}{\partial z} \\ C_{31}^{(l)} &= \frac{\partial V}{\partial x} \\ C_{33}^{(l)} &= \frac{\partial V}{\partial z} \end{aligned} \tag{6.1}$$

The restoring force can be written on matrix and compact form as:

$$\begin{pmatrix} \Delta x_1 & \Delta z_1 & 0 & 0 \\ \Delta x_2 & \Delta z_2 & 0 & 0 \\ 0 & 0 & \Delta x_1 & \Delta z_1 \\ 0 & 0 & \Delta x_2 & \Delta z_2 \end{pmatrix} \begin{pmatrix} \frac{\partial H}{\partial x} \\ \frac{\partial H}{\partial z} \\ \frac{\partial V}{\partial x} \\ \frac{\partial V}{\partial z} \end{pmatrix} = \begin{pmatrix} \Delta H_1 \\ \Delta H_2 \\ \Delta V_1 \\ \Delta V_2 \end{pmatrix} \tag{6.2}$$

$$\mathbf{Ax} = \Delta\mathbf{F} \tag{6.3}$$

And the restoring force coefficients on compact form are found as:

$$\mathbf{x} = \mathbf{A}^{-1}\Delta\mathbf{F} \tag{6.4}$$

Each mooring line will be subjected to direct action of waves and current, but the principal loads are the forces transmitted by the moored structure. By assuming a horizontal sea bed, and neglecting bending stiffness, dynamic effects in the line and current forces, the x- and z-coordinates can therefore be found quasi-statically for a range of horizontal force levels by applying the catenary equations. In cases with high tension in the line, stretching becomes important. The effect of axial elasticity can be included to form the elastic catenary equations as shown by Triantafyllou (1990). Elasticity effects are accounted for in the present study. The equations are derived in Appendix A.

A Matlab routine (Nielsen, 2004) for computing mooring line geometry and restoring characteristics for multi-segment mooring lines has been modified and adapted to quasi-static analysis of the mooring system concepts presented in this study. The mooring lines are modelled as continuous lines, not accounting for the stiffness effect of the delta-lines. The weight of the upper segment is therefore adjusted according to the weight of the delta-lines. Quasi-static analysis is very convenient in the initial design phase due to the minimal computational effort required.

6.2 Eigenvalue analysis

Finding the natural frequencies of an inclined catenary is not straight forward as the static quantities are varying in space. By modelling a single mooring line in Riflex, the lines' eigenfrequencies and eigenvectors can be found by using the built-in eigenvalue analysis option. Lancros' method for solution of eigenvalue problems is utilized.

6.3 Motion decay test

6.3.1 General

A motion decay test, often called a free oscillation test, is carried out by giving the system an initial displacement and then leaving the system free to oscillate. After the system is released, and by assuming linear damping, the motion in the degree of freedom regarded can be described by:

$$M\ddot{x} + B\dot{x} + kx = 0 \tag{6.5}$$

where M is the structural and added mass of the system, B is the linear damping coefficient and k is the stiffness coefficient. x, $\dot{x}$ and $\ddot{x}$ are the translation/rotation, velocity and acceleration of the system respectively.

By using the dynamic nodal forces option in Riflex, a motion decay test can be simulated by applying a ramp force/moment to the COG of the structure in the desired degree of freedom. When the ramp force is switched off, the system is released and free to oscillate. Natural periods and damping levels can be found from the decay test, and the respective procedures are reviewed in the following.

6.3.2 Natural periods

The natural periods may be obtained from the decay time series by measuring the time difference between two consecutive peaks. Another method, which is utilized here, is to apply a Fast Fourier Transform (FFT) on the time series. The natural period is then taken as the period corresponding to the frequency level containing the most energy in the power spectrum.

6.3.3 Damping

By assuming quadratic damping, the damping term of equation (6.5) becomes:

$$F_D(\dot{x}) = B_1\dot{x} + B_2\dot{x}\,|\,\dot{x}\,| \tag{6.6}$$

We see that the damping force is split into two contributions, where the first term represents the linear damping force proportional to the velocity, while the second term represents the quadratic damping force proportional to the velocity squared.

The linear damping term includes hydrodynamic damping from wave generation in addition to structural damping, while the quadratic damping term includes the eddy-making damping or drag damping.

By dividing both sides of (6.5) with M and insert (6.6), we get:

$$\ddot{x} + b_1\dot{x} + b_2\dot{x}\,|\,\dot{x}\,| + b_3 x = 0 \tag{6.7}$$

where b_1, b_2 and b_3 are the linear and quadratic damping coefficients and the stiffness coefficient divided by M respectively.

Nielsen (2007) showed that equation (6.7) can be linearized by introducing an equivalent damping coefficient b_e:

$$\ddot{x} + b_e\dot{x} + b_3 x = 0 \tag{6.8}$$

For a motion decay signal with n cycles, the equivalent linearized damping can be expressed as:

$$b_e = b_1 + K_L^* b_2 = b_1 + \frac{16}{3}\frac{x_n}{T_n} b_2 \tag{6.9}$$

where x_n and T_n are the motion amplitude and period for cycle n respectively, and K_L^* is the linearization coefficient. The linearization coefficient is found by using the value that will minimize the error (Larsen 2010).

The equivalent linear damping may be estimated within each half cycle of the decay signal by using the logarithmic decrement. By considering two consecutive peaks in the motion decay signal, as shown in figure 6-1, we can define the logarithmic decrement as:

$$\delta = \ln\left|\frac{x_n}{x_{n+1}}\right| \tag{6.10}$$

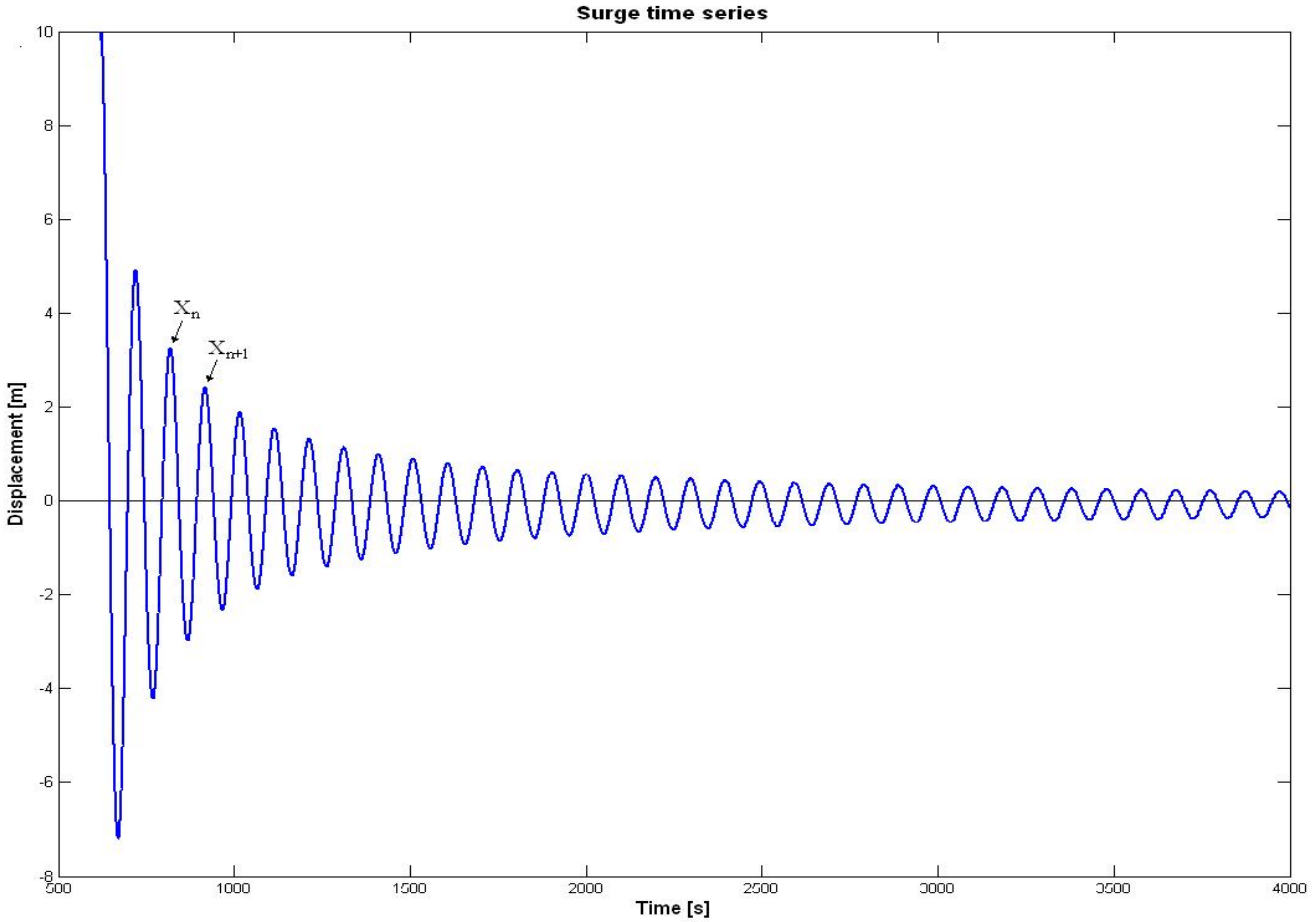

Figure 6-1: Motion decay signal

Furthermore we introduce the relative damping, which can be expressed as a function of the logarithmic decrement:

$$\zeta(\delta) = \frac{\delta}{\sqrt{4\pi^2 + \delta^2}} \tag{6.11}$$

The critical damping is given as:

$$b_{crit} = \frac{B_{crit}}{M} = 2\omega_0 = \frac{4\pi}{T_0} \tag{6.12}$$

By expressing the relative damping as a fraction of the critical damping, we get:

$$\zeta = \frac{b_e}{b_{crit}} = b_e \frac{T_0}{4\pi} \tag{6.13}$$

The equivalent linearized damping is now found from the decay signal as:

$$b_e = \zeta b_{crit} = \frac{4\pi}{T_0} \frac{\delta}{\sqrt{4\pi^2 + \delta^2}} \tag{6.14}$$

The measurements in equation (6.14) can be fitted to equation (6.9); and by linear regression the linear and quadratic contribution to the damping can be estimated as a function of motion amplitude.

6.4 Time domain analysis procedure

The equations of motions can be solved in the time domain by dividing the desired time period into a number of time steps and perform equilibrium iterations at each time step. The solution is obtained by using the start conditions from the previous time step and assuming a motion pattern. The solution will then in turn become the start conditions for the next time step.

According to the theory manual, non-linear time domain analysis in Riflex, which is utilized in this study, is performed by using a true Newton-Raphson type of equilibrium iteration. This implies recalculating the tangential mass, damping and stiffness matrices at each iteration cycle. The procedure offers a quadratic convergency rate. A modified Euclidean displacement norm is used as convergence criterion, i.e. the sum of displacements must be below a certain value.

The numerical integration is based on the Newmark β-family. By assuming an acceleration pattern, i.e. choosing the parameters β and γ; and denoting the time step increment $\Delta\tau$, the velocity and displacement at time step $t + \Delta\tau$ is found as:

$$\begin{aligned} \dot{r}_{t+\Delta\tau} &= \ddot{r}_t + (1-\gamma)\ddot{r}_{t+\Delta\tau}\Delta\tau + \gamma\ddot{r}_{t+\Delta\tau}\Delta\tau \\ r_{t+\Delta\tau} &= r_t + \dot{r}_t\Delta\tau + \left(\frac{1}{2} - \beta\right)\ddot{r}_t(\Delta\tau)^2 + \beta\ddot{r}_{t+\Delta\tau}(\Delta\tau)^2 \end{aligned} \tag{6.15}$$

A β-value of ¼ gives constant average acceleration, while a γ-value of ½ gives no numerical damping. For all the analyses presented in this study, these values are used.

The overall structural damping matrix is described by a Rayleigh damping formulation:

$$\mathbf{C} = \alpha_1\mathbf{M} + \alpha_2\mathbf{K} \tag{6.16}$$

The global mass proportional damping contribution (α_1) is omitted to avoid unphysical structural damping due to rigid body motions. The global stiffness proportional damping contribution (α_2) shall give a realistic energy dissipation at the peak period of the loading. Since α_1 is omitted, α_2 simply becomes $2\lambda/\omega$ and is set to 0,01. λ is the relative structural damping.

At each time step, the external loads are updated due to improved estimates of structural velocities. The other contributions to the load vector are kept constant.

The hydrodynamic contributions to the external forces are found by using a long wave length approximation for the wave-induced excitation forces and a generalized Morison's equation formulation for the viscous forces. They are calculated to the actual instantaneous structural position.

6.5 Data handling

A Matlab routine is developed to run the coupled software programs described in Chapter 5 and implement the theory described in this chapter. The structural properties and main dimensions of the three models with different mooring system concepts are incorporated in Excel. The same is the case for the environmental input and time domain simulation parameters. Matlab reads data from Excel and applies it to the selected types of analysis to be performed. Postprocessing data and calculating statistics from time domain simulations are also incorporated.

Because this study includes a large number of analyses with different system configurations, the Matlab routine and Excel sheets are proven invaluable. In Excel, system properties and simulation parameters are easily altered and presented in a clear manner, while Matlab is an excellent tool for handling large amount of data and for postprocessing purposes.

An overview of the analysis methods is shown in figure 6-2.

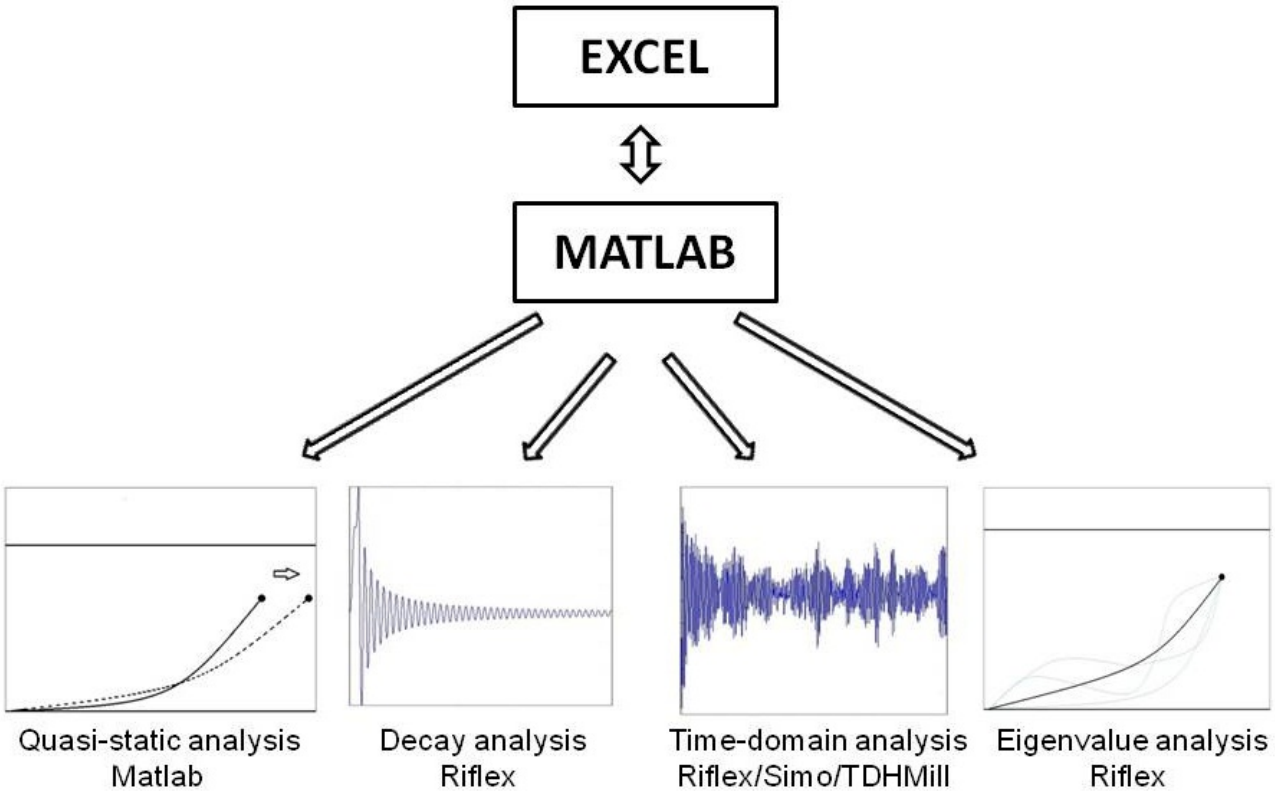

Figure 6-2: Overview of analysis methods

7. Concept selection

7.1 General

In this chapter, the three different mooring system concepts introduced in Chapter 5 are compared and one of the concepts is selected for further studies based on the results.

The concepts are analysed quasi-statically to obtain line configuration and mooring line characteristics. Furthermore, motion decay tests are performed in surge, heave and pitch to find natural periods and damping levels. Finally, dynamic response and statistics are obtained for operational and severe environmental conditions by the means of non-linear time domain analysis.

7.2 Quasi-static analysis

By varying the horizontal force levels, line configurations for the three mooring system concepts are obtained as shown in figure 7-1.

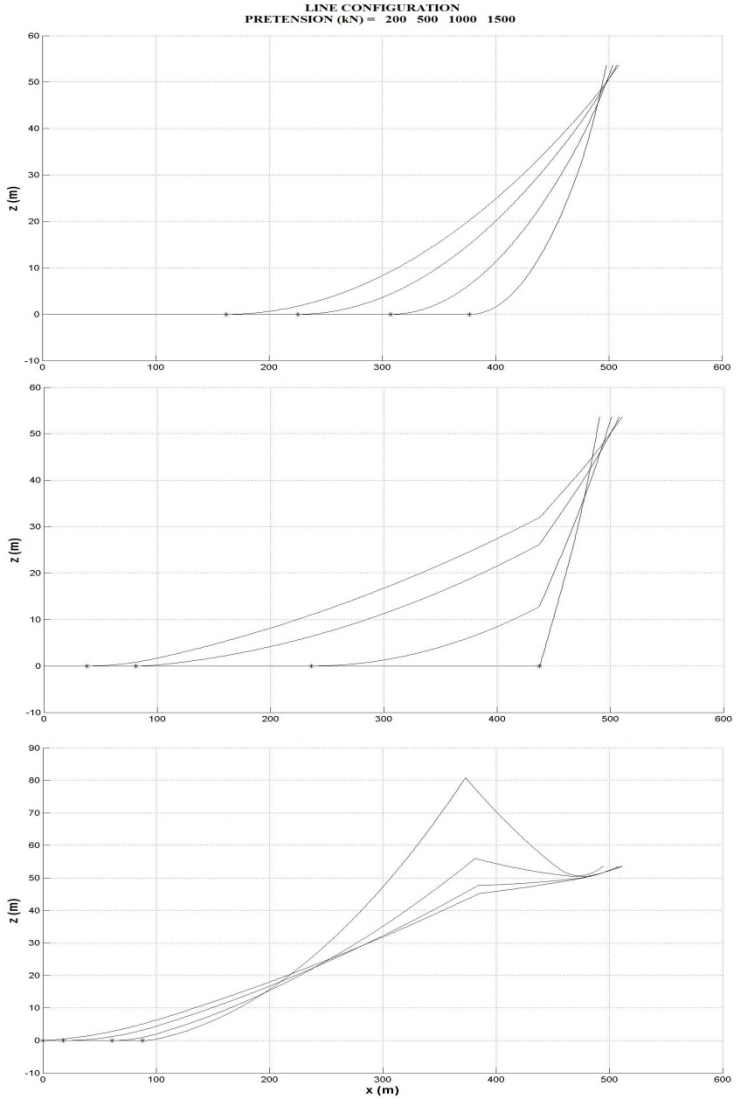

Figure 7-1: Mooring line configuration
Top: Distributed mass mooring system, Middle: Clump weight mooring system, Bottom: Buoyancy element mooring system

We see that as the horizontal force is increased, the catenary geometry changes due to fairlead displacements and consequently chain lifted off from the sea bottom. For the buoyancy element mooring system, no line is left resting at the sea bottom as the horizontal force reaches the largest value of 1500 kN. For the other two concepts however, a great portion of the line is still left on the sea bottom at the same horizontal force level.

The mooring line characteristics are shown in figure 7-2. Both the horizontal top tension and the total top tension is plotted for the three mooring system concepts.

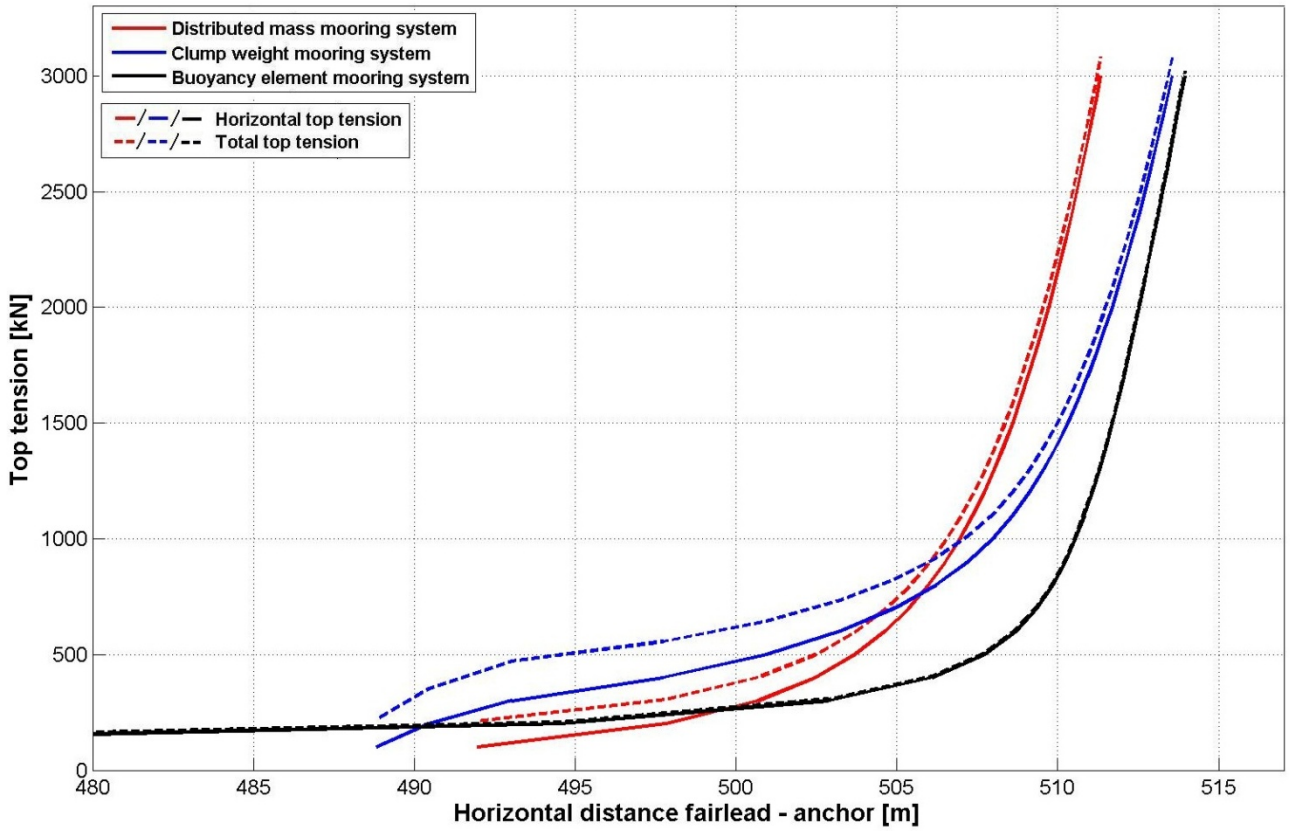

Figure 7-2: Mooring line characteristics for three mooring system concepts

Because of the buoys attached to the lines of the buoyancy element mooring system, it is seen that initially for a large fairlead displacement range, the top tension is kept almost constant as the line between the fairlead and the buoy is "tightened up" (see figure 7-1). A further increase in displacement beyond this range will give non-linear restoring forces from the geometric stiffness as line is lifted off from the sea bottom. However, already at a top tension of approximately 1200 kN, the whole line length is suspended, i.e. all the line is lifted from the sea bottom. Additional increase in top tension beyond this point is therefore due to the combined effects of non-linear restoring forces from the change in geometry as the buoy is pulled down, and linear restoring forces from elasticity in the line. As a result of the buoys effect on the line configuration, the total top tension will be almost identical to the horizontal top tension for the whole tension range considered.

The distributed mass mooring system, solely consisting of chain segments, will respond by an increase in top tension as soon as the fairlead displacements increase. Because of the large submerged weight of the line, parts of the line remain resting on the sea bottom through the whole top tension range considered. This provides geometric stiffness contributions to the restoring forces. However, the large axial stiffness of the chain segments leads to increasingly mooring line response due to stretching as the tension increases.

For the clump weight mooring system, the tension-displacement curve will initially be steep due to the increased stiffness when the clump weight is partially lifted off the sea bottom. Furthermore, when fairlead displacements increase, the wire segments in the lines will reduce the stiffness of the system, resulting in a smaller top tension gradient than the case with the distributed mass mooring system. Because of the clump weight's effect on the line configuration (see figure 7-1) the total top tension will have a significant vertical component. The effect is primarily seen for low top tension levels.

7.3 Motion decay analysis

Motion decay tests have been carried out on the test model. Results for vertical and longitudinal motion modes for the three different mooring system concepts are found.

The structure is initially given 500 s to obtain equilibrium before the ramp force is applied for 600 s. For translational motion modes (surge and heave) the ramp force is 5 kN/s, while for the rotational motion mode (pitch) the ramp force is 1500 kNm/s. For all three concepts, the anchors where given a prescribed displacement corresponding to a pretension of 500 kN.

The main results are presented in the following.

7.3.1 Natural periods

The natural periods obtained from the motion decay tests are presented in table 7-1.

Mooring system concept	Degree of freedom	Natural period [s]
Distributed mass	Surge	54,1
	Heave	28,8
	Pitch	25,6
Clump weight	Surge	82,5
	Heave	27,5
	Pitch	25,4
Buoyancy element	Surge	52,4
	Heave	26,4
	Pitch	26,4

Table 7-1: Natural periods

It is seen that the natural periods in all the degrees of freedom considered are above the WF range, i.e. resonant WF motions are avoided. The surge natural period is significantly larger for the clump weight mooring system than for the others. This is because all three mooring systems have an equal pretension of 500 kN, and with respect to the mooring line characteristics (see figure 7-2) we see that the clump weight mooring system is significantly "softer" than the other concepts at low tension levels. For the buoyancy element mooring system it is seen that the heave and pitch natural periods are identical and possible Mathieu effects must be considered. It is however important to note that the natural periods of the system are not tuned for these initial concept studies.

7.3.2 Damping

The relative damping (ζ) from the logarithmic decrement is presented as a function of surge displacement in figure 7-3 (left), while the ratio between linear and quadratic damping as a function of surge displacement is shown in figure 7-3 (right).

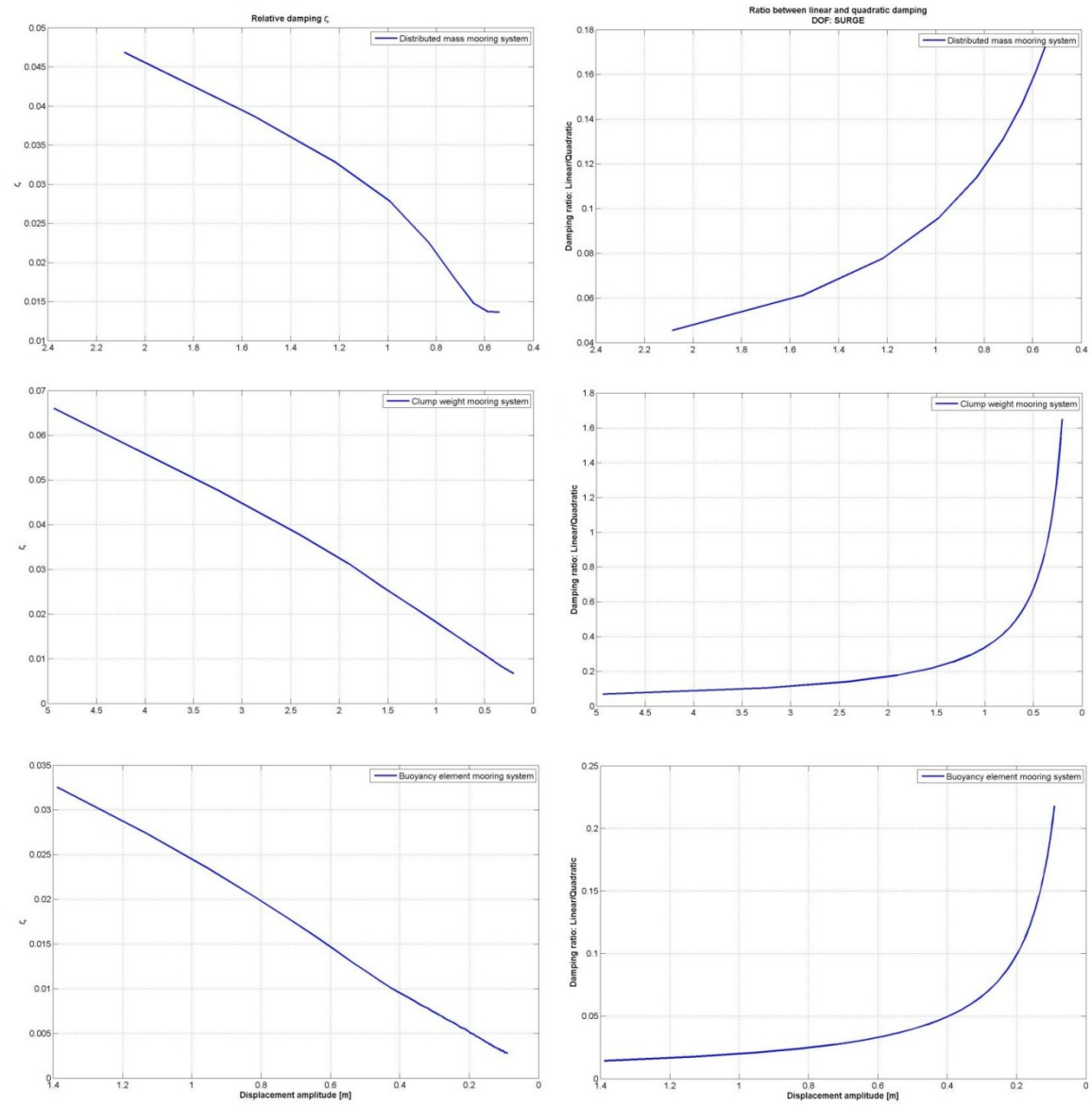

Figure 7-3: Surge damping
Left: Relative damping (ζ) as function of surge displacement. Right: Damping ratio (linear/quadratic) as function of surge displacement
Top: Distributed mass-. Middle: Clump weight-. Bottom: Buoyancy element mooring system.

Generally, the relative damping decreases with decreasing motion amplitudes which is obvious from studying figure 7-3 (left). From the plots on the right side, it is seen that the effect from quadratic viscous damping is prominent for large motion amplitudes, while we are left with the linear damping as the motion amplitudes approaches zero. The mooring system itself has little effect on the overall system damping, and the differences are mainly due to different displacement levels.

For the other motion modes considered (heave and pitch), the viscous damping is not as prominent as for surge. For heave, the linear damping contribution is in order of 10-100 times larger than the

viscous damping, and is therefore close to constant; while a larger viscous damping contribution is seen in pitch. The relative damping levels presented in table 7-2 are mean values over the decay signal considered. As expected, the type of mooring system has negligible effect on the heave and pitch damping.

Mooring concept	**Distributed mass**	**Clump weight**	**Buoyancy element**
Degree of freedom	Relative damping ζ	Relative damping ζ	Relative damping ζ
Heave	0,0295	0,0283	0,0266
Pitch	0,0201	0,0196	0,0203

Table 7-2: Relative damping, heave and pitch

7.4 Time domain analysis

In order to compare the different concept's response to environmental loads and capture dynamic effects in the mooring lines, time domain analysis is performed. Two environmental load conditions are considered. The first condition, denoted operational condition, is taken as an environmental condition where the wind turbine is operating at maximum effect, i.e. with wind speeds close to the rated wind speed. The second condition, denoted storm condition, is taken as a non-operating condition with combination of wind and waves with 100-year return periods and current with 10-year return period. Typical values for the Northern North Sea as given in DNV-OS-E301 are used.

The environmental conditions are shown in table 7-3.

		Opertional Condition	**Storm Condition**
Wave	H_s [m]	1,0	15,0
	T_p [s]	6,6	16,0
Wind	U_{mean} [m/s]	11,0	40,5
	Turb. Intensity	0,1	0,1
Current	V_0 [m/s]	0,5	1,6
	V_{20} [m/s]	0,4	1,1
	V_{40} [m/s]	0,3	1,1
	V_{60} [m/s]	0,2	0,7
	V_{80} [m/s]	0,1	0,7
	V_{100} [m/s]	0,0	0,6

Table 7-3: Environmental conditions

All the environmental loads are applied to the structure with a heading of 0° relative to the x-axis, in the direction of the anchorline parallel to the x-axis (Anch.line 1). The anchor nodes are given a prescribed displacement corresponding to a pretension of 500 kN for all three concepts. An 1-hour simulation is carried out for each environmental condition and the main results are presented for the operational- and storm condition in table 7-4 and 7-5 respectively.

Mooring system concept	Distributed mass				Clump weight				Buoyancy element			
Response	Mean	Std.	Min	Max	Mean	Std.	Min	Max	Mean	Std.	Min	Max
Surge - Waterline [m]	4,8	0,7	2,0	6,8	7,3	0,7	4,0	9,4	4,8	0,7	2,1	6,7
Sway - Waterline [m]	0,0	0,0	-0,1	0,1	0,0	0,0	-0,1	0,1	0,0	0,1	-0,1	0,1
Heave - Waterline [m]	4,1	0,1	3,6	4,5	3,6	0,2	3,1	4,1	6,8	0,2	6,2	7,3
Pitch - Waterline [m]	3,9	0,8	1,0	6,2	3,8	0,8	0,9	6,1	4,2	0,8	1,4	6,6
Tower bottom heave [m]	-75,7	0,1	-76,2	-75,3	-76,3	0,1	-76,7	-75,8	-73,0	0,2	-73,8	-72,4
Axial force - DL1 [kN]	462,4	16,3	400,7	510,0	433,7	11,7	382,1	471,1	408,7	15,6	351,9	458,0
Axial force - DL2 [kN]	462,5	15,7	407,7	501,6	433,8	11,3	390,5	467,6	408,7	15,9	352,2	457,1
Axial force - DL3 [kN]	364,4	11,9	318,8	401,4	352,0	14,2	305,4	396,7	257,9	3,9	245,9	270,2
Axial force - DL4 [kN]	253,6	12,9	214,3	306,9	239,4	14,4	199,7	294,4	244,9	3,3	235,4	262,7
Axial force - DL5 [kN]	253,7	13,2	214,3	309,8	239,3	14,7	201,1	298,8	244,9	3,7	234,6	260,6
Axial force - DL6 [kN]	364,3	12,1	316,9	403,5	352,0	14,5	303,9	399,8	257,9	3,3	248,0	274,5
Axial force - Anch. Line 1 [kN]	829,4	31,8	713,6	913,6	816,6	22,7	728,1	879,8	801,9	30,5	692,8	895,1
Axial force - Anch. Line 2 [kN]	516,9	5,4	499,2	540,9	527,8	4,4	516,1	547,3	493,4	5,6	478,7	517,4
Axial force - Anch. Line 3 [kN]	516,8	5,5	498,8	541,3	527,7	4,4	516,1	547,4	493,4	5,7	479,0	517,9

Table 7-4: Response statistics, operational condition

Mooring system concept	Distributed mass				Clump weight				Buoyancy element			
Response	Mean	Std.	Min	Max	Mean	Std.	Min	Max	Mean	Std.	Min	Max
Surge - Waterline [m]	3,8	4,8	-12,8	18,4	7,3	4,8	-8,8	21,6	3,1	5,0	-13,3	21,4
Sway - Waterline [m]	0,0	0,0	-0,1	0,0	0,0	0,0	0,0	0,0	0,0	0,0	0,0	0,1
Heave - Waterline [m]	3,5	1,4	-1,4	8,3	3,0	1,5	-2,7	8,4	5,0	3,7	-11,8	17,0
Pitch - Waterline [m]	2,0	3,0	-8,5	12,2	1,9	3,1	-9,8	12,3	2,1	3,2	-7,9	14,7
Tower bottom heave [m]	-76,3	1,3	-81,3	-71,7	-76,8	1,5	-82,4	-71,5	-74,8	3,7	-91,7	-62,9
Axial force - DL1 [kN]	570,1	353,7	-105,1	2459,8	535,5	156,4	83,7	1454,0	591,5	453,2	-75,1	3101,2
Axial force - DL2 [kN]	584,0	385,8	-100,9	2487,6	542,4	194,2	63,6	1557,7	603,0	462,7	-56,7	3145,3
Axial force - DL3 [kN]	332,0	64,2	83,3	726,3	316,8	77,4	101,2	501,7	343,4	163,1	125,5	1321,4
Axial force - DL4 [kN]	252,7	89,4	62,6	856,7	254,4	83,8	85,5	523,5	203,1	70,2	51,1	782,4
Axial force - DL5 [kN]	259,7	98,7	31,6	907,3	258,1	86,4	86,6	553,7	208,3	66,2	61,7	743,9
Axial force - DL6 [kN]	325,0	42,4	85,9	573,5	312,7	75,8	97,0	474,8	337,6	144,7	139,9	1159,6
Axial force - Anch. Line 1 [kN]	1061,7	746,6	-332,2	4875,5	1030,4	354,1	114,4	2942,2	1176,4	912,5	-150,4	6211,9
Axial force - Anch. Line 2 [kN]	481,9	118,6	33,2	1272,7	506,5	23,8	430,0	649,4	537,0	173,5	273,2	1537,1
Axial force - Anch. Line 3 [kN]	481,6	118,7	41,4	1270,6	506,1	23,4	425,6	636,3	536,3	173,9	275,8	1583,5

Table 7-5: Response statistics, storm condition

See figure 5-1 for definition of the anchorline directions. Waterline is referring to the waterline at zero-load initial configuration*.

Generally, it is seen that the mean mooring line tensions are approximately equal for the three concepts for both environmental conditions. For the operational condition, the mean mooring line tension is slightly larger for the clump weight concept than for the other two concepts; while for the storm condition, the buoyancy element concept experiences the largest mean mooring line tension. The maximum values and variation in line tension (expressed in terms of the standard deviation) are however significantly larger for the concepts utilizing distributed mass and buoyancy element than for the clump weight concept**.

The effects described above can be explained by the mooring line characteristics (see figure 7-2). At the applied pretension level, the total tension is significantly larger for the clump weight mooring

* Mean heave response should be zero at the actual waterline.

** The negative minimum values for axial force are not physical, i.e. chain segments are not in compression.

concept than for the other two concepts, i.e. the vertical tension component is larger. At the same time, the tension-excursion curve gradient is smaller. When the environmental load is applied, the clump weight concept will therefore experience a large surge offset due to the load while the line tension remains approximately the same as for the other concepts. Due to the large gradients of the tension-excursion curves, the distributed mass- and buoyancy element concepts will have large tension variations even for relatively small variations in horizontal offset. Actually, for the buoyancy element concept in storm condition, maximum line tension in the most heavily loaded line reaches a value above 6000 kN, while the same value is just below 5000 kN and 3000 kN for the distributed mass- and clump weight concept respectively. The same effect is observed for the most heavily loaded delta-lines.

It is observed that even though the initial gap between the tower bottom and sea bottom was only 20 m, neither of the concepts are risking bottom contact during the storm condition.

The complete response time series from the concept comparison are found in Appendix B.

7.5 Conclusion and selection of concept for further studies

By studying the three concepts, pros and cons for each concept are revealed.

The buoyancy element concept is desirable for deep water mooring systems because the weight and stiffness is reduced, and dynamic effects in the mooring line are limited to the part of the line extending from the buoy to the sea bottom. For the application investigated in this study however, the buoyancy element concept is failing when it comes to limiting the maximum line tension. Because the suspended length of the line is very limited for the water depth considered, the soft nature of the mooring system will result in large peak tensions. Also, the buoy may cause challenges during installation and handling. Furthermore, by using the present layout we risk having vertical forces on the anchor. This can be resolved by increasing the line length or bottom segment weight, further complicating the handling and compromising on the mooring system cost.

The distributed mass concept may be the most desirable when it comes to installation and handling purposes. In addition, the large submerged weight allows for short line lengths and ensures no vertical forces on the anchor. However, the large tension-excursion curve gradient gives large tension variations during severe weather conditions.

When it comes to limiting maximum line tension, the clump weight concept is superior to the other two concepts. The relatively small tension-excursion curve gradient over a large displacement range ensures good control with the line tension even in severe weather conditions. As for the distributed mass concept, the large submerged weight allows for shorter line lengths and limits the risk of vertical forces on the anchor. The drawback is that the horizontal offset will be large, resulting in a large footprint and possibly inflicting damage on the power cable. The offset can however be controlled by tuning the pretension, compromising on the maximum line tension level.

Based on the discussion in this chapter, the clump weight mooring system is selected for further studies. The two other concepts will not be further discussed.

8. Mooring system optimisation

8.1 General

A number of key parameters defining the mooring system have been selected and subjected to a parameter study. Their effects on the system performance are investigated in order to optimise the mooring system. The main concerns that need to be considered when selecting the design parameters may be summarized as:

- Avoiding vertical forces on the anchors
- Select segments with adequate breaking strength to resist the maximum line tension with sufficient margins
- Avoiding clump weight touchdown
- Keeping the mooring lines as short as possible
- Utilize the geometric stiffness range by tuning the pretension

For a mooring system with clump weights, the most influential design parameters are the size (mass) of the clump weights and their position along the mooring line. Emphasis is therefore put on these two design parameters.

Other parameters that are investigated include:

- Pretension
- Overall length of the mooring system
- Chain and wire weight/dimension
- Vertical fairlead position
- Delta-line length

The parameter study is carried out by the means of quasi-static and dynamic analysis. The clump weight size and position are investigated by utilizing a quasi-static approach. Furthermore, by applying the optimised values for the clump weight size and position; the pretension, overall length of the mooring system and chain- and wire weight/dimension are determined by the means of time domain analysis. The storm condition defined in Chapter 7 is applied with environmental loading acting with an heading of 0° relative to the x-axis. The vertical fairlead position and delta-line lengths are selected based on theoretical considerations.

8.2 Clump weight size

In order to investigate the effect of the clump weight size, all other parameters are kept constant while the clump weight size is varied according to table 8-1.

Diameter [m]	Volume [m^3]	Mass [tons]	Gyration radius [m]	Buoyancy force [kN]	Gravity force [kN]	Weight in water [kN/m]
1	0,79	6,17	0,35	7,90	60,48	52,58
2	3,14	24,66	0,53	31,59	241,93	210,34
3	7,07	55,49	0,76	71,08	544,34	473,26
4	12,57	98,65	1,01	126,36	967,72	841,36
5	19,63	154,13	1,25	197,43	1512,06	1314,62

Table 8-1: Clump weight size

The resulting line configuration, here presented for a pretension level of 700 kN, is shown in figure 8-1.

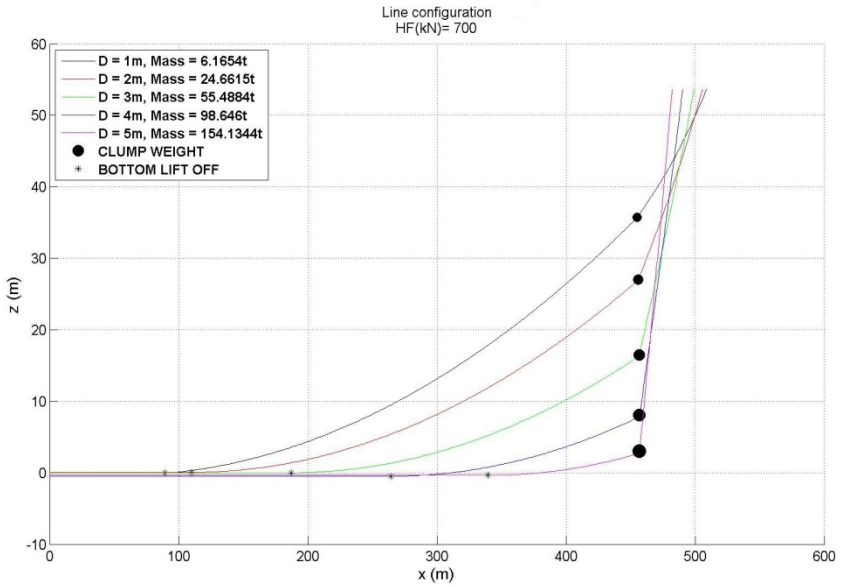

Figure 8-1: Line configuration for various clump weight sizes

As the line configuration is determined by the submerged weight of the line, it is seen that the size of the clump weight is of major importance for the configuration. For the largest clump weights, the short suspended part of the mooring line is close to vertical while the major part of the line is resting on the sea bottom. Even in equilibrium position, the largest clump weights are close to the sea bottom and will therefore experience touchdown on the leeward side when the floater is displaced due to environmental loading. This will not be the case for the smaller clump weights as the reduced weight ensures adequate vertical distance to the sea bottom. Problems with possible vertical forces on the anchors may occur however, as the catenary sag is relatively small.

The mooring line characteristics for the selection of clump weights are shown in figure 8-2.

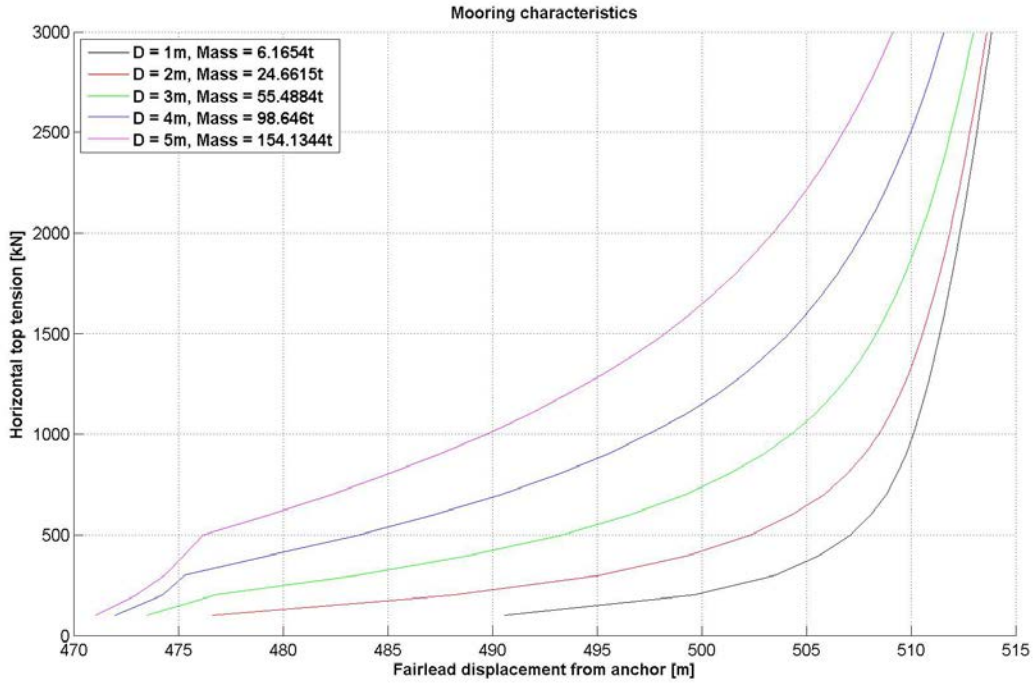

Figure 8-2: Mooring line characteristics for various clump weight sizes

It is seen that for all the applications, the tension-extension curves initially have small gradients at low and moderate horizontal top tension levels. The restoring forces are obtained from the catenary (geometric) stiffness contribution as the line curvature changes when bottom chain is lifted off due to increasing fairlead displacements. For higher tension levels, the lines will respond increasingly by stretching, i.e. the elastic stiffness contribution is governing the restoring forces. The tension-extension curve will eventually approach a straight line and the mooring lines will fail structurally when the breaking strength is exceeded. The dynamic tension may become very large in the elastic region as a small change in displacement causes large changes in tension. The transition to the elastic region occurs at much lower tension levels for the small clump weights than for the larger ones. For the large clump weights, the weights will be resting on the sea bottom for low horizontal top tension levels. A large pretension is thus required to prevent leeward weights from touchdown, which in turn can give rise to large impact forces.

Ultimately, the choice of clump weight size becomes a trade-off between increased pretension and reduced dynamic tension for the large weights; and reduced pretension and increased dynamic tension for the smaller weights. The latter will be preferable in most operational conditions, but will fail to limit the peak tension in severe weather conditions.

A clump weight with diameter 3,5 m and mass 75,5 t is selected. By choosing this relatively large clump weight size, we ensure that the non-linear restoring forces from the catenary stiffness are acting over a large top tension range; hence limiting the maximum tension. Though even larger clump weights would give slightly more favourable line characteristics in the high tension range, a large pretension would be required to prevent clump weight touchdown on the leeward side, resulting in larger mean tension in the lines. In addition, very large clump weights would increase the cost and complicate the installation.

8.3 Clump weight position

By varying the distance between the clump weight and the fairlead, and keeping all other parameters constant, the effect of the clump weight position can be investigated. The distance between the fairlead and the clump weight is increased in steps of 5 m. Mooring line characteristics for 6 different clump weight positions are shown in figure 8-3.

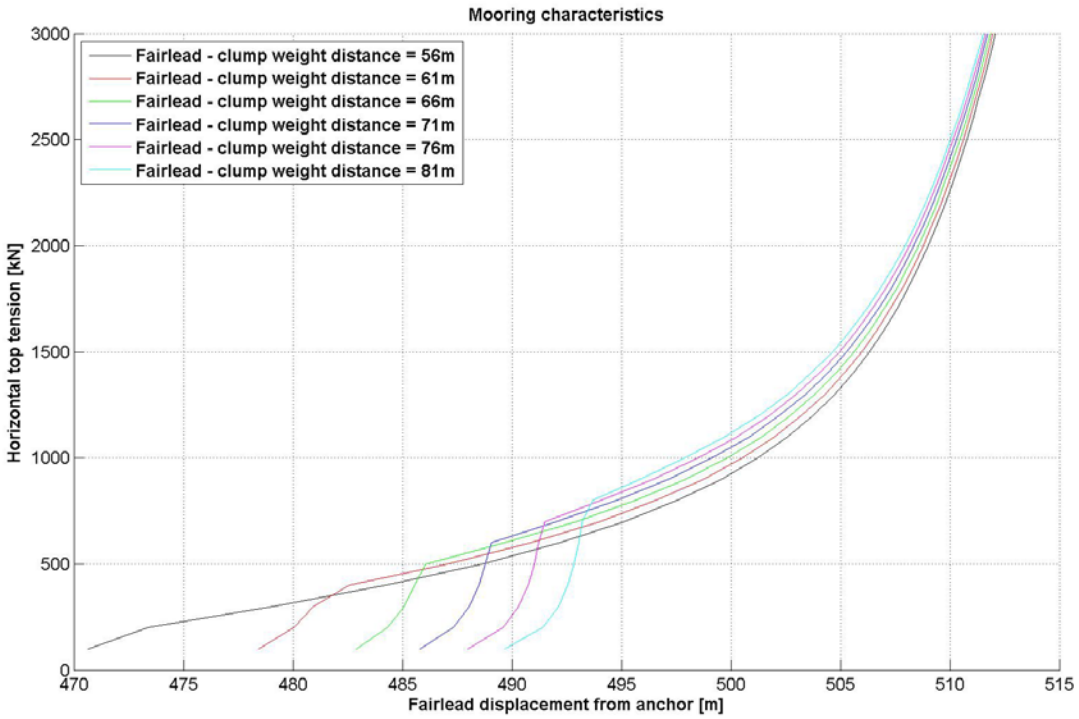

Figure 8-3: Mooring line characteristics for various clump weight positions

We see that after the clump weights are lifted from the sea bottom, the horizontal top tension levels are almost identical for all applications. This is due to the fact that only the clump weight position is varied, i.e. the submerged weight of the mooring lines which governs the top tension is constant.

The vertical distance between the fairlead and the sea bottom is only 54 m, and in addition, delta-lines are used. Attaching clump weights to the delta-lines is not desirable as this will add further complexity to the system, especially with respect to installation. It may also influence the delta-lines' effect on the yaw restoring coefficient. Depending on the size of the clump weight and the pretension in the lines, we are therefore left with a narrow range of positions for where the clump weight may be attached to the main mooring line. As the position is not affecting the tension in the lines much, a clump weight position close to the delta-lines is preferred. This will reduce the possibility of clump weight touchdown on leeward side during severe weather conditions.

A distance of 56 m along the cable from the fairlead to the clump weight is selected. This is sufficiently close to the delta-lines so that problems with clump weight touchdown on the leeward lines are avoided. It will also allow us to use a short wire segment between the delta-lines and the clump weight, introducing some additional elasticity to the upper part of the mooring lines.

8.4 Pretension

The pretension of a mooring system is important for limiting the horizontal offset. For the considered mooring system, the pretension is tuned by analysing the line tension and horizontal offset for various pretension levels. The surge response and axial forces in the most heavily loaded line (Anch.line 1) and one of the leeward lines (Anch.line 2) are presented in table 8-2.

Response	Surge - Waterline [m]				Axial force - Anch.line 1 [kN]				Axial force - Anch.line 2 [kN]			
Pretension	Mean	Std	Min	Max	Mean	Std	Min	Max	Mean	Std	Min	Max
300 kN	17,60	4,91	2,64	37,85	1027,23	65,62	883,87	1643,65	455,56	267,35	-261,39	1106,34
500 kN	13,13	5,23	-2,34	32,10	1225,02	114,23	934,65	2211,16	763,40	73,77	-117,22	1021,04
600 kN	11,04	5,26	-4,64	29,74	1312,71	149,60	870,49	2608,74	834,77	23,89	405,22	933,73
700 kN	9,34	5,27	-6,65	27,75	1400,95	186,08	821,16	2965,65	902,31	24,09	791,24	1034,93
900 kN	6,83	5,32	-9,83	24,91	1588,42	276,89	749,02	3713,12	1052,32	38,15	893,62	1280,41
1100 kN	5,24	5,38	-11,99	23,23	1776,36	383,90	641,61	4479,17	1209,98	59,92	993,40	1585,92

Table 8-2: Dynamic response as function of pretension

We see from the results that low pretension is favourable with respect to limiting the mean and maximum tension in the lines. However, the lines on the leeward side may become slack which can give rise to snap loads and impact forces from clump weight touchdown. For large pretension values, the mean- and maximum tension in the lines are increased, and the standard variation of axial force in the most heavily loaded line increases due to stretching.

For conventional offshore production units, the risers are limiting the permissible horizontal offsets. This does not apply to the considered application, but it is important to limit offsets of concern to the power cable and adjacent structures.

A pretension level of 700 kN is selected. This will give a reasonable compromise between line tension and floater excursions. It is important to note that the pretension is not given explicitly as input to Riflex. The input is given as prescribed displacements of the anchors, which in turn will govern the pretension. The relationship between the two is found quasi-statically. Since the quasi-static analysis is not accounting properly for the effect of the delta-lines, the pretensions given in table 8-2 will slightly overestimate the actual horizontal top tension as it appears from the time domain analysis.

8.4 Total line length

By increasing the horizontal distance between the anchor and the fairlead, the total length of the mooring system is increased. All other parameters are kept constant while the lower wire segment length is varied. The effect on the mooring line characteristics is presented in figure 8-4.

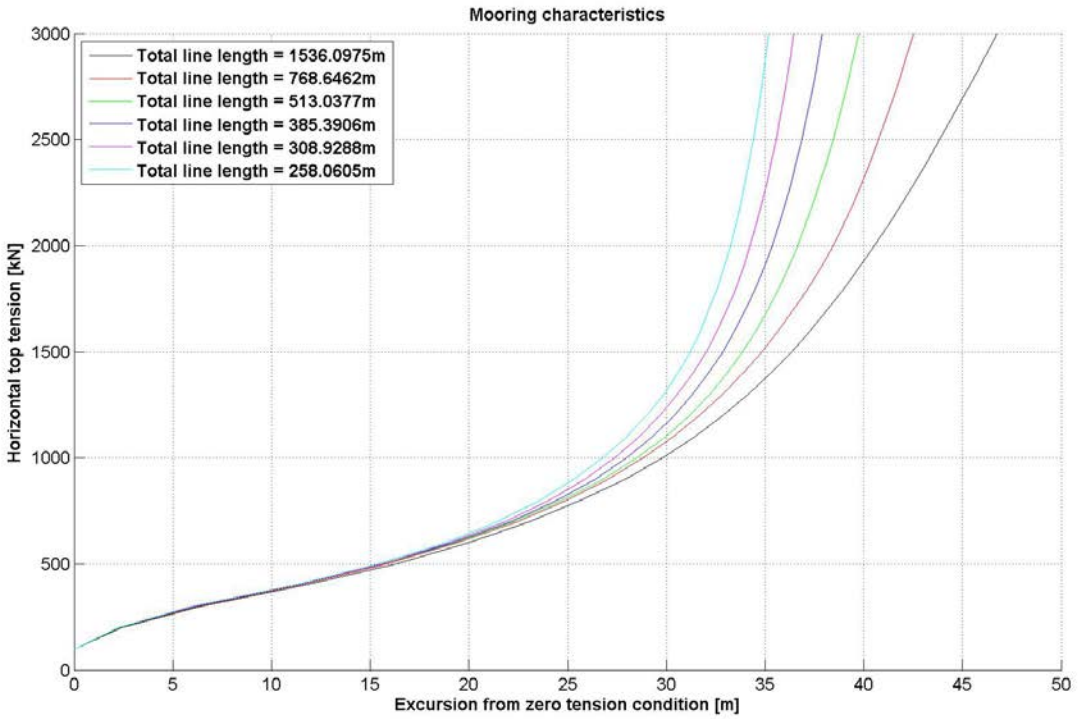

Figure 8-4: Mooring line characteristics for various line lengths

As expected, the length of the line has no effect on the line characteristics for low tension levels. Part of the line is resting on the sea bottom for all considered applications, providing the same restoring forces. As the top tension increases however, we see that the transition to elastic stiffness dominance appear earlier for the shorter lines. This is simply because they have less bottom line length; which thus will be exhausted at smaller excursion levels than for the longer lines.

Ideally, one would want as short lines as possible. This is favourable because it will reduce the cost of the mooring system. If we also assume that the floating wind turbine is one of multiple turbines in a wind farm, reducing the mooring line length will increase the income as more wind turbines can be installed in the same area.

However, the most important from a design perspective is that we limit the peak tension and ensure no vertical forces on the anchor. The mooring line length must therefore be determined by analysing in the time domain. The three shortest line lengths from figure 8-4 are analysed, and it is checked for vertical forces on the anchor of Anchorline 1 during the time of maximum surge offset of the floater.

The results are presented in table 8-3.

Mooring line length [m]	Vertical force on anchor
385,4	YES
513	NEGLIGIBLE
768,6	NO

Table 8-3: Check of vertical forces on anchor

For the shortest line length, maximum vertical forces in the order of 10^2 kN are observed on the anchor. For the line of length 513 m, the line 10 m from the anchor was lifted only a few centimetres above the sea bottom during the instant of maximum line tension; hence the vertical force on the anchor will be very small compared to the weight of the anchor. For the longest line length, no line lift-up close to the anchor was observed. Based on the results, mooring lines with a total length of 513 m are selected.

8.5 Chain and wire dimension

Changing the weight of the suspended chain and wire segments to manipulate the mooring line characteristics is unnecessary as the weight of the suspended catenary effectively can be controlled by the clump weight size. Our only concern when choosing chain and wire dimensions will therefore be to provide sufficient breaking strength to resist the maximum tension with adequate safety margins.

The effect of the bottom chain weight has been investigated quasi-statically. The results showed that for the mooring system considered, the mooring line characteristics are not very sensitive to this parameter. However, due to the fact that analysis showed a very small vertical force on the anchor for the selected line length, bottom chain slightly heavier than the chain used in the suspended line is selected. The length of the bottom chain is 150 m. As tensions in the delta-lines are approximately half the tensions in the upper part of the main mooring line, the delta-line chains are somewhat reduced in dimension compared to the chain segments in the main mooring line.

The chain and wire diameter is selected to fulfil the design criteria, based on the maximum tension values in table 8-2. Data is taken from Vryhof anchors (2010) and presented in table 8-4. For details on how the design mooring system components are modelled in Riflex, see Appendix C.

	Component type			
	Chain - Connectors	**Chain - Delta lines**	**Chain - Bottom**	**Wire**
Class/Type	R4-RQ4 studless	R4-RQ4 studless	R4-RQ4 studless	Six strand wire rope
Diameter [mm]	87	73	105	96
Proof load [kN]	5355	3884	7497	-
Break load [kN]	7682	5572	10754	6965
Weight [kg/m]	151	107	221	40,5
Axial stiffness [MN]	-	-	-	483,8

Table 8-4: Chain and wire properties

Studless chain is applied as recommended for permanent moorings. This type of chain is attractive with respect to the fatigue life and weight per unit strength ratio. For the wire segments, six strand wire rope is applied. This gives high elasticity and flexibility, and relatively low axial stiffness. The drawback is that it is only recommended for up to 10 years design life.

8.6 Vertical fairlead position

Ideally, the vertical fairlead position should be located at a point where there is no coupling between surge and pitch, i.e. at the vertical position of the centre of rotation. By doing so, the wind and wave induced dynamic loading in the mooring lines will be minimized. According to Nielsen (2009), this position will for a deep-draft floating wind turbine structure oscillating at its pitch natural period be located somewhere between the COB and COG, closer to the COG. However, since the vertical distribution of wave forces is frequency dependent, so is the vertical position of the centre of rotation.

This frequency dependency can be shown mathematically. By utilizing the description of the motion of any point on the floating body, as shown by Faltinsen (1990), we get:

$$\begin{aligned}\mathbf{s} = &(\eta_1 + z\eta_5 - y\eta_6)\mathbf{i} + (\eta_2 - z\eta_4 + x\eta_6)\mathbf{j} \\ &+ (\eta_3 + y\eta_4 - x\eta_5)\mathbf{k}\end{aligned} \tag{8.1}$$

where η_{1-6} are the translational and angular rigid body motions. Furthermore, by choosing a point z' close to the COG of the body, Nielsen (2009) demonstrated that the horizontal motion of this point is described by:

$$\eta_1(z') = \eta_1 + z'\eta_5 \tag{8.2}$$

The vertical position of the centre of rotation will then be the point where the horizontal motion of z' is zero, hence:

$$z'_{rot} = -\frac{\eta_1}{\eta_5} \tag{8.3}$$

By assuming zero damping, and surge and pitch excitation forces in phase, the motions in surge and pitch may be approximated as:

$$\begin{aligned}\eta_1 &\simeq \frac{F_1}{-\omega^2(m + A_{11}) + C_{11}} \\ \eta_5 &\simeq \frac{F_5}{-\omega^2(I_{55} + A_{55}) + C_{55}}\end{aligned} \tag{8.4}$$

If z'_F is the resultant position of the horizontal wave forces, the pitch moment may be approximated as $F_5 \simeq F_1 z'_F$. Furthermore $C_{11} \simeq 0$ and $(I_{55} + A_{55}) \simeq (m + A_{11})r^2 = Mr^2$, where r is the radius of inertia in pitch.

The vertical position of the centre of rotation is then obtained as:

$$z'_{rot} \simeq -\frac{F_1}{F_1 z_F}\frac{-\omega^2 Mr^2 + C_{55}}{-\omega^2 M} = -\frac{1}{z_F}\left[r^2 - \frac{C_{55}}{\omega^2 M}\right] \tag{8.5}$$

When excited by waves of high frequency, the vertical centre of rotation will be located close to the bottom of the cylinder; while it moves towards plus infinity as the excitation frequency goes to zero.

It is obvious that we cannot choose a single point that will have no coupling between surge and pitch for the whole WF range. A fairlead connection point far up on the cylinder will be favourable in survival conditions, while moving the point down towards the bottom of the cylinder is favourable for most operational conditions. It is also important to consider that lowering the fairlead position will increase the overturning moment on the support structure from the wind thrust, and hence increase the static pitch angle.

With respect to the design of the mooring system, the most important consideration is however to choose a fairlead position that will give sufficiently suspended line length to achieve the desired mooring line characteristics. With the COG located 28 m from the bottom of the cylinder, i.e. only 48 m from the sea bottom, it is obvious that the fairlead has to be located above the COG. Especially since the length of the delta-lines further limits the length of suspended main mooring line to play with. The vertical fairlead position has not been subjected to a parameter study like other key parameters of the mooring line. It is chosen based on the issues discussed here and is subsequently verified by the means of time domain analysis. The mooring lines are attached to the fairlead 46,4 m below the mean water line as indicated in figure 8-5.

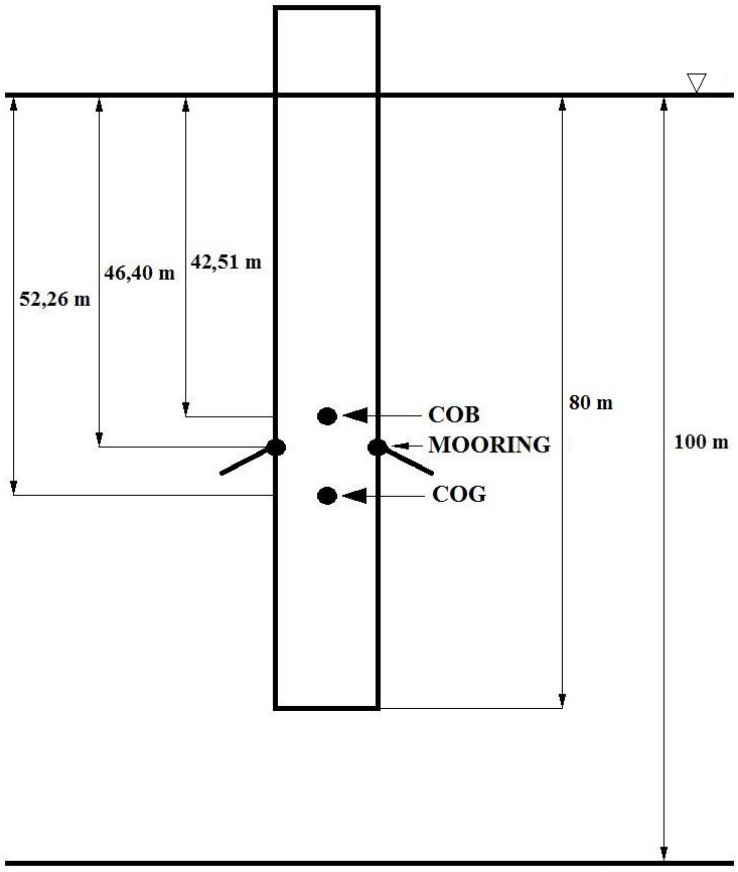

Figure 8-5: Vertical fairlead position

8.7 Delta-line length

The delta-lines will contribute to increased yaw stiffness because they are attached to the fairlead with an angle to the centre line of the structure. Nielsen (2009) demonstrated that the yaw restoring coefficient can be written as:

$$C_{66} = \sum_{i=1}^{n} TR\cos\varphi\left(1+\frac{R}{L_H}\right) \tag{8.6}$$

where T is the top tension, R is the distance from the centre of the structure to the "effective" mooring line connection point, φ is the top angle between the mooring line and the horizontal plane, and L_H is the horizontal distance from the "effective" mooring line connection point to the anchor. n is the number of mooring lines. When delta-lines are applied, the "effective" mooring line connection point is the point where the two delta-lines meet the main mooring line (see figure 8-6).

Furthermore, the delta-lines will act as a rigid connection as long as they are in tension, which is governed by the yaw angle. Nielsen (2009) showed that the delta-lines are in tension as long as the yaw angle is less than given by:

$$\eta_6 < \frac{L_H}{L_H + R}\tan\beta \tag{8.7}$$

Here η_6 is the yaw angle in radians and β is the angle between the delta-lines and the centre line of the structure, as indicated in figure 8-6.

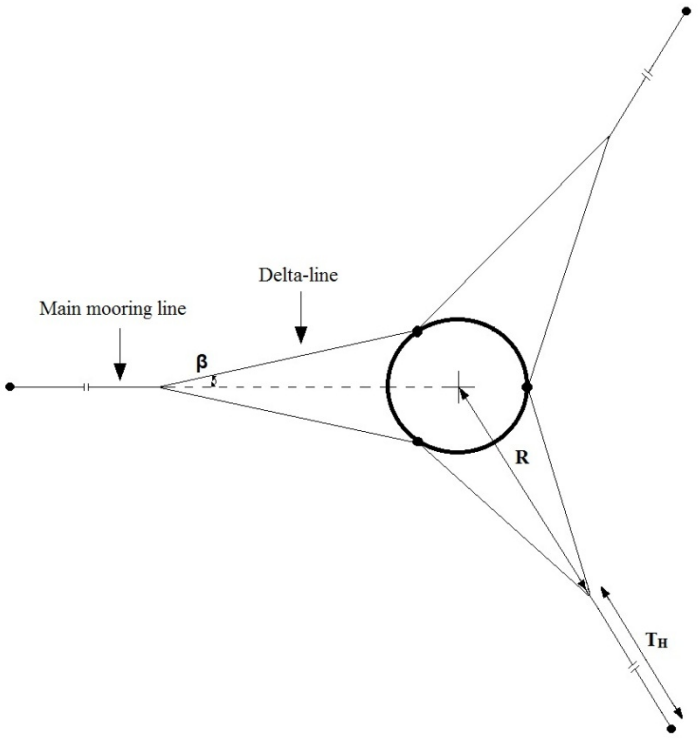

Figure 8-6: Mooring system layout

By assuming that the total mooring line length is constant, it is seen that by using long delta-lines, the maximum yaw angle before the delta-lines go slack is reduced, and the yaw restoring coefficient is increased. Shorter delta-lines will allow for larger yaw angles before the delta-lines go slack, but the restoring coefficient is reduced and the yaw natural period will increase. From equation (8.6) we see that the yaw restoring coefficient, and consequently the natural period can however be effectively controlled by the pretension.

The main consideration when selecting the delta-line length will be the water depth. As discussed earlier, the clump weight should preferable not be attached to the delta-lines. Hence, the delta-lines must be relatively short in order to achieve adequate length of main mooring line to play with. A length of 40 m is selected for the delta-lines, which means that the yaw angle must be below 6° in order to maintain tension in the delta-lines.

With all the other parameters defined as given in the previous sections, we get the top tension $T \simeq 807\,kN$ (total top tension from stamod), the angle $\varphi \simeq 43°$, $R = 42{,}15\,m$ and $L_H = 457{,}3\,m$. By using the data from figure 5-2 we get $I_6 = 6{,}28E07\,kgm^2$. Hence the yaw restoring coefficient will be $81{,}5\,MNm/rad$ and a natural period in yaw of approximately $5{,}5\,s$ is obtained. The low natural period will contribute to minimize rotations induced by asymmetric forces on the rotor.

8.8 Design mooring system

In this section, some key features of the design mooring system are presented.

The static equilibrium configuration is shown in figure 8-7.

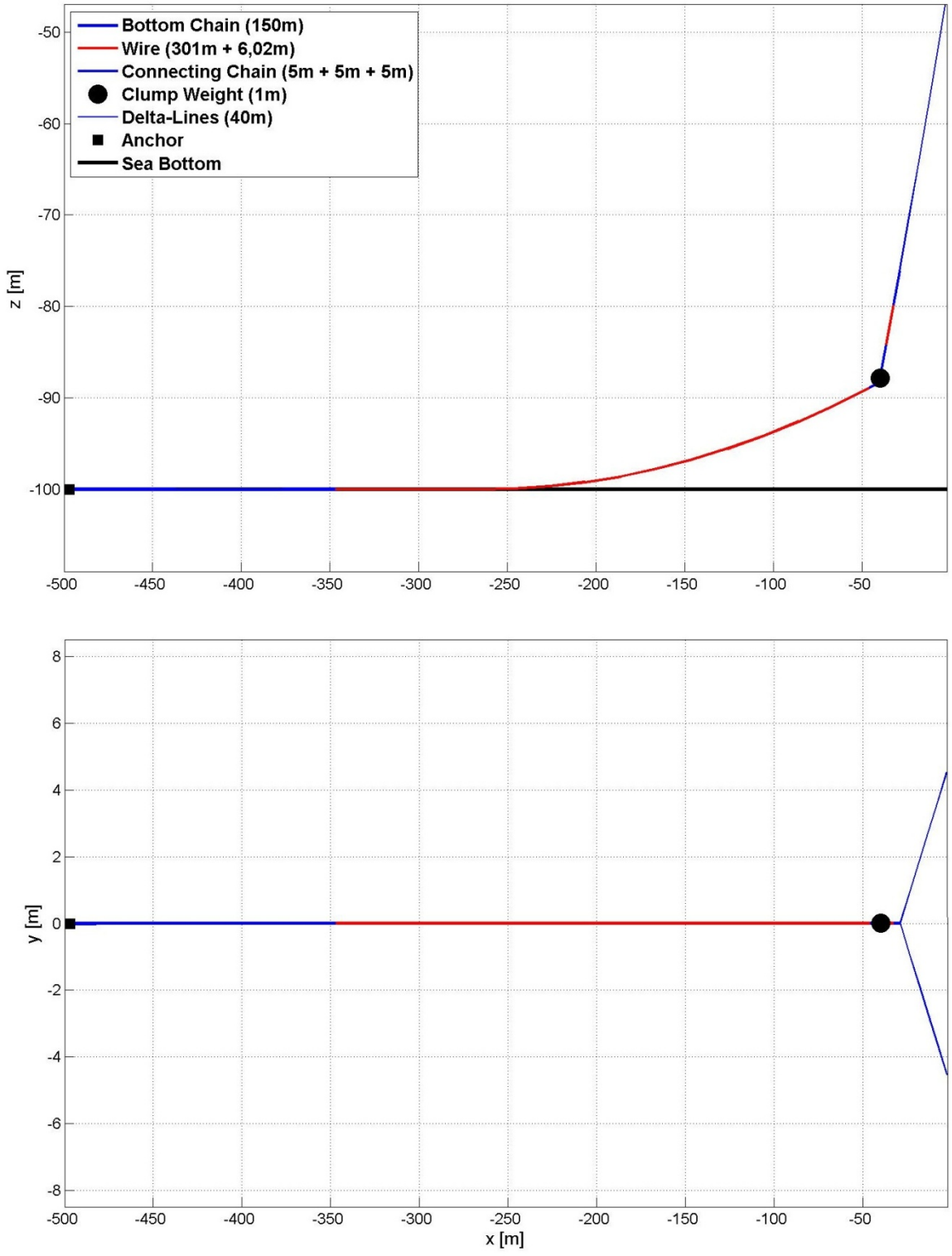

Figure 8-7: Static equilibrium configuration
Top: x-z-plane, Bottom: x-y-plane

The results obtained from 1-hour time domain analysis in operational- and storm conditions (from Chapter 7) are presented in table 8-5. Note that the standard deviation of surge motion is significantly smaller at the fairleads than in the waterline and at the rotor.

	Operational condition				Storm condition			
Response	**Mean**	**Std**	**Min**	**Max**	**Mean**	**Std**	**Min**	**Max**
Surge - Waterline [m]	7,37	0,69	3,88	9,46	9,34	5,27	-6,65	27,75
Sway - Waterline [m]	0,00	0,00	0,00	0,00	0,00	0,00	0,00	0,01
Heave - Waterline [m]	-0,60	0,10	-0,93	-0,31	-1,01	1,09	-5,63	2,43
Pitch - Waterline [deg]	3,29	0,67	0,95	5,67	1,77	3,78	-9,61	14,86
Surge - Rotor [m]	11,12	1,39	5,45	15,40	11,34	9,51	-17,57	44,11
Sway - Rotor [m]	0,00	0,00	0,00	0,00	0,00	0,00	0,00	0,00
Heave - Rotor [m]	63,28	0,13	62,77	63,66	62,82	1,19	57,63	66,27
Surge - Fairlead [m]	4,73	0,39	2,79	5,64	7,91	2,37	0,90	16,16
Sway - Fairlead [m]	0,00	0,00	0,00	0,00	0,00	0,00	0,00	0,01
Heave - Fairlead [m]	-46,92	0,08	-47,18	-46,68	-47,29	1,06	-51,88	-43,79
Z-pos - Clump weight 1 [m]	-83,49	0,44	-85,66	-82,39	-79,81	3,88	-90,91	-62,92
Z-pos - Clump weight 2 [m]	-90,42	0,18	-90,92	-89,57	-91,89	1,36	-97,87	-88,18
Z-pos - Clump weight 3 [m]	-90,42	0,18	-90,92	-89,57	-91,89	1,36	-97,87	-88,18
Axial force - Anch.line 1 [kN]	1177,97	18,75	1090,65	1231,36	1400,95	186,08	821,16	2965,65
Axial force - Anch.line 2 [kN]	939,82	4,82	926,62	966,23	902,31	24,09	791,24	1034,88
Axial force - Anch.line 3 [kN]	939,82	4,82	926,62	966,23	902,31	24,09	791,24	1034,93
Axial force - DL1 [kN]	616,73	9,18	574,19	643,02	721,21	94,17	405,83	1501,65
Axial force - DL2 [kN]	616,73	9,18	574,19	643,02	721,20	94,16	405,63	1501,65
Axial force - DL3 [kN]	625,13	30,16	525,94	728,00	578,18	195,33	28,56	927,62
Axial force - DL4 [kN]	377,52	30,14	281,73	476,77	389,33	203,57	-11,39	1002,68
Axial force - DL5 [kN]	377,52	30,14	281,73	476,77	389,32	203,57	-11,41	1002,72
Axial force - DL6 [kN]	625,13	30,16	525,94	728,00	578,18	195,33	28,56	927,81
Heave - Tower bottom [m]	-80,47	0,08	-80,71	-80,24	-80,80	1,06	-85,46	-77,18
Total surface elevation [m]	0,00	0,25	-0,94	0,85	0,00	3,74	-12,47	11,89
Wind speed [m/s]	10,97	1,19	6,24	14,46	40,45	3,11	27,63	50,98
Vertical force on anchor	NO				NO			

Table 8-5: Response from time domain analysis

The natural periods of the whole system and for one single line are presented in table 8-6 and 8-7 respectively.

Degree of freedom	**Natural period** [s]
Surge	84,6
Heave	27,7
Pitch	23,9

Table 8-6: System natural periods

It is seen that all the natural periods are above the WF range. Furthermore, Mathieu effects due to coincident heave and pitch natural periods are avoided; while the critical wave period $T_{wave,cr} = 13\,s$ may excite pitch resonance.

Pretension [kN]	Mode	Eigenvalue	Circular frequency [rad/s]	Natural period [s]
700	1	0,62	0,79	7,96
	2	6,76	2,60	2,42
	3	20,88	4,57	1,38
	4	28,21	5,31	1,18
	5	28,65	5,35	1,17

Table 8-7: Single line natural periods

From table 8-7 it is seen that only the 1st natural period is in the wave period range, while the other modes have lower natural periods. It is therefore checked for resonance in the mooring lines by exposing the system for waves with peak periods close to the 1st natural period. The results are shown in table 8-8. No significant increase of the axial force and motions in the mooring lines are observed, i.e. no mooring line resonance. This is probably due to the large drag damping in the mooring lines; in addition to the fact that for the considered wave periods, almost all wave kinematics are eliminated at the depth of the mooring lines.

Significant wave height	Peak period	Response							
		Axial force anchorline 1				X-pos - anchorline top			
Hs [m]	Tp [m]	Mean	Std	Min	Max	Mean	Std	Min	Max
4	7,66	1451,33	35,26	1305,12	1580,54	-30,56	0,05	-30,83	-30,33
4	7,96	1450,62	34,55	1307,06	1576,41	-30,56	0,05	-30,83	-30,37
4	8,26	1450,04	33,90	1300,81	1575,57	-30,56	0,05	-30,83	-30,38

Table 8-8: Mooring line resonance test

9. Design check

9.1 General

Since floating offshore wind turbines is a relatively new concept that has yet to be fully commercialized, there is currently no unique standard governing the design of such structures. Until a standard that fully covers these structures is established, DNV proposed to use the standard DNV-OS-J101 “Design of Offshore Wind Turbine Structures” together with DNV Guideline for Offshore Floating Wind Turbine Structures. The former provides principles, technical requirements and guidance for design, construction and in-service inspection of offshore wind turbine structures. The latter discusses issues related to design principles, site conditions, loads, stability and stationkeeping of floating wind turbine structures.

The guideline states that: “Until loads and response of catenary moored floating wind turbine structures are more thoroughly understood, the permanent mooring line tension as well as the dynamic mooring line tension shall be taken according to DNV-OS-E301 “Position Mooring”, which applies to the design of the mooring line as well as to the design of the anchor that transfers the loads to the supporting seabed soils.” DNV-OS-E301 “Position Mooring” is henceforth referred to as OS-E301. It provides environmental conditions and methods for mooring system analysis, in addition to requirements regarding mooring equipment.

When it comes to mooring line components, requirements concerning materials, manufacture, testing, dimensions and tolerances are given for mooring chain and steel wire ropes in DNV-OS-E302 “Offshore Mooring Chain” and DNV-OS-E304 “Offshore Mooring Steel Wire Ropes” respectively.

Figure 9-1 illustrates the relationships discussed here, and how the standards are referring to each other.

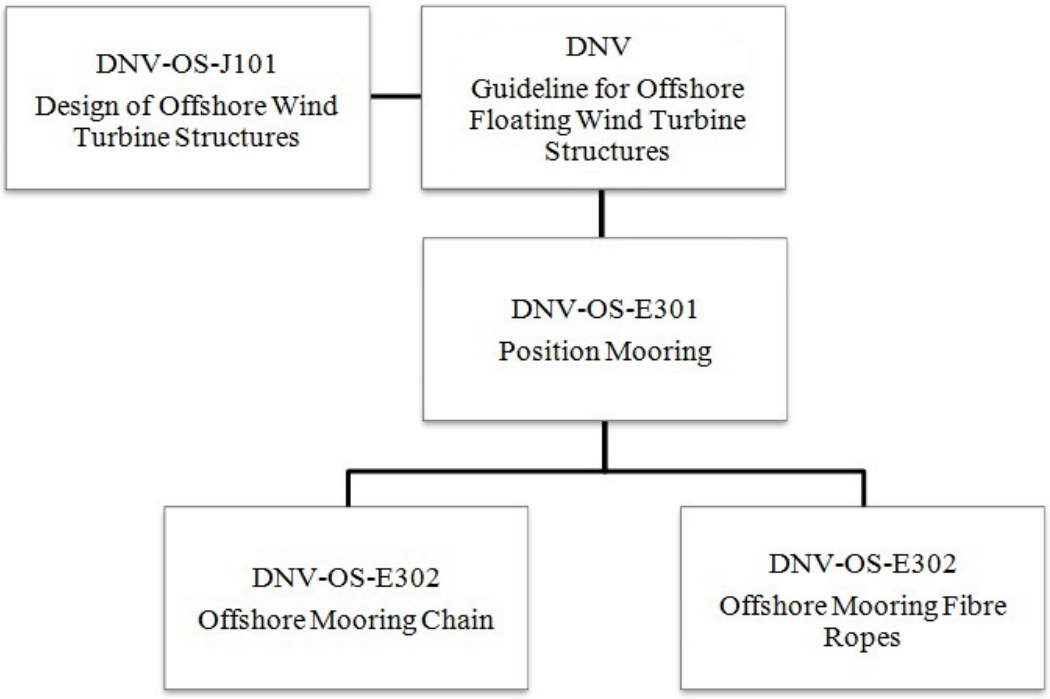

Figure 9-1: Overview of standards

9.2 Limit states

The Framework Regulations enforced by the Norwegian Petroleum Safety Authority, refers to NORSOK Standards when it comes to design of offshore structures. The NORSOK standards will in turn refer to the rules of classification societies, as represented with DNV in the previous section. According to Haver (2007), the structural design of offshore structures is based on the limit states design method; where a limit state is referred to as a state where the structure or a part of the structure no longer fulfils the requirements ensuring that the structure performs according to the design specification.

The four limit states are recognized as:

- Ultimate limit state
- Accidental limit state
- Fatigue limit state
- Serviceability limit state

9.2.1 Ultimate limit state (ULS)

The ultimate limit state (ULS) corresponds to the resistance to maximum applied loads. The control shall demonstrate that all foreseen loads can be resisted with an adequate margin.

Typically, according to ISO 19900, the ULS for offshore structures include:

- Loss of static equilibrium of the structure (e.g. overturning or capsizing)
- Failure caused by exceeding the ultimate strength
- Transformation of the structure into a mechanism
- Loss of structural stability
- Sinking
- Loss of stationkeeping

With respect to the ULS, control against loss of stationkeeping, as given in OS-E301, is emphasized in this study. It is stated that the ULS is introduced to ensure that the individual mooring lines have adequate strength to withstand the load effects imposed by extreme environmental conditions.

9.2.2 Accidental limit state (ALS)

The accidental limit state (ALS) corresponds to accidental situations or abnormal events. The control ensures that a given accidental scenario does not lead to a complete loss of the integrity of the structure. Also some very rare accidental loads are to be checked under the ALS.

As for the ULS, the ALS requirements for the stationkeeping system, as given in OS-E301, are emphasized in this study. The limit state is introduced to ensure that the mooring system has adequate capacity to withstand the failure of one mooring line. For cases where the mooring lines are equipped with clump weights, the loss of a clump weight due to failure of the connection to the mooring line is included as a single failure event.

9.2.3 Fatigue limit state (FLS)

The fatigue limit state (FLS) refers to the cumulative damage due to repeated loads. The control ensures that the structure is designed with proper margins against fatigue failure. The FLS control is not considered in this study.

9.2.4 Serviceability limit state (SLS)

The serviceability limit state (SLS) addresses the effect on comfort and non-structural components from the motions and structural responses. The control is carried out to ensure that the structure fulfils the functional requirements adequately. The SLS control is not considered in this study.

9.3 Environmental conditions

For details on environmental conditions, DNV standards generally refer to DNV-RP-C205 "Environmental Conditions and Environmental Loads". However, for simplicity, the environmental conditions applied here are taken directly from OS-E301. Northern North Sea – Troll field is selected as design location. This location has a water depth of slightly above 300 m, while the water depth in this study is set to 100 m. The current profile is therefore adjusted, while the wave and wind conditions are taken as given in OS-E301. In the following, details about the waves, wind and current are given, in addition to the drag force coefficients.

9.3.1 Waves

Sea states with return periods of 100 years shall normally be used. Combinations of significant wave height and peak period along the 100-year contour, defined by the inverse FORM technique, shall be applied. In cases with limited environmental data, typical sea states for specific areas can be applied for preliminary design. This is utilized in the present study. The peak period is then determined from the range of peak periods given by the means of a sensitivity analysis.

The 100-year sea state for the Troll field is given in table 9-1.

	H_s [m]	T_p [s]
Northern North Sea - Troll field	15,0	15,5 - 17,5

Table 9-1: Troll field sea state

Based on the maximum axial force response in the anchor lines for the peak period range considered, a design peak period of 16,5 s was selected. A JONSWAP wave spectrum is used for modelling the sea state. The waves are given with an average propagation direction including a cosine spreading function.

9.3.2 Wind

According to OS-E301, a mean wind speed 10 m above sea level, with a return period of 100 years based on the marginal distribution of wind speeds at the specific location, should normally be used. The wind load is treated as a steady component in combination with a time varying gust component. The time varying wind is here described by a Kaimal wind spectrum.

In the standard, a 1-hour mean wind speed 10 m above the sea level, with a return period of 100 years is given. This is taken as the 3-hour mean wind speed at hub height in the analysis. The turbulence intensity is set to 0,1.

The 100-year mean wind speed for the Troll field is given in table 9-2.

	U [m/s]
Northern North Sea - Troll field	40,5

Table 9-2: Troll field wind speed

9.3.3 Current

OS-E301 states that a surface current speed with a 10-year return period should normally be used, based on the marginal distribution of current speeds at the location. Based on measurements from the Troll field, Mathiesen et al. (2008) proposed a current profile. Since the water depth at the Troll field far exceeds the water depth used in this study, only the part of the profile down to a water depth of 100 m is used.

The 10-year current profile applied is given in table 9-3.

	U [m/s]	Level [m]
Northern North Sea - Troll field	1,59	0
	1,14	-20
	1,06	-40
	0,72	-60
	0,72	-80
	0,72	-100

Table 9-3: Modified Troll field current profile

9.3.4 Directions

All the environmental loads are assumed to be acting in the same direction. All directions from 0° to 360°, with a spacing of 30°, are investigated. 0° is along the positive x-axis, while the other directions are defined clockwise accordingly as shown in figure 9-2.

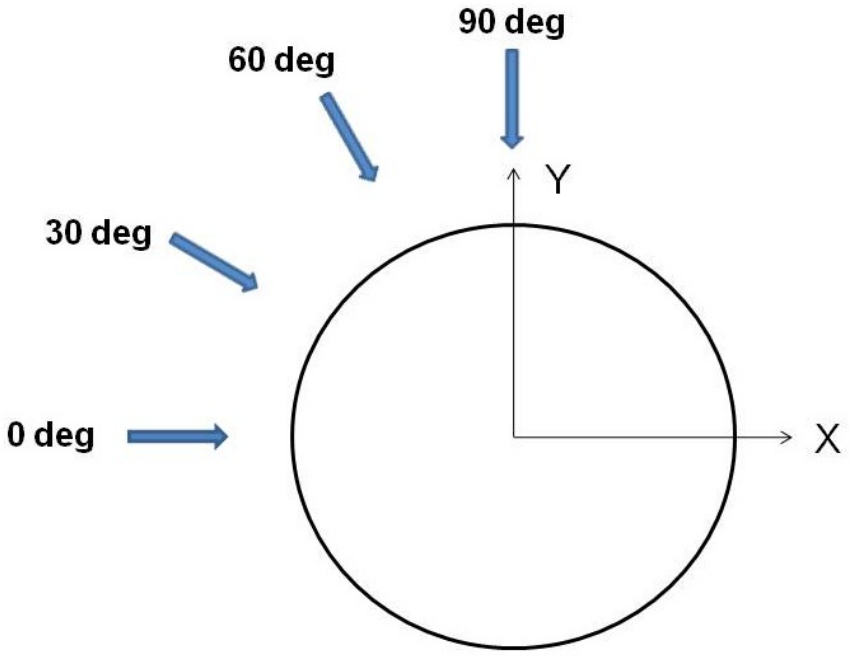

Figure 9-2: Definition of directions

9.3.5 Drag force coefficients

The drag force coefficients for the mooring line components are taken according to OS-E301 and presented in table 9-4.

	Drag coefficients, C_d	
Component type	**Transverse**	**Longitudinal**
Studless chain	2,4	1,15
Stranded rope	1,8	-

Table 9-4: Drag force coefficients

Marine growth and special sea bed soil conditions are not considered in this study.

9.4 Mooring system analysis

According to OS-E301, mooring system analysis can be performed by applying a frequency domain or a time domain method. The latter is utilized in this study, due to the possibility of including drag forces and non-linear mooring systems.

9.4.1 Time domain analysis

In general, the required simulation length is governed by the number of maxima per unit time of the combined WF/LF process. The duration of an environmental state is usually taken as 3 hours, which is the simulation length used here.

From one 3-hour time series, a global maximum, which forms the basis for the extreme value statistics, is referred to as the maximum response between two successive mean-up-crossings. The global maxima are assumed to be independent stochastic variables.

The required extreme value for the line tension is taken as the Most Probable Maximum (MPM) value of the extreme value distribution. This distribution is found by simulating, say 20, realizations of duration 3 hours. The largest global maxima from each realization form the extreme sample, which then is fitted to an extreme value distribution. For a large extreme sample, the distribution will approach a Gumbel distribution; and the MPM value will correspond to the 37% percentile, i.e. 63% probability of exceedance. An alternative approach could be to use the expected value from the extreme sample. This would be conservative as it corresponds to the 57% percentile value of the Gumbel distribution.

9.4.2 Characteristic line tension

In the standard, two components of the characteristic line tension are considered:

- $T_{C\text{-}mean}$ – The characteristic mean line tension, due to pretension and mean environmental loads.
- $T_{C\text{-}dyn}$ – The characteristic dynamic line tension, induced by LF and WF motions.

When analysing in the time domain, the former is taken as the mean of the time series. The latter is taken as the difference between the MPM value of the extreme value distribution and the characteristic mean line tension. The characteristic line tensions are thus found as:

$T_{C\text{-}mean}$ = mean tension of the time series
$T_{C\text{-}dyn} = T_{MPM} - T_{C\text{-}mean}$

9.4.3 Characteristic capacity

For cases where statistics for the breaking strength of mooring line components are not available, the characteristic strength may be taken according to

$$S_C = 0,95 S_{mbs} \tag{9.1}$$

where S_{mbs} is the minimum breaking strength for new components as given in table 8-4.

9.4.4 Design equation and partial safety factors

In OS-E301, the mooring system is categorized according to the consequences of mooring system failure. The two categories are:

Class 1 - Mooring system failure is unlikely to lead to unacceptable consequences such as loss of life, collision with adjacent platform, capsize or sinking.
Class 2 - Mooring system failure may well lead to unacceptable consequences of these types.

Furthermore, the design equation is introduced as:

$$S_C - T_{C-mean}\gamma_{mean} - T_{C-dyn}\gamma_{dyn} \geq 0 \tag{9.2}$$

where the characteristic quantities are defined in the previous sections, and the partial safety factors are given in table 9-5.

	ULS		ALS	
	Partial safety factor on mean tension	Partial safety factor on dynamic tension	Partial safety factor on mean tension	Partial safety factor on dynamic tension
Consequence class	γ_{mean}	γ_{dyn}	γ_{mean}	γ_{dyn}
1	1,10	1,50	1,00	1,10
2	1,40	2,10	1,00	1,25

Table 9-5: Partial safety factors

It is seen that the safety factors for ALS are relatively small. Conservatism is however ensured by the very small probability of coincident line failure and characteristic loads with return period of 100 years.

9.4.5 Horizontal offset and permissible line length

The standard states that the horizontal offset of a given reference point shall be within the operational service limitation both for intact mooring system and in the case of a single line failure. For riser applications, the riser manufacture specification will govern the maximum permissible horizontal offset. Floating wind turbine applications are not specifically addressed in the standards; it is however obvious that the horizontal offset will be limited by the power cable configuration and the distance to adjacent structures.

When it comes to permissible line lengths, the following applies to design where anchors that cannot take uplift forces are used:

- The mooring lines shall have enough length to avoid uplift at anchors for all relevant design conditions in the ULS.
- Vertical forces on the anchors can be accepted in the ALS, if it is documented that these forces will not significantly reduce the characteristic resistance of the anchors.

Furthermore, it is stated that the maximum permissible line length is limited to the suspended length at a line tension equal to the breaking strength of the line plus 500 m.

9.5 Results – ULS

For the ULS, analyses of duration 3 hours are carried out with the mooring system in intact condition. The environmental conditions described in Chapter 9.3 are applied. Analyses are performed with environmental loads from 0° to 360° with an angular increment of 30° according to figure 9-2, i.e. a total of 12 analyses. The main results are presented in table 9-6, while complete results are found on the attached DVD.

Direction	Axial forces [kN]				Max Lift-off [m]	Anch. line nu.	Horizontal plane excursion [m]
	Chain segment		Wire segment				
	Mean	Max	Mean	Max			
0	1399,35	3547,12	1397,56	3546,26	0,01	1	30,74
30	1370,86	2682,69	1368,93	2681,46	0,02	1	31,97
60	1296,66	1934,28	1294,43	1932,64	0,00	1	38,91
90	1299,14	2391,42	1297,10	2390,09	0,00	2	30,14
120	1340,95	2912,33	1339,08	2911,36	0,01	2	29,25
150	1300,81	2169,52	1298,79	2167,71	0,00	2	28,26
180	1188,83	1657,21	1186,44	1655,57	0,00	2	38,49
210	1294,93	2165,74	1292,90	2163,87	0,00	3	28,68
240	1336,88	3234,03	1335,00	3233,07	0,02	3	29,17
270	1296,52	2531,76	1294,48	2530,43	0,00	3	30,65
300	1294,50	1682,10	1292,27	1680,23	0,00	1	35,39
330	1367,88	2964,16	1365,95	2963,26	0,01	1	32,56

Table 9-6: Results ULS analysis

We see that as expected, the maximum tension will be largest in the cases where the environmental loads are acting directly towards one of the anchorlines, i.e. for directions 0°, 120° and 240°. This is because almost all the forces are taken up by only one anchorline in these cases. For all directions, very small differences are observed between the most heavily loaded chain segment and the most heavily loaded wire segment.

The anchorline number refers to the most heavily loaded anchorline in each case. See figure 5-1 for definition of anchorline numbering.

The horizontal plane excursion refers to the maximum horizontal offset during each of the 3 hours simulations. The maximum offsets vary between 28 m and 39 m. We see that the largest offsets occur in cases where the environmental loads are acting in between adjacent lines. The maximum tension in these cases are however limited because the forces are distributed almost evenly between two lines instead of only one. Since the power cable configuration nor the possibility of adjacent wind turbines is investigated in this study, the ULS requirements regarding permissible horizontal offset are assumed fulfilled.

Maximum lift-off refers to the maximum lift-off of a point located 10 m from the anchor of the most heavily loaded anchorline during each 3 hour simulation. This value will thus strongly indicate whether we are experiencing vertical forces on the anchors or not. Lift-off is only observed for cases

where the environmental loads are acting close to or directly towards an anchorline. However, when accounting for the weight of the anchor, a lift-off of 2 cm of a point 10 m from the anchor will give negligible vertical forces on the anchor.

Ideally, 20 simulations of duration 3 hours should be performed for each direction in order to establish an extreme value distribution for the line tension. This would however demand an unrealistic amount of computational effort. The extreme value distribution is therefore conservatively fitted to 20 3-hour simulations for the case with largest maximum line tension, i.e. environmental loads with a direction of 0°. By using different seed number for each simulation and fitting the extreme line tension sample to a Gumbel distribution, the extreme value distribution is obtained as shown in figure 9-3. The Gumbel parameters are obtained according to Leira (2010). Complete results from all the 20 simulations are found on the attached DVD.

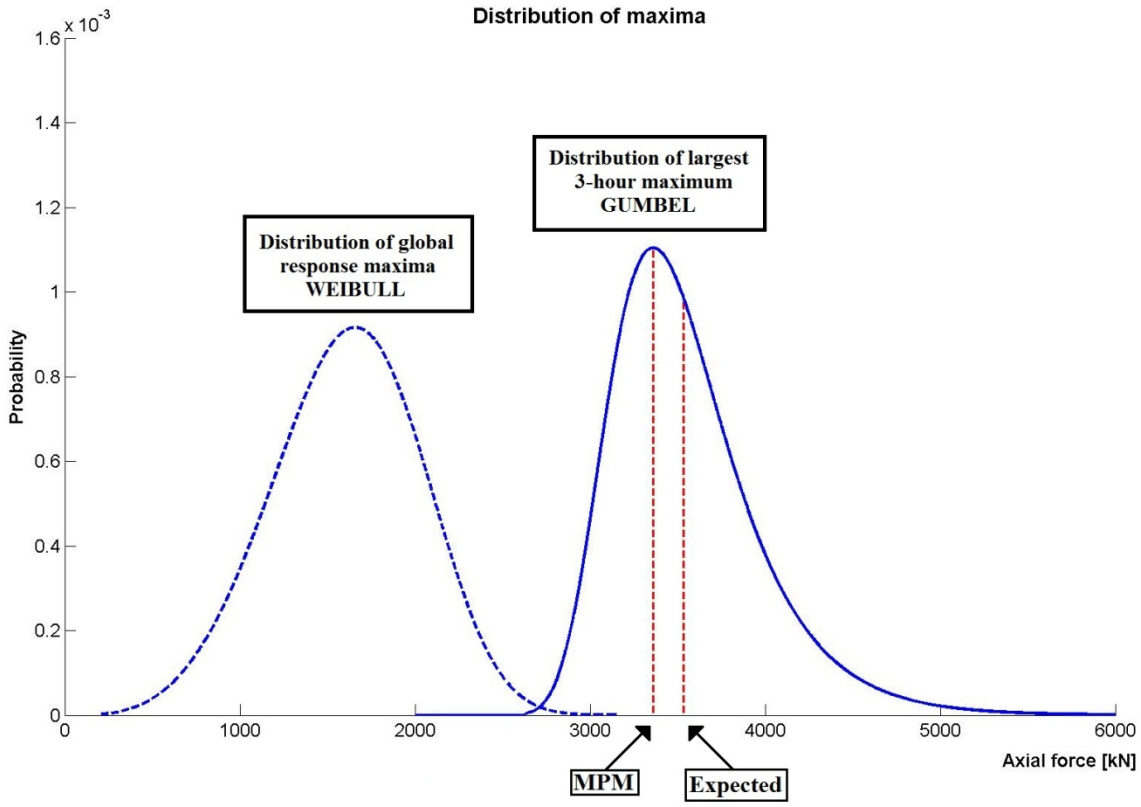

Figure 9-3: Distribution of maximum line tension ULS

The distribution of global maxima from a single 3-hour simulation is fitted to a Weibull distribution and plotted in dotted lines. Both distributions shown are for the most heavily loaded chain segment. The MPM- and expected value for the maximum line tension is indicated in dotted red lines, and correspond to the 37% percentile and 57% percentile value of the Gumbel distribution respectively. The results are presented in table 9-7 for both the most heavily loaded chain- and wire segment.

	Chain	Wire
MPM value [kN]	3534,90	3534,04
Expected value [kN]	3362,37	3361,43

Table 9-7: MPM and expected value for maximum line tension ULS

By applying the MPM value when calculating the characteristic dynamic line tension, the design equation (eq. 9-2) is presented for all considered directions in table 9-8.

Direction	Consequence class	Design equation	
		Chain	Wire
0	1	2814,09	2133,62
	2	1216,47	536,03
30	1	2802,69	2122,17
	2	1196,53	515,99
60	1	2773,01	2092,37
	2	1144,59	463,84
90	1	2774,01	2093,44
	2	1146,33	465,71
120	1	2790,73	2110,23
	2	1175,60	495,10
150	1	2774,68	2094,11
	2	1147,50	466,89
180	1	2729,88	2049,18
	2	1069,11	388,25
210	1	2772,32	2091,76
	2	1143,38	462,77
240	1	2789,10	2108,60
	2	1172,75	492,24
270	1	2772,96	2092,39
	2	1144,49	463,88
300	1	2772,15	2091,51
	2	1143,08	462,33
330	1	2801,50	2120,98
	2	1194,45	513,90

Table 9-8: Design equation results ULS

We see that for both consequence classes 1 and 2, all values are positive, and the design equation is hence fulfilled for all directions. It is safe to assume that unless the structure is placed in a wind farm very close to adjacent structures, a floating wind turbine will be classified as a class 1 type of structure. Regardless, the criteria given in the ULS control will be fulfilled.

9.6 Results – ALS

For the ALS, analyses of duration 3 hours are carried out with the mooring system in damaged condition. Two damaged conditions are examined. The first is investigating the case of loss of one anchorline, while the second case investigates the loss of a clump weight. The environmental conditions described in Chapter 9.3 are applied. Analyses are performed with environmental loads from 0° to 360° with an angular increment of 30° according to figure 9-2, i.e. a total of 12 analyses for each of the two ALS cases. The main results are presented here, while complete results are found on the attached DVD.

9.6.1 Loss of one line

For the purpose of analysing the effect of loss of an anchorline, a new Riflex analysis model is made with anchorline 1 missing. The new finite element model is presented in figure 9-4.

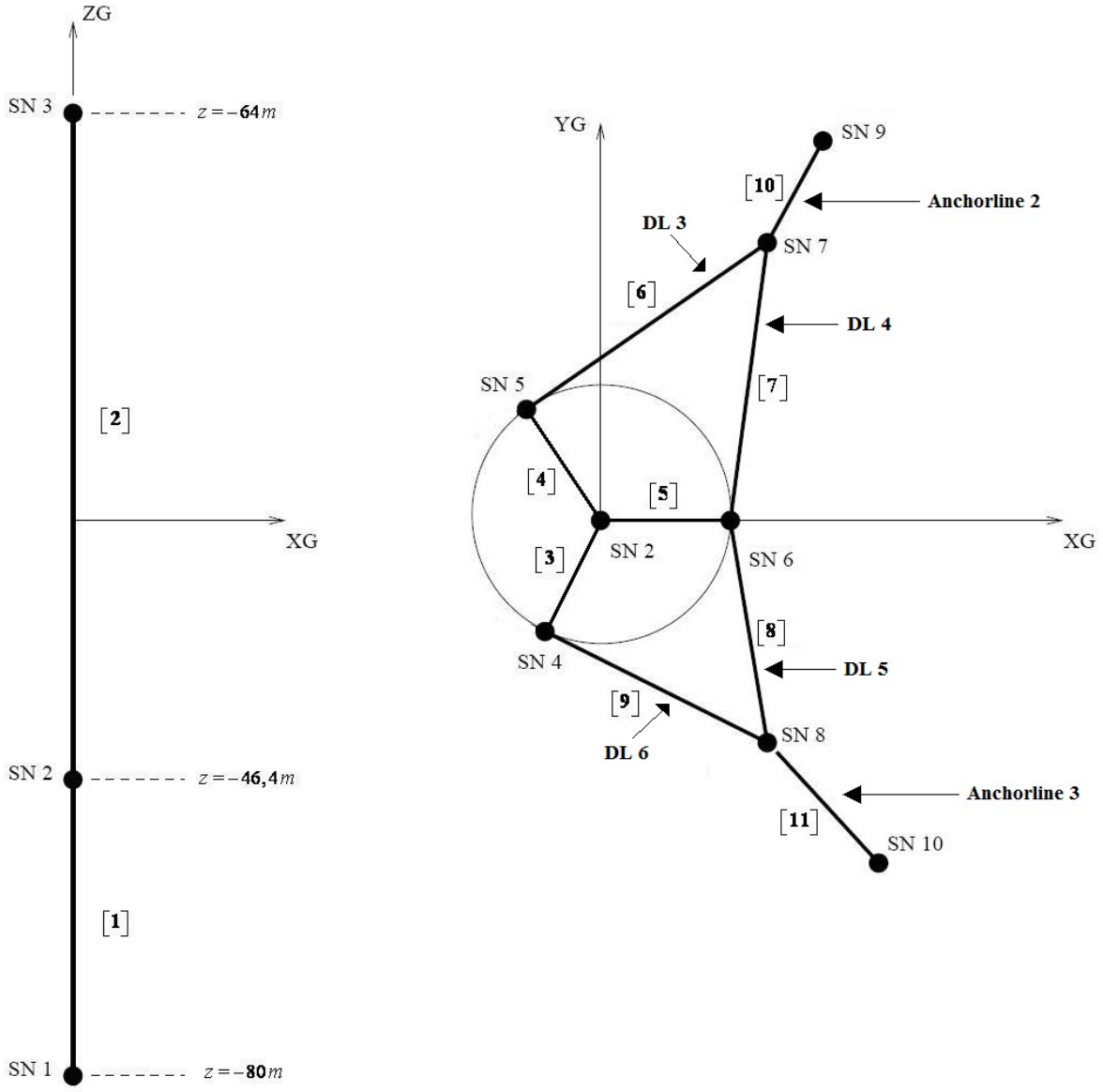

Figure 9-4: Finite element model, ALS – Loss of line

The results from the 12 analyses are presented in table 9-9.

Direction	Axial forces [kN]				Max Lift-off [m]	Anch. line nu.	Max horizontal-plane excursions [m]	Yaw angle [deg]	
	Chain segment		Wire segment						
	Mean	Max	Mean	Max				Mean	Max
0	968,27	1154,54	965,40	1152,07	0,00	3	500,04	52,38	66,28
30	932,16	1203,16	929,32	1201,46	0,00	2	484,86	54,06	64,54
60	905,14	1288,62	902,28	1285,98	0,00	2	407,71	47,00	51,76
90	450,82	4620,97	446,96	4749,10	0,00	3	228,02	28,75	30,56
120	519,88	2911,31	516,00	2291,19	0,00	3	47,55	4,73	7,47
150	961,97	1282,92	959,23	1280,18	0,00	2	29,75	0,83	3,52
180	900,75	1040,48	897,73	1035,78	0,00	3	25,90	0,00	0,00
210	963,59	1282,55	960,86	1280,14	0,00	3	29,54	-0,86	-5,07
240	910,97	1253,22	908,15	1250,29	0,00	3	47,61	-4,73	-8,04
270	450,97	5631,22	447,12	5653,40	0,00	2	226,54	-28,70	-30,54
300	905,01	1288,85	902,15	1286,22	0,00	3	407,80	-47,03	-51,76
330	928,57	1149,49	925,72	1147,20	0,00	3	483,09	-54,20	-62,86

Table 9-9: Results ALS analysis – Loss of line

We see that as one anchorline is removed, the horizontal plane excursions are significantly increased. This is especially prominent for the directions where the environmental loads are acting towards the removed anchorline, i.e. for directions 0°-90° and 270°-330°. The same directions are also associated with very large mean and maximum yaw angles. Because there is no anchorline present to resist the motions, the floater will drift off and rotate around its z-axis (yaw) until the two originally leeward anchorlines are tightened and equilibrium is regained. In practice, this new equilibrium position would cause very large tension levels in the delta-lines as the two delta-lines on the leeward side of the new equilibrium position will be pinched around the floater circumference. This does not appear from the analyses however, as the delta-lines go directly through the body of the floater in a non-physical manner. It is therefore fair to assume, though it is not supported by the analyses, that when environmental loads with a return period of 100 years are applied on the structure from the discussed directions, we run an impending risk of losing additional anchorlines. Hence, the mooring system lacks redundancy for these directions. It is also obvious that with horizontal offsets up to 500 m, there is a large risk of running into adjacent structures if we assume that the floating wind turbine is located in a wind farm.

For the other directions considered, 120°-240°, sufficient restoring forces are provided by the remaining two anchorlines. Mean and maximum tension in the most heavily loaded anchorline will be relatively low and horizontal plane excursions are somewhat in the same range as experienced in the ULS case.

Vertical forces on the anchors are not observed for any of the directions considered.

Using the worst case as basis for calculating extreme value statistics will be futile as the missing anchorline makes the response for each case strongly dependent on the direction of the environmental loads. The maximum value from each simulation is therefore taken as the MPM value when performing the design check; the design equation is calculated for consequence class 1 and 2 for each direction. The results are found in Appendix D. The design equation is satisfied for all directions except for environmental loads from 90° and 270°. However, the results can as mentioned not be taken as the truth as larger tension levels are expected in real life. When the large horizontal offset values are

added, the conclusion is that when considering the case of loss of one anchorline, the mooring system fails to meet the criteria given in the ALS.

9.6.2 Loss of one clump weight

For these analyses, the clump weight on anchorline 1 is removed from the Riflex model and replaced by a regular chain segment. The results from the 12 analyses are presented in table 9-10.

Direction	Axial forces [kN]				Max Lift-off [m]	Anch. line nu.	Max horizontal-plane excursions [m]
	Chain segment		Wire segment				
	Mean	Max	Mean	Max			
0	1130,30	6916,15	1130,09	6916,42	2,05	1	32,43
30	1085,61	6492,04	1085,23	6492,23	1,80	1	34,10
60	962,56	4317,20	961,89	4317,10	1,14	1	37,10
90	1159,58	2187,49	1157,30	2186,14	0,00	2	38,90
120	1152,37	2113,67	1150,16	2111,95	0,00	2	26,32
150	1075,56	1549,36	1073,11	1546,78	0,00	2	20,36
180	972,76	1162,27	969,91	1159,67	0,00	2	18,04
210	1076,54	2231,08	1074,09	2229,61	0,00	3	27,27
240	1151,45	1893,37	1149,25	1891,36	0,00	3	25,80
270	1156,56	1801,67	1154,27	1799,67	0,00	3	34,60
300	960,12	4242,72	959,46	4242,69	1,00	3	38,60
330	1080,96	6093,79	1080,59	6093,98	1,84	3	34,16

Table 9-10: Results ALS analysis – Loss of clump weight

The results show that we can expect large peak tensions in the mooring lines for the directions where the environmental loads are acting towards the removed clump weight. The effect is prominent for the directions 0°-60° and for 300°-330°. This is due to the fact that when the clump weight is removed from an anchorline, the restoring forces from the geometric stiffness contribution of the considered line are dramatically reduced. Hence, the line will respond by stretching and the elastic stiffness contribution will govern the restoring forces. It is also seen that the horizontal plane excursions are larger for these directions, and that vertical forces on the anchors are expected. The sum of these effects may result in loss of the anchorline, and we are back to the first ALS case discussed in the previous section.

For the other directions considered, the results are similar to the ULS case.

As for the first ALS case, the maximum line tension from each of the 12 simulations is taken as the MPM value when checking the design equation. The results, which are found in Appendix E, show that the design equation is not fulfilled for directions 0°, 30°, 300° and 330°.

The mooring system is seen not to fulfil the design criteria for neither of the two investigated ALS cases. Introducing additional anchorlines to increase the redundancy of the mooring system may therefore be considered.

10. Conclusion

The purpose of this study has been to select and optimise the mooring system design for floating offshore wind turbine structures in shallow water. Furthermore, methods for designing the mooring system according to the governing standards were demonstrated.

The design of the floating support structure was based on the Hywind concept, utilizing a deep-draft Spar floater. The draft of the substructure was reduced to 80 m to accommodate to the water depth of only 100 m. Only catenary mooring systems were considered since other types of stationkeeping systems would compromise the design concept. Three types of catenary mooring systems were defined, distributed mass-, clump weight- and buoyancy element mooring system. They were analysed by the means of quasi-static and dynamic analysis in order to determine the system behaviour. The mooring line characteristics obtained from quasi-static analysis showed that the clump weight mooring system had favourable characteristics compared to the other two mooring system concepts considered. The relatively low submerged weight of the buoyancy element mooring system will reduce the geometric stiffness. When the horizontal offset is increased, the line length would therefore have to be very large in order to ensure non-linear restoring forces and preventing vertical forces on the anchors. The distributed mass mooring system had a larger submerged weight and consequently more geometric stiffness. The large axial stiffness of the chain gave however a large elastic stiffness, and a transition to the elastic stiffness range was quickly observed as the horizontal offset increased. The clump weight mooring system had large geometric stiffness due to the large catenary sag from the clump weight, while the elastic stiffness was reduced due to the wire segments in the mooring lines. This combination of stiffness contributions was proven effective, as the transition to the elastic stiffness range was observed to occur at larger tension levels than for the other two concepts. Peak tensions in the mooring lines were then limited. This was also supported by time domain analysis, which demonstrated that the maximum tension observed in the mooring lines during a 1-hour simulation in severe environmental conditions were 40% and 53% larger for the distributed mass- and buoyancy element mooring system respectively than for the clump weight mooring system.

Sensitivity studies were carried out with respect to a number of mooring system parameters. As the main problem was to get sufficient geometric stiffness from the limited suspended line length, the size of the clump weight was seen to be the most influential parameter on the system behaviour. Various sizes, ranging from 6 – 154 tons were investigated. The heaviest ones had major impact on the catenary sag, resulting in favourable mooring line characteristics. However, using clump weights with mass above 100 tons would require very large pretension in order to prevent clump weight touchdown on leeward lines when the floater is offset. In addition, issues related to installation and handling arise for the largest clump weights. Clump weights of size 75 tons were therefore selected. As the suspended line length was limited, and attaching the clump weights to the delta-lines not desirable, a clump weight position on the main mooring line very close to the delta-lines was selected. The pretension needed to be large enough to avoid slack leeward lines and small enough to limit the mean and maximum tension in the weather ward lines. A pretension corresponding to a horizontal top tension of 700 kN was used. The total line length and chain and wire segments were selected to meet the criteria given in the standards with respect to vertical forces on the anchors and permissible line tension. The vertical fairlead position and the length of the delta-lines were merely assessed by theoretical considerations. The former is ideally located close to the vertical centre of rotation, which was shown to be frequency dependent. The vertical fairlead position was set to a point between the centre of gravity and the centre of buoyancy of the floating structure, mainly to provide enough suspended line length. The delta-line length, which influences the yaw restoring coefficient and consequently the yaw natural period was set to 40 m. As the vertical distance between the sea bottom and the fairlead is only 53,6 m, this gave some suspended main mooring line length left to play with. The yaw natural period was estimated to 5,5 s, while the natural periods for the other motion modes were kept above the wave period range.

There is no unique standard governing the design of floating wind turbines, but a guideline assessing the key issues regarding the floating body of such structures is established by DNV. The guideline refers to DNV-OS-E301 “Position Mooring” for design of mooring system. The Troll field was selected as design location, and analyses were carried out against the ULS and ALS. Environmental loading from a total of 12 directions were considered for each limit state, ranging from 0°-360° relative to the floating structure. The results showed that the line tensions were within the acceptable limits for all directions in the ULS. For the ALS, both the cases of loss of line and loss of clump weight were considered. For the first case, large tensions exceeding the criteria given by the standard were observed when the environmental loads were acting in the direction of the missing line. Very large horizontal offsets in the range of the length of the mooring system were also observed. For the case with the loss of clump weight, tensions exceeding the permissible limits and vertical forces on the anchor were observed for directions were the environmental loads were acting towards the line with the missing clump weight. The ALS analyses proved the lack of redundancy in the mooring system in the cases of line breakage and loss of clump weight. Using more than three mooring lines must be considered in order to limit the mooring line tension and horizontal offsets in the ALS cases.

11. Recommendations for further work

The detail design of the clump weights is not studied here, but must be investigated if such components are to be used in a mooring system. E.g. by designing a round or coned clump weight without a large suction surface, the clump weight may partly rest on the sea bottom which will improve the mooring line characteristics. This is especially relevant for shallow water applications, as utilizing larger clump weights would increase the geometric stiffness contribution to the restoring forces. Other aspects concerning the detail design of the clump weights include selecting material and investigate how they should be installed and attached to the mooring line.

In this study, the design check focused on the ultimate limit state and the accidental limit state. In order to complete the design check, also the fatigue limit state should be assessed. This involves calculating the fatigue damage arising in the long term environment the mooring system is subjected to, represented by a number of discrete environmental conditions. Furthermore, VIV analyses must be carried out both for the ULS and for the ALS to include the VIV effects on the mean and low-frequency components of line tension. Related to the ALS control, one would need to adjust the design (e.g. by adding additional anchorlines) so that the redundancy of the system increases. This can be challenging as the diameter of the substructure is small, and one would want to include delta-lines to maintain the low yaw natural periods.

As floating wind turbines are intended to be installed in wind farms consisting of a large number of structures, issues related to the mooring system arise. When using catenary moorings, the mooring system may in fact be the limiting factor on how close the wind turbines can be installed; especially if one assumes a design where mooring lines for different structures are not crossing. To save cost on the anchors, one may also investigate the possibility of using one common anchor point for two or several mooring lines of different structures.

References

Chakrabarti, Subrata (2005) Handbook of Offshore Engineering Volume 1. Illinois, USA: Elsevier Science.

Faltinsen, O.M. (1990): Sea Loads on Ships and Offshore Structures. Cambridge, UK: Cambridge University Press.

Furunes, E.W. (2010) "Floating Wind Turbines at Medium Water Depths". M.Sc. thesis, Dept. of Structural Engineering, NTNU, Trondheim.

Haslum, H.A. (2000) "Simplified methods applied to non-linear motion of spar platform". Dr.ing thesis, Dept. Of marine hydrodynamics, NTNU, Trondheim.

Haver, Sverre K. (2007): "Prediction of Characteristics Response for Design Purposes". Lecture notes in TMR4195 Design of Offshore Structures. Trondheim; Norway: Norwegian University of Science and Technology.

Haver, Sverre K. (2010): Lecture notes in TMR4195 Design of Offshore Structures. Trondheim; Norway: Norwegian University of Science and Technology.

Hordvik, T. (2010) "Alternative Design of Anchor Systems for Floating Windmills". Pre-project, Dept. of marine hydrodynamics, NTNU, Trondheim.

Langen, I., Sigbjørnsson,R. (1979) Dynamisk Analyse av Konstruksjoner. Trondheim; Norway: SINTEF, Avdeling for Konstruksjonsteknikk.

Larsen, C.M. (2010) Lectures notes for special topic: Dynamic analysis of marine structures. Trondheim; Norway: Norwegian University of Science and Technology.

Leira (2010) Lecture notes in TMR4235 Stochastic theory of sea loads. Trondheim; Norway: Norwegian University of Science and Technology.

Loukogeorgaki, E., Angelides, D. C. "Stiffness of Mooring Lines and Performance of Floating Breakwater in Three Dimensions". Division of Hydraulics and Environmental Engineering, Department of Civil Engineering, Aristotle University. Thessaloniki, Greece: Elsevier Science Limited

Luo, Y. (1992) "Optimum Design of Clump Weights for Offshore Mooring Systems". Published in the proceedings of the Proceedings of the Second International Offshore and Polar Engineering Conference, USA. Noble Denton. London, U.K.

Mathiesen, M., Nygaard, E. (2008):	"Hywind Metocean Design Basis". Statoil internal document.
Nielsen, F.G. (2004)	Matlab catenary calculations routine (mooring_characteristics.m). Statoil internal file.
Nielsen, F.G. (2007):	"Design Brief for Offshore Floating Wind-Mills". Statoil internal document.
Nielsen, F.G. (2009):	"Tuning the Geometric and Mass Properties of Hywind". Statoil internal document.
Nielsen, F.G. (2011)	Personal communication.
Triantafyllou, M.S. (1990)	"Cable Mechanics with Marine Applications". Dept. of Ocean Engineering, Massachusetts Institute of Technology, Cambridge, USA.
Yttervik, R. (2009)	TDHMILL3D User Documentation. Statoil internal document.

DNV Guideline for Offshore Floating Wind Turbine Structures

DNV-OS-J101	Design of Offshore Wind Turbine Structures.
DNV-OS-E301	Position mooring.
DNV-OS-E302	Offshore Mooring Chain
DNV-OS-E304	Offshore Mooring Steel Wire Ropes
DNV-RP-C205	Environmental Conditions and Environmental Loads
ISO 19900	Petroleum and Natural Gas Industries – General Requirements for Offshore Structures

Riflex Theory Manual

Riflex User Manual

SIMO Theory Manual

SIMO User Manual

Vryhof anchors (2010)	Anchor manual. Capelle a/d Yssel, the Netherlands.

www.statoil.com

Appendices

List of appendices

Appendix A: Catenary equations, including the effect of elasticity

Deriving the catenary equations is taken from Faltinsen (1990).

Bending stiffness and dynamic effects in the line are neglected and we assume a horizontal seabed.

In figure A1 an element of the line is shown. The mean hydrodynamic forces per unit length in the normal and tangential direction are denoted D and F respectively. W is the submerged weight of the line per unit length, A is the cross-sectional, E is the elastic modulus and T is the line tension. Due to the submerged weight, the correction forces $-\rho gAz$ and $-\rho gAZ - \rho gAdz$ are introduced at the end of the element.

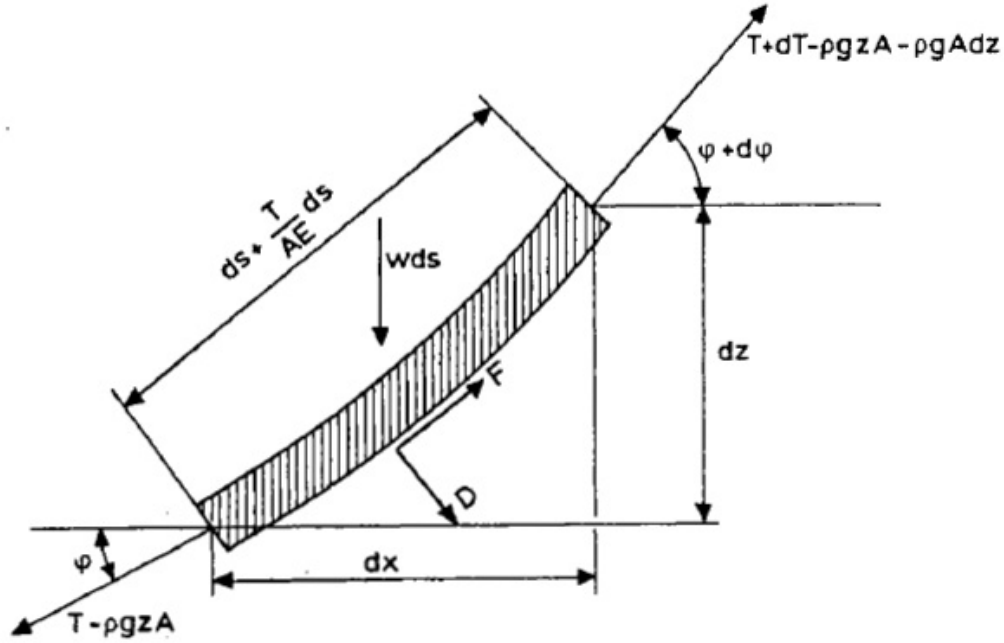

Figure A1: Forces acting on an element of an anchor line (Source: Faltinsen (1990))

From equilibrium we find

$$dT - \rho gAdz = \left[w\sin\phi - F(1 + T/(AE)) \right] ds \tag{3}$$

$$Td\phi - \rho gAzd\phi = \left[w\cos\phi + D(1 + T/(AE)) \right] \tag{4}$$

By neglecting the effect of current forces F and D, and neglect the effect of elasticity the analysis is simplified. The cable line is assumed to have constant weight per unit length.

Introducing

$$T' = T - \rho gzA \tag{5}$$

And write

$$dT' = w \sin\phi ds \tag{6}$$

$$T' d\phi = w \cos\phi ds \tag{7}$$

Eq. (4) and (5) can be divided to obtain

$$\frac{dT'}{T'} = \frac{\sin\phi}{\cos\phi} d\phi \tag{8}$$

$$T' = T_0' \frac{\cos\phi_0}{\cos\phi} \tag{9}$$

By integration we get

$$s - s_0 = \frac{1}{w} \int_{\phi_0}^{\phi} \frac{T_0'}{\cos\theta} \frac{\cos\phi_0}{\cos\theta} d\theta = \frac{T_0' \cos\phi_0}{w} [\tan\phi - \tan\phi_0] \tag{10}$$

$dx = \cos\phi$ and we can write

$$\begin{aligned} x - x_0 &= \frac{1}{w} \int_{\phi_0}^{\phi} \frac{T_0' \cos\phi_0}{\cos\theta} d\theta \\ &= \frac{T_0' \cos\phi_0}{w} \left(\log\left(\frac{1}{\cos\phi} + \tan\phi \right) - \log\left(\frac{1}{\cos\phi_0} + \tan\phi_0 \right) \right) \end{aligned} \tag{11}$$

$dz = \sin\phi$ and we can write

$$\begin{aligned} z - z_0 &= \frac{1}{w} \int_{\phi_0}^{\phi} \frac{T_0 \cos\phi_0 \sin\theta}{\cos^2\theta} d\theta \\ &= \frac{T_0' \cos\phi_0}{w} \left[\frac{1}{\cos\phi} - \frac{1}{\cos\phi_0} \right] \end{aligned} \tag{12}$$

If ϕ_0 is the point of contact between the cable line and the sea bed so $\phi_0 = 0$, we see that

$$T_0' = T' \cos\phi \tag{13}$$

The horizontal component of the tension at the sea bed can be written as

$$T_H = T \cos\phi_w \tag{14}$$

By comparison we see that

$$T_0' = T_H$$

The angle φ can be eliminated from Eq.(8) and (10), and (9) can be written as

$$\frac{xw}{T_H} = \log\left(\frac{1+\sin\phi}{\cos\phi}\right)$$

And

$$\sinh\left(\frac{wx}{T_H}\right) = \frac{1}{2}\left(\frac{1+\sin\phi}{\cos\phi} - \frac{\cos\phi}{1+\sin\phi}\right) = \tan\phi$$

$$\cosh\left(\frac{wx}{T_H}\right) = \frac{1}{2}\left(\frac{1+\sin\phi}{\cos\phi} + \frac{\cos\phi}{1+\sin\phi}\right) = \frac{1}{\cos\phi}$$

And we may write

$$s = \frac{T_H}{w}\sinh\left(\frac{w}{T_H}x\right) \tag{15}$$

$$z + h = \frac{T_H}{w}\left[\cosh\left(\frac{w}{T_H}x\right) - 1\right] \tag{16}$$

By combining Eq. (3), (10) and (11) the line tension can be found as

$$T - \rho g z A = \frac{T_H}{\cos\phi} = T_H + w(z+h)$$

i.e.

$$T = T_H + wh + (w + \rho g A)z \tag{17}$$

In the waterplane we have

$$T_z = ws \tag{18}$$

By using the above derived formulas, the following quantities can be found with reference to figure A2.

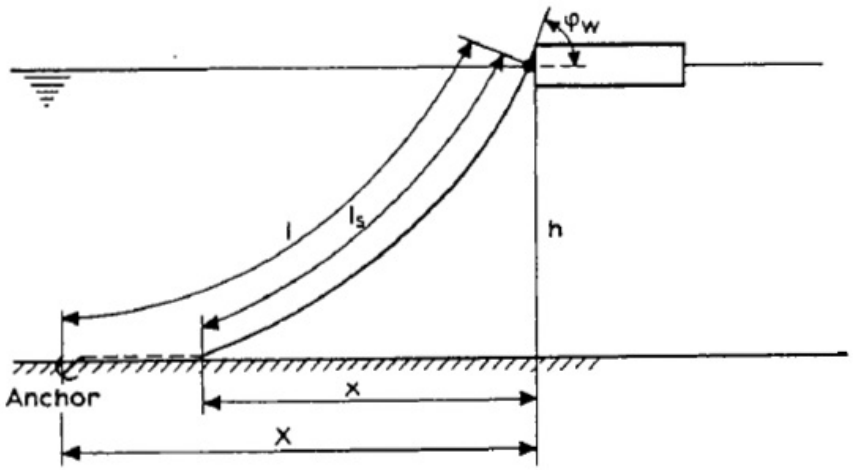

Figure A2: Vessel moored with one anchor line (Source: Faltinsen (1990))

$$l_s = a \sin\left(\frac{x}{a}\right) \tag{19}$$

$$h = a\left[\cosh\left(\frac{x}{a}\right) - 1\right] \tag{20}$$

where

$$a = \frac{T_H}{w} \tag{21}$$

By a combination of Eq. (17) and (18) we obtain

$$l_s^2 = h^2 + 2ha \tag{22}$$

The maximum tension in the cable can be written as

$$T_{\max} = T_H + wh \tag{23}$$

And the minimum length of the cable becomes

$$l_{\min} = h\left(2\frac{T_{\max}}{wh} - 1\right)^{\frac{1}{2}} \tag{24}$$

The horizontal distance X is found as

$$X = l - l_s + x \tag{25}$$

Triantafyllou (1990) showed how the effects of stretch could be accounted for in the catenary equations. By assuming that the cross-sectional area after stretching A, has been replaced by the unstretched area A_0, the x-coordinate is obtained by integration and reads:

$$\frac{dx}{ds} = \cos\phi(1+e) \cong \cos\phi\left(1+\frac{T_e}{EA_0}\right) = \cos\phi + \frac{H}{EA_0}$$
$$x = \frac{H}{w_0}\left[\sinh^{-1}\left(\frac{V - w_0(l-s)}{H}\right) - \sinh^{-1}\left(\frac{V - w_0 l}{H}\right)\right] + \frac{Hs}{EA_0} \tag{26}$$

The z-coordinate is obtained in a similar fashion and reads:

$$\frac{dz}{ds} = \sin\phi(1+e) \cong \sin\phi\left(1+\frac{T_e}{EA_0}\right) = \sin\phi + \frac{V - w_0(l-s)}{EA_0}$$
$$z = \frac{H}{w_0}\left\{\left[1+\left(\frac{V - w_0(l-s)}{H}\right)^2\right]^{\frac{1}{2}} - \left[1+\left(\frac{V - w_0 l}{H}\right)^2\right]^{\frac{1}{2}}\right\} \tag{27}$$
$$+\frac{1}{EA_0}\left[Vs - w_0 ls + \frac{1}{2}w_0 s^2\right]$$

Appendix B: Time series, comparison of mooring system concepts

B.1 Operational condition

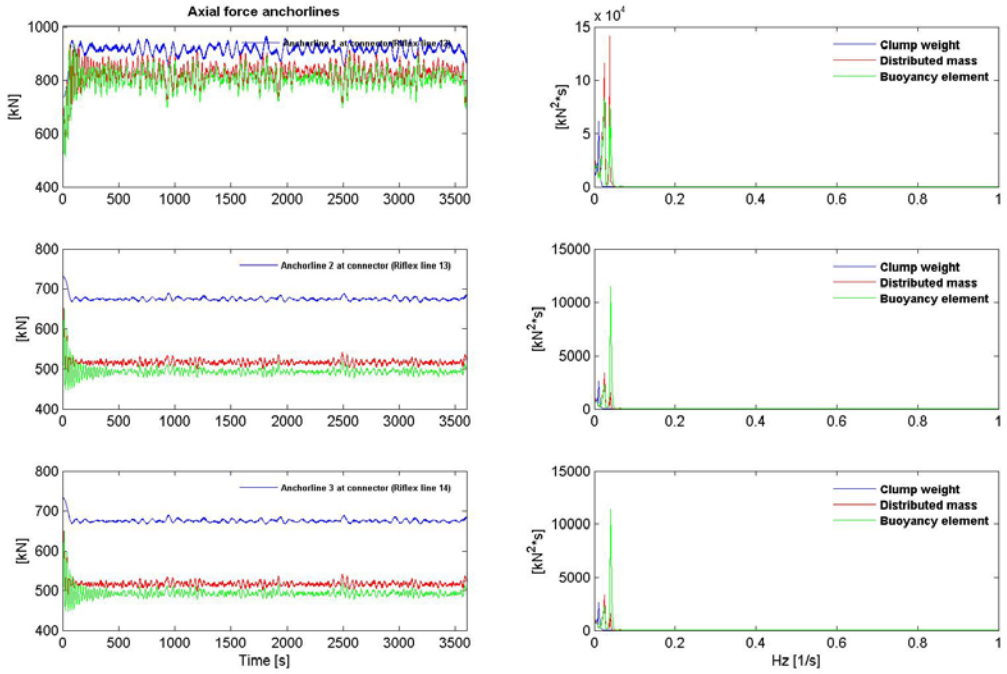

Figure B1: Comparison of axial forces – main mooring lines

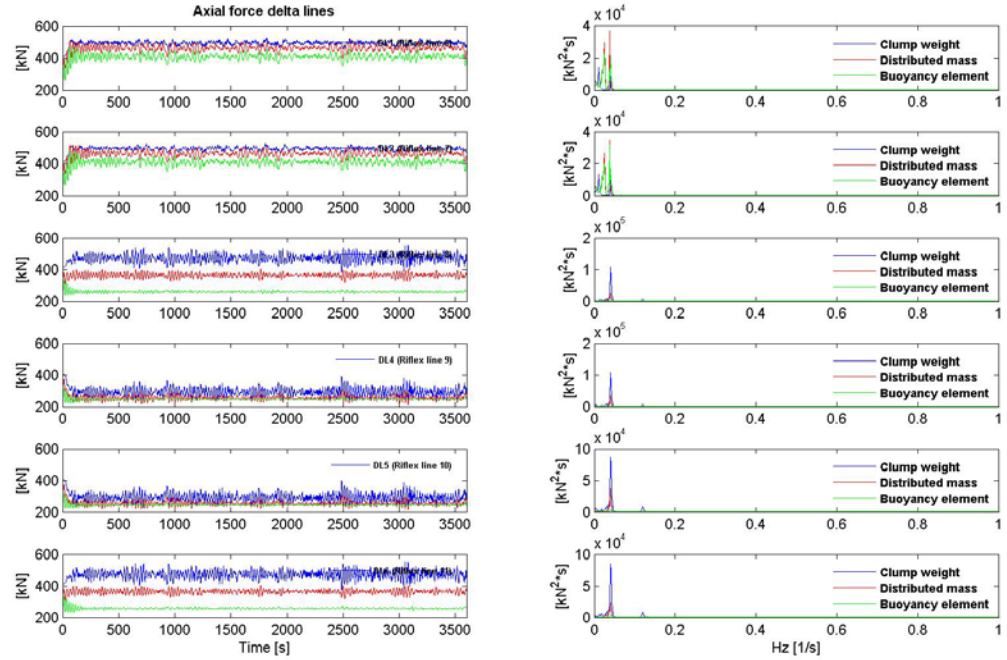

Figure B2: Comparison of axial forces – delta-lines

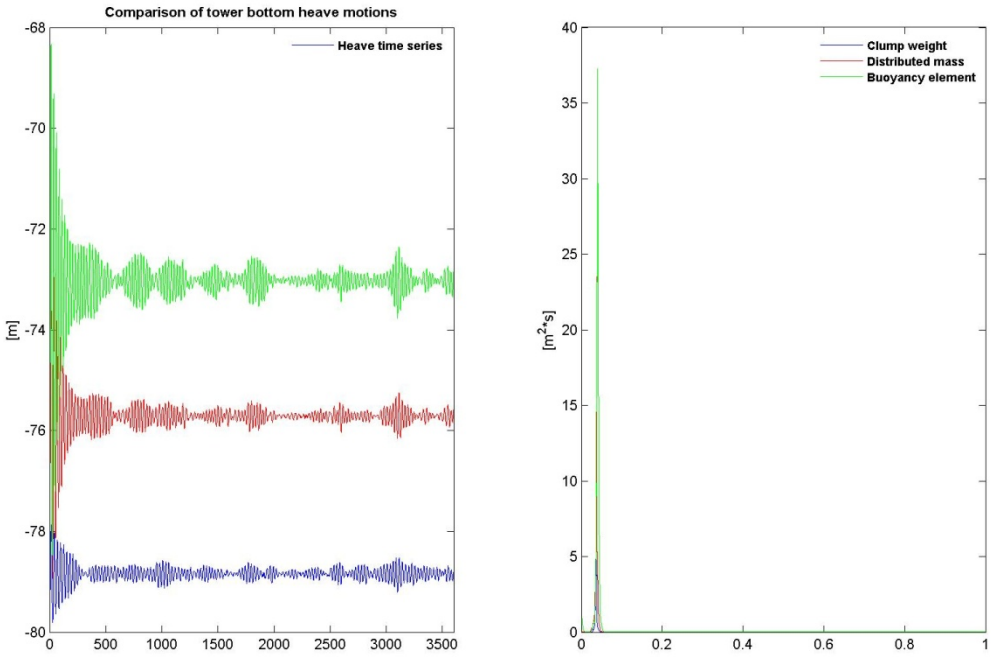

Figure B3: Comparison of tower bottom heave motions

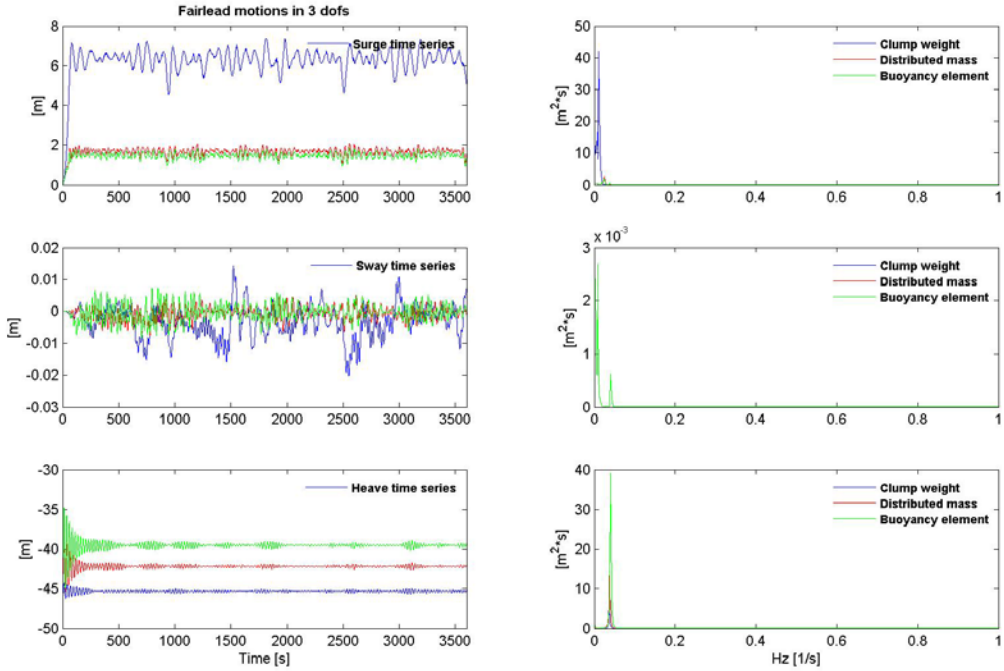

Figure B4: Comparison of fairlead translations

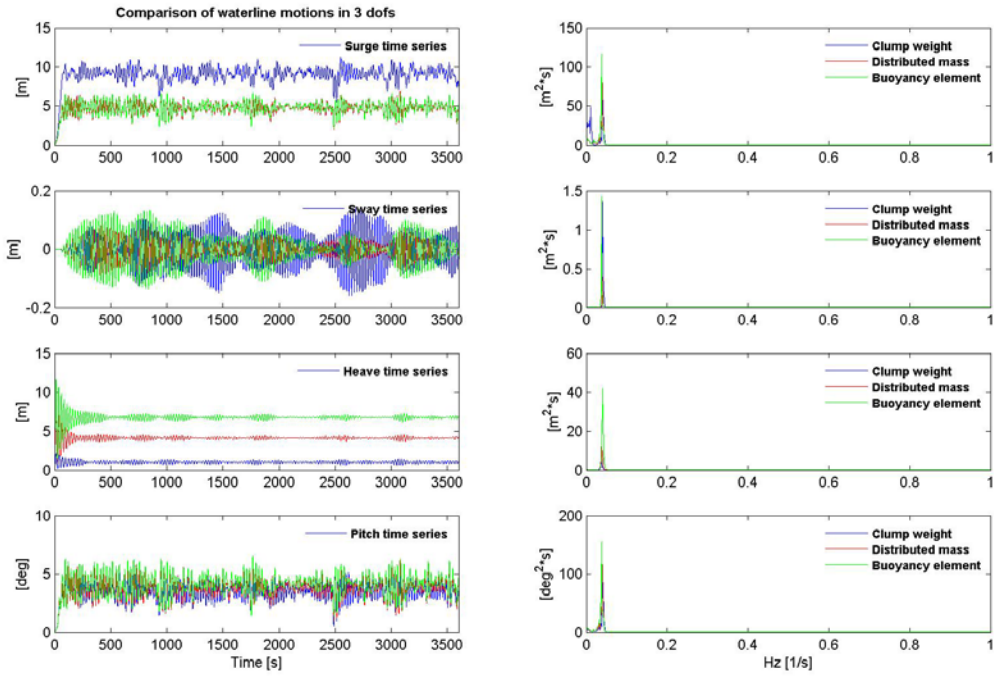

Figure B5: Comparison of waterline translations

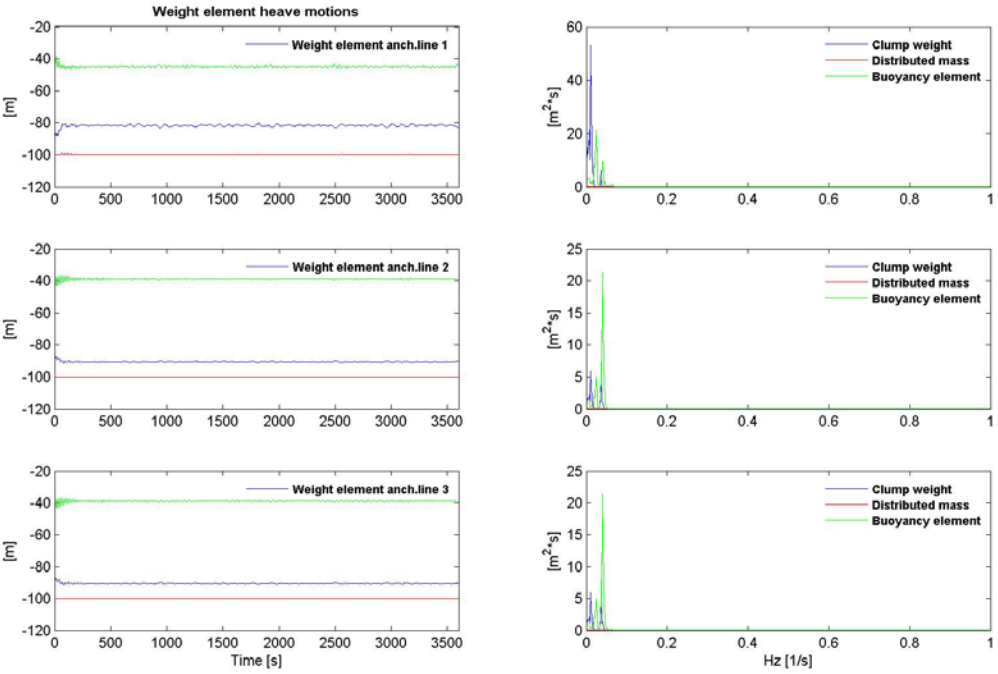

Figure B6: Comparison of weight element heave motions

B.2 Storm condition

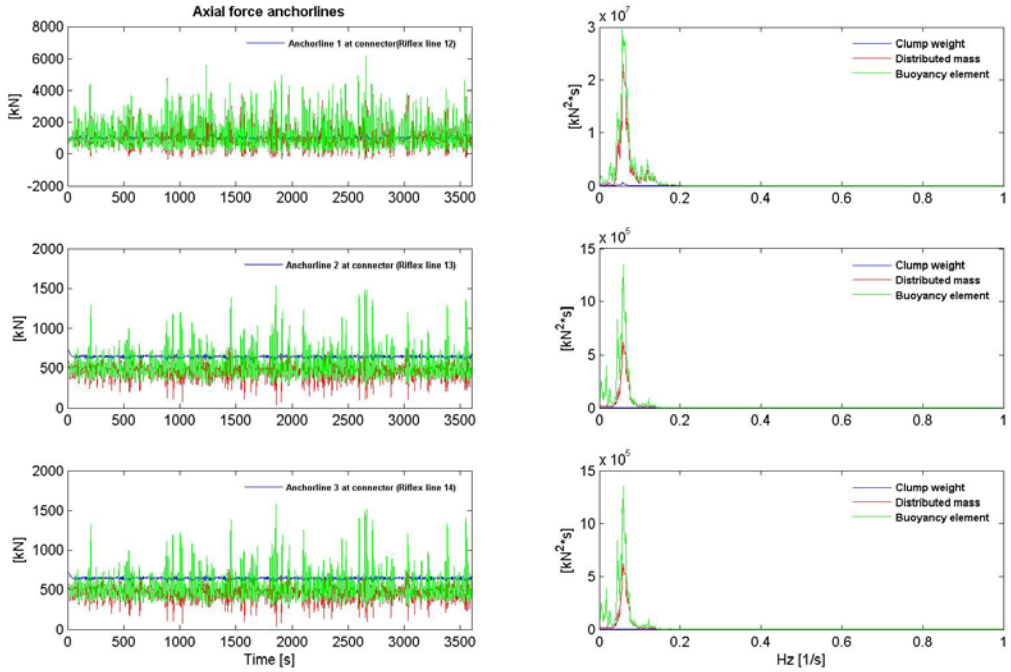

Figure B7: Comparison of axial forces – main mooring lines

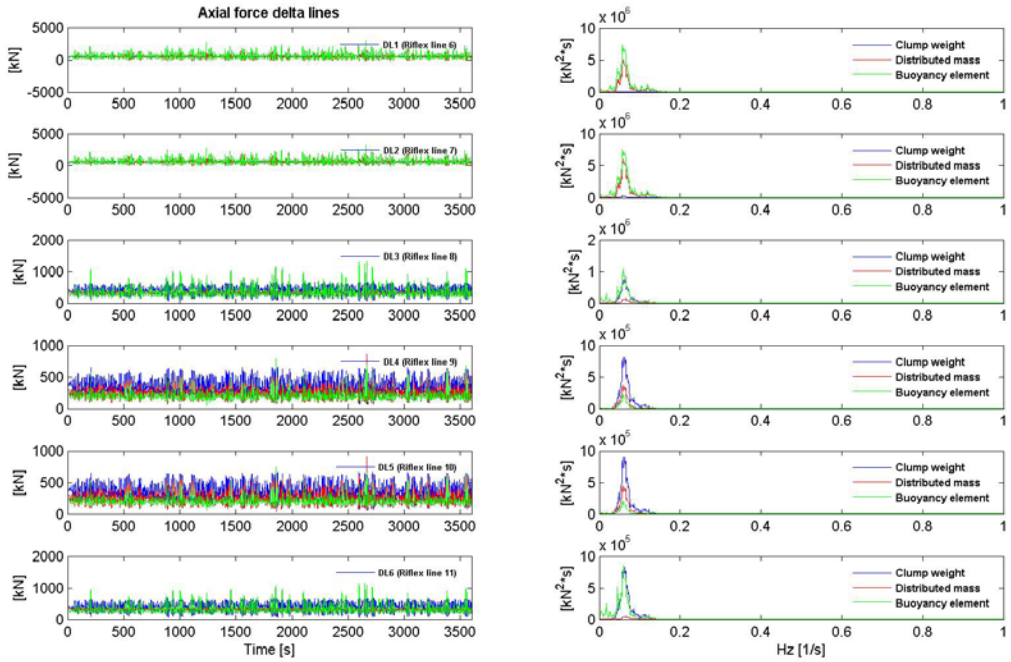

Figure B8: Comparison of axial forces – delta-lines

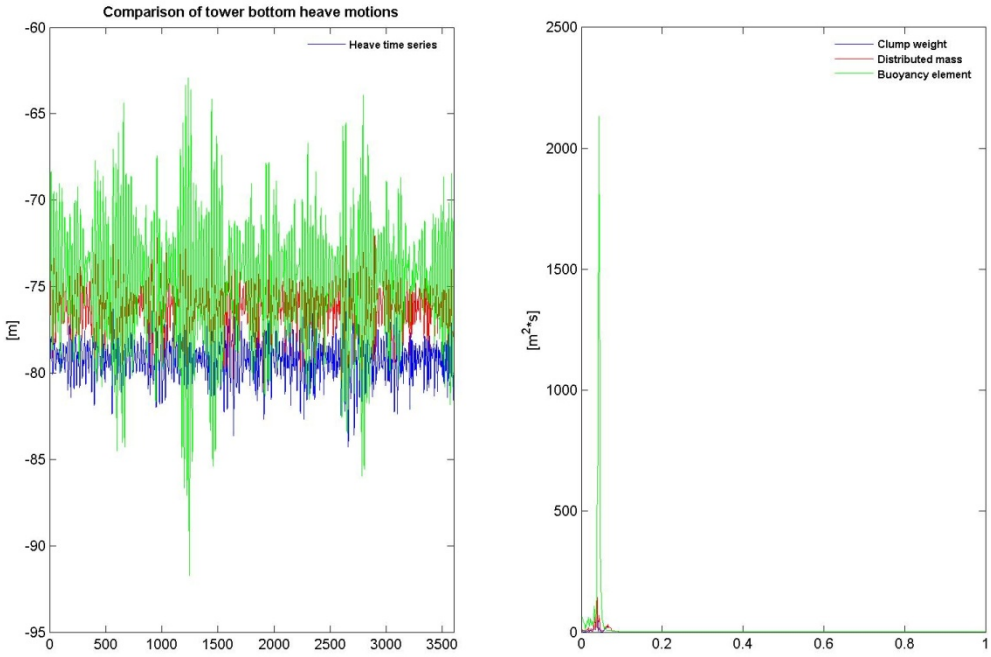

Figure B9: Comparison of tower bottom heave motions

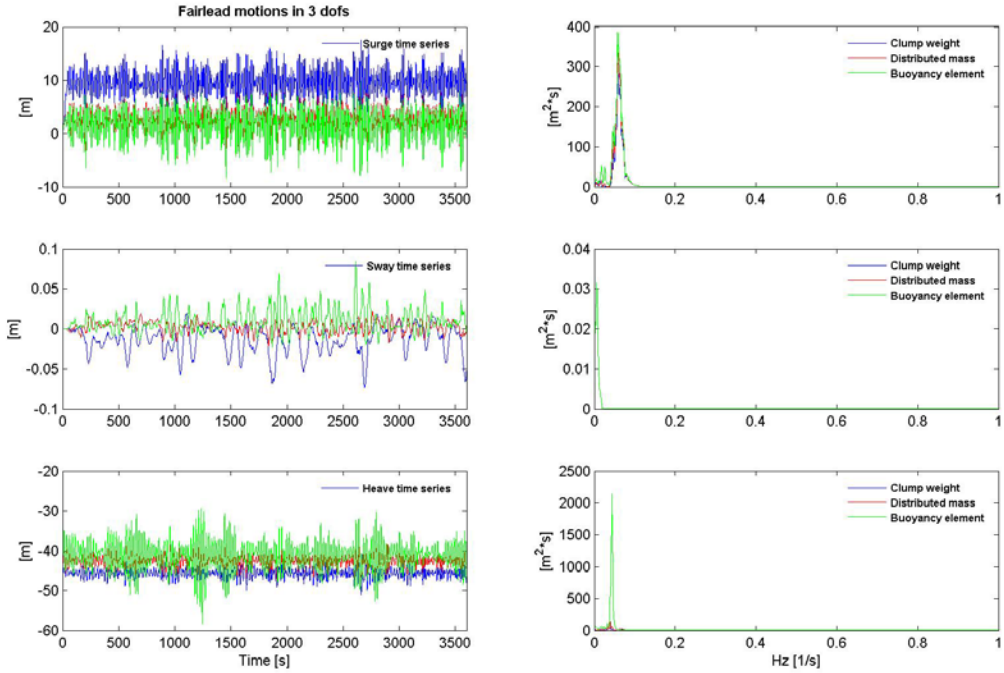

Figure B10: Comparison of fairlead translations

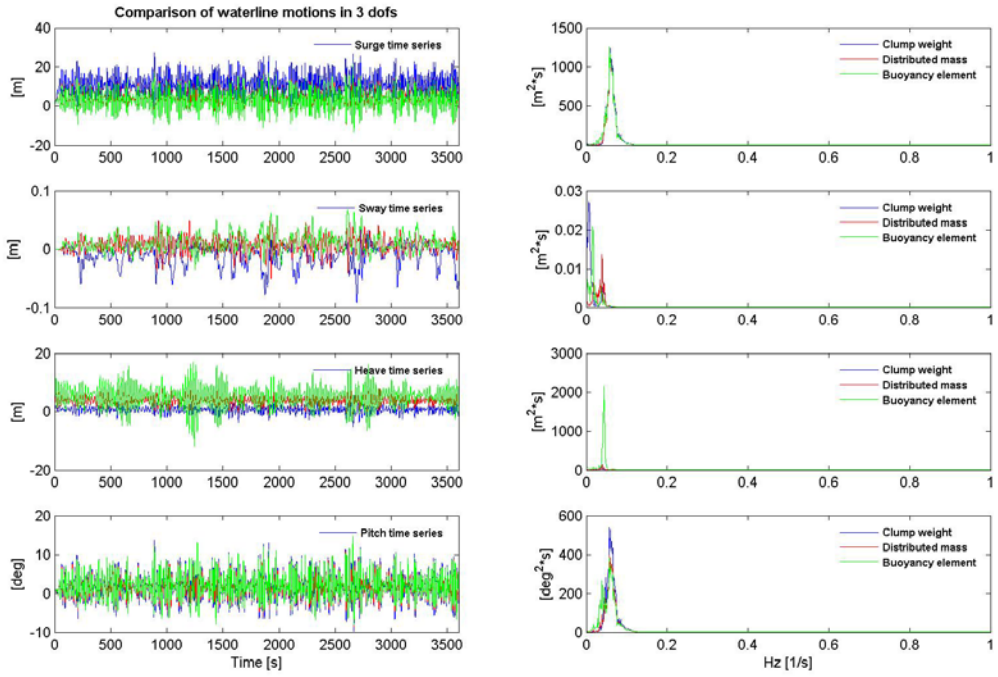

Figure B11: Comparison of waterline translations

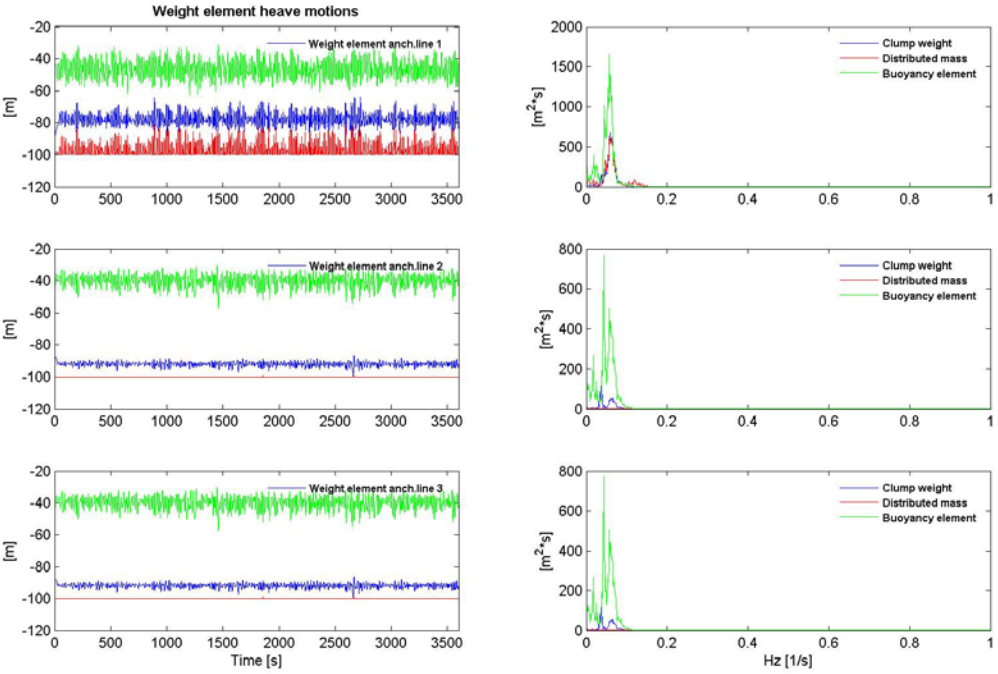

Figure B12: Comparison of weight element heave motions

Appendix C: Riflex modelling of design mooring system components

The design mooring system components are modelled in Riflex according to table C1.

		Component type				
Parameter	**Dimension**	**Chain (Connectors)**	**Chain (Delta-lines)**	**Chain (Bottom)**	**Wire**	**Clump weight**
AMS	[t/m]	0,151	0,107	0,221	0,0405	75,526
AE	[m^2]	0,01189	0,00837	0,0173	0,00724	9,6211
AI	[m^2]	0	0	0	0	0
RGYR	[m]	0	0	0	0	0,88510
AST	[m^2]	0,01189	0,00837	0,0173	0,00724	78,54
WST	[m^3]	0,0001827	0,0001079	0,0003208	0,0000869	98,175
EA	[kN]	7,09E+05	7,09E+05	7,09E+05	4,84E+05	1,92E+09
D	[m]	0,174	0,146	0,21	0,096	3,5

Table C0-1: Riflex modelling of mooring system segments

Appendix D: Design equation results ALS – Loss of line

The results from calculating the design equation for the 12 directions considered in the ALS – Loss of line are shown in table D1.

Direction	Consequence class	Design equation	
		Chain	Wire
0	1	6124,74	5259,34
	2	6096,80	5231,34
30	1	6067,64	5115,94
	2	6027,00	5075,12
60	1	5970,94	4908,69
	2	5913,41	4851,14
90	1	2259,91	-2864,70
	2	1634,39	-3510,03
120	1	4147,45	2372,85
	2	3788,73	2106,57
150	1	5982,89	4983,53
	2	5934,75	4935,38
180	1	6243,45	5429,11
	2	6222,49	5408,41
210	1	5983,45	4985,40
	2	5935,61	4937,50
240	1	6010,46	4990,10
	2	5959,12	4938,78
270	1	1148,65	-4763,56
	2	371,62	-5544,51
300	1	6392,89	4908,06
	2	6392,89	4850,45
330	1	6369,33	5225,92
	2	6369,33	5192,70

Table D0-1: Design equation results ALS – Loss of line

Appendix E: Design equation results ALS – Loss of clump weight

The results from calculating the design equation for the 12 directions considered in the ALS – Loss of line are shown in table E1.

Direction	Consequence class	Design equation	
		Chain	Wire
0	1	-196,83	-6664,63
	2	-1064,71	-7532,58
30	1	265,22	-5823,17
	2	-545,74	-6634,22
60	1	2645,23	-1391,09
	2	2142,04	-1894,37
90	1	5007,62	3298,90
	2	4853,43	3144,57
120	1	5088,10	3446,83
	2	4943,91	3302,56
150	1	5701,16	4548,94
	2	5630,10	4477,89
180	1	6116,68	5248,35
	2	6088,25	5219,89
210	1	4951,37	3116,08
	2	4778,19	2942,75
240	1	5330,34	3909,07
	2	5219,05	3797,76
270	1	5431,72	4107,14
	2	5334,95	4010,33
300	1	6337,78	-1237,50
	2	6337,78	-1729,98
330	1	6216,94	-4991,96
	2	6216,94	-5743,97

Table D1: Design equation results ALS – Loss of clump weight

Appendix F: Content on the attached DVD

F.1 T. Hordvik Master Thesis 2011 – 2 sided print (pdf -file):

Master thesis.

F.2 Presentation_Statoil_09062011 (power-point presentation):

Power point presentation for Statoil research centre 09.06.2011. Summarizes the highlights of the study.

F.3 Other matlab routines (folder):

Contains matlab scripts and functions that are not directly related to running the analyses.

Scripts:

- damping.m
  - Finding linear and quadratic damping from decay test. Calls on subroutine SPEGEN_T.m.
- design_config.m
  - Plot static equilibrium configuration of mooring system from Riflex stamod results.
- Gumbel_fit.m
  - Fit extreme sample to Gumbel distribution and plot. Calls on subroutine weibull.m
- JONSWAP.m
  - Plots JONSWAP-spectrum from given Hs and Tp

Functions:

- SPEGEN_T.m
  - FFT-routine for generating power spectrum from given time history xt. By Finn Gunnar Nielsen.
- weibull.m
  - Fits sample to a Weibull distribution.

F.4 Analyses (folder):

Contains the input files and results (tables and plots) from all the analyses. Contains 4 subfolders.

1. RUN - Comparison (subfolder):

Contains the input files and results (tables and plots) from the comparison analyses.

- model.xls
  - All structural properties, environmental input and simulation parameters defined in excel.

Scripts :

- Run_script.m
  - The main script which controls the analyses. Calls on numerous subroutine

Functions:

- make_directories.m
    - Make directories for saving the results from the analyses.
- user_input.m
    - Controls the user interface of the program.

Subfolders:

- Anchor routines (folder)
    - Contains all the subroutines necessary for running the catenary and mooring system calculations.
- Decay test (folder)
    - Contains all the input files and subroutines necessary for running the decay analysis.
- Dynamic analysis routines (folder)
    - Contains all the input files and subroutines necessary for running the dynamic analysis.
- Eigenvalue analysis routines (folder)
    - Contains all the input files and subroutines necessary for running the eigenvalue analysis.
- Results (folder)
    - Contains plots and statistics for various analyses of the different mooring system concepts, and also the results for the sensitivity analyses. The Riflex result files are not included due to the size of these files.

2. RUN – Optimized system (subfolder):

Contains the input files and results (tables and plots) from the comparison analyses.

- model.xls
    - All structural properties, environmental input and simulation parameters defined in excel.

Scripts:

- Run_script.m
    - The main script which controls the analyses. Calls on numerous subroutines.

Functions:

- make_directories.m
    - Make directories for saving the results from the analyses.
- user_input.m
    - Controls the user interface of the program.

Subfolders:

- Anchor routines (folder)

    - Contains all the subroutines necessary for running the catenary and mooring system calculations.
- Decay test (folder)
    - Contains all the input files and subroutines necessary for running the decay analysis.
- Dynamic analysis routines (folder)
    - Contains all the input files and subroutines necessary for running the dynamic analysis.
- Eigenvalue analysis routines (folder)
    - Contains all the input files and subroutines necessary for running the eigenvalue analysis.
- Results (folder)
    - Contains plots and statistics for various analyses of the optimized mooring system. The Riflex result files are not included due to the size of these files.

3. Parameter study (subfolder):

Contains the input files and results for all the parameters that are studied by the means of quasi-static analysis.

4. Design check (subfolder):

Contains the input files and results for the design check.

Subfolders:

- ALS (folder)
    - Input files and results from two ALS cases
- ULS (folder)
    - Input files and results from one ULS case